OFFICE OF CIVILIAN RADIOACTIVE WASTE MANAGEMENT CALCULATION COVER SHEET	1. QA: QA Page: 1 Of: 76

2. Calculation Title Thermal Hydrology EBS Design Sensitivity Analysis	
3. Document Identifier (including Revision Number) CAL-EBS-HS-000003 Rev 00 ICN 01	
4. Total Attachments 4	5. Attachment Numbers – Number of pages in each I – 8pages, II – 3pages, III – 6pages, IV – 4pages

	Print Name	Signature	Date
6. Originator	Bryan E. Dunlap Junghun Leem	Bryan Dunlap Jhun Leem	4-25-01 4-25-01
7. Checker	Michael T. Itamura	Michael T Itamura	4/29/01
8. Lead	Robert J. MacKinnon	Robert J MacKinnon	04/29/01

1. Remarks

J. Leem is responsible for Section 5.9, the data transmittal for this calculation, MO0008SPATH03.001 and MO0103MWDTHS03.001, and the attachments

B. Dunlap is responsible for the remainder.

Revision History

10. Revision No.	11. Description of Revision
Rev 00	Initial Issue
Rev 00 ICN 01	Section 5.9 added for the lower temperature operating mode scenarios (DTN: MO0103MWDTHS03.001). Attachment IV was modified for DTN: MO0103MWDTHS03.001

CONTENTS

Page

FIGURES

Page

TABLES

Page

1. PURPOSE

In the Technical Change Request titled "Site Recommendation Design Baseline," (CRWMS M&O 2000h, attachment LV.RSO.EPS.1/00-004) repository design bounds for performance assessment models were defined. These repository design bounds could possibly affect the thermal hydrologic model results. Therefore a scoping calculation was required in order to assess the sensitivity of the thermal-hydrological system performance to each bounded design parameter. Calculations were performed to determine the thermal-hydrologic system sensitivity to lineal heat loading (by changing waste package to waste package spacing), ranging from 0.90kW/m to 1.60kW/m. Calculations were simultaneously performed to determine the system sensitivity to preclosure active ventilation duration, ranging from 0 to 100 years of active ventilation. Also, an upper and lower bounded range of hydrologic property sets were used in each of the sensitivity calculations performed in order to gain an understanding of the dependence or independence of each design parameter to the hydrologic property values. Other design parameters that were investigated in order to determine whether further sensitivity analyses were required include: backfill versus no backfill, invert thermal conductivity, drift-to drift spacing adjustment, and active ventilation heat removal efficiency. This calculation was performed under procedure AP-3.12Q, Rev. 0/ICN 3, *Calculations*. It is directed by the development plan TDP-EBS-HS-000004 (CRWMS M&O 2000j) which was developed under procedure AP-2.13Q, *Technical Product Development Plans* for use in Performance Assessment activities. Though AP-2.13Q has been replaced by AP-2.21Q, *Quality Determinations and Planning for Scientific, Engineering, and Regulatory Compliance Activities*, for this activity the development plan remains in effect.

2. METHOD

This calculation applies two models, a two dimensional (2D) thermal-hydrologic submodel and a three dimensional (3D) thermal (conduction-only) submodel that were described in the *Multiscale Thermohydrologic Model* (CRWMS M&O 2000f, section 6.3 and 6.5), the non-backfilled versions of these submodel files are contained in DTN: LL000509112312.003 (Mean Infiltration Case), DTN: LL000509012312.002 (High Infiltration Case), and DTN: LL000509212312.004 (Low Infiltration Case). These submodels were extracted to compute thermal response sensitivities to various parameter adjustments. Standard graphing packages (described in section 4) are used to visualize resulting thermal response curves parsed from the thermal-hydrologic sensitivity runs.

The methods used to control the electronic management of data as required by AP-SV.1Q*, Control of the Electronic Management of Information*, were not specified in the Development Plan*, Development Plan for Thermal Hydrology EBS Design Sensitivity Analysis* (CRWMS M&O 2000j). With regard to the development of this calculation, the control of electronic management of data was evaluated in accordance with YAP-SV.1Q, *Control of the Electronic Management of Data*. The Evaluation (CRWMS M&O 2000g) determined that the current work processes and procedures are adequate for the control of electronic management of data for this activity. Though YAP-SV.1Q has been replaced by AP-SV.1Q, this evaluation remains in effect.

3. ASSUMPTIONS

3.1 It is assumed that the line-loaded, drift-scale, thermal-hydrologic (LDTH) submodel, L4C4, that was extracted from the Multiscale Thermohydrologic Model (MSTHM) is representative of an average location in the repository footprint. This assumption is based on the selected submodel's physical location relative to the geometric center of the repository footprint (Easting:170,501m, Northing:233,808m). No further confirmation is needed for this assumption since the goal of this calculation report simply requires that each sensitivity analysis is performed with like models in order to quantify the sensitivity of the chosen parameter. This assumption is used throughout this calculation report.

3.2 It is assumed that the second 21PWR package in the extracted discrete, drift-scale, thermal conduction-only (DDT) model will be representative of the hotter packages to be contained in the repository. This assumption is based on the observation that the second 21PWR returns the highest temperatures of any package in a 3D drift-scale model that is representative of an average repository drift section. No further confirmation of this assumption is necessary since due to the order in which packages are located in the 3D drift-scale section model the greatest concentration of thermal output for the modeled section length is centralized at the second 21PWR. This assumption is used in section 5.8.

3.3 It is assumed that the first co-disposal high-level waste (HLW) package in the extracted DDT model will be representative of the cooler packages to be contained in the repository. This assumption is based on the observation that the HLW package is the lowest temperature package in the 3D drift-scale model that is representative of an average repository drift section. No further confirmation of this assumption is necessary since due to the order in which packages are located in the 3D drift-scale section model the lowest concentration of thermal output for the modeled section length is centralized at the HLW package. This assumption is used in section 5.8.

3.4 During ventilated preclosure period 70% of the decay heat output is removed from the system. Because of this assumption it is accurate to model the preclosure period by simply reducing the decay heat output to 30% of its non-ventilated rate. The basis of this assumption is provided in the document "Ventilation Model" (CRWMS M&O 2000k, section 7.) and described in the *Monitored Geologic Repository: Project Description Document* (CRWMS M&O 2000d, section 2.7). No further confirmation is needed for this assumption since the goal of this calculation report simply requires that each sensitivity analysis is performed with like models in order to quantify the sensitivity of the chosen parameter. This assumption is used throughout this report. Section 5.6 test the design's sensitivity to this assumption.

3.5 The average age of the commercial spent nuclear fuel (CSNF) is assumed to be 26 years at year equal 0 in each of the simulations performed. This assumption is based on a requirement contained in the direction paper, "Direction to Transition to Enhanced Design Alternative II" (Wilkens, D.R. and Heath, C.A. 1999, enclosure 2, requirement 17). No further confirmation is needed for this assumption since the goal of this calculation report simply requires that each sensitivity analysis is performed with like models in order to quantify the sensitivity of the chosen parameter. This assumption is used throughout this report.

3.6 The capacity of the repository is assumed to be 70,000 metric tons of heavy metal (MTHM), consisting of 63,000 MTHM of CSNF and 7,000 MTHM of a combination of vitrified HLW and DOE spent nuclear fuel (DSNF) (CRWMS M&O 1999a, section 2). This assumption is consistent with the LADS and TSPA-SR models. No further confirmation is needed for this assumption since the goal of this calculation report simply requires that each sensitivity analysis is performed with like models in order to quantify the sensitivity of the chosen parameter. This assumption is used throughout this report.

3.7 The emplacement drifts will be arranged with a uniform 81 meter spacing between their centerlines (CRWMS M&O 1999a, table O-6). This assumption is consistent with the LADS and TSPA-SR models. No further confirmation is needed for this assumption since the goal of this calculation report simply requires that each sensitivity analysis is performed with like models in order to quantify the sensitivity of the chosen parameter. This assumption is used throughout this report. Section 5.7.2 tests the model's sensitivity to this assumption by adjusting the emplacement drift spacing parameter.

3.8 The waste packages will be arranged with a uniform 0.1 meter spacing between each package (CRWMS M&O 1999a, table O-6) that is emplaced at a reference package loading of 1.45 kW/m (Stroupe, E.P. 2000, table on page 2). This assumption is consistent with the TSPA-SR models. No further confirmation is needed for this assumption since the goal of this calculation report simply requires that each sensitivity analysis is performed with like models in order to quantify the sensitivity of the chosen parameter. This assumption is used throughout this report. Section 5.7.1 tests the model's sensitivity to this assumption by adjusting the waste package spacing parameter.

4. USE OF COMPUTER SOFTWARE AND MODELS

4.1 SOFTWARE APPROVED FOR QA WORK

The software package NUFT V3.0s (STN: 10088-3.0s-00) was used to perform the thermal-hydrologic simulations. The NUFT 3.0s software was obtained from Configuration Management in accordance with the AP-SI series of procedures. The following UNIX workstations were used to run the NUFT 3.0s software package: picard.nwer.sandia.gov (Sun SparcUltra 4, SunOS 5.7, serial #738F0958, ID #R431923, Albuquerque, NM), borg.nwer.sandia.gov (Sun SparcUltra 4, SunOS 5.7, serial #701V0015, ID #S819978, Albuquerque, NM), worf.nwer.sandia.gov (Sun SparcUltra 4, SunOS 5.7, serial #926H3DAC, ID #R404810, Albuquerque, NM), and dryheat.ymp.gov (Sun SparcUltra2, SunOS 5.7, M&O #117147, Las Vegas, NV). The software package, NUFT V3.0s is capable of heat & mass transfer modeling in porous media and is appropriate for this application. The software package, NUFT 3.0s, was used within its range of validation.

The software package mView V2.20 (STN: 10072-2.20-00) was used to post-process the data produced by the NUFT models used in this report. The mView V2.20 software package was obtained from Configuration Management in accordance with the AP-SI series of procedures. The mView software was run on the UNIX workstation odin.ymp.gov (Hewlett-Packard Visualize J-2240, HP-UX 10.20, M&O #700889). The software package mView V2.20 is appropriate for this application and was used within its range of validation.

The commercially available software program Microsoft Excel97 is used to graphically present the trends of thermal responses predicted by the sensitivity models. The Excel97 work was performed on a DELL powerEdge 2200 computer using the Windows NT operating system, M&O #111593. This software was used for presentation purposes only (e.g., graphical presentations) which is exempt from qualification or validation requirements in accordance with AP-SI.1Q, *Software Management*, Section 2. There are no other applications (routines or macros) developed using this commercial software.

4.2 SOFTWARE ROUTINES

No Software routines were used in this calculation.

4.3 MODELS

This calculation applies 2D thermal-hydrologic and 3D thermal (conduction-only) submodels that were extracted from the non-backfilled submodeling data submittals of the *Multiscale Thermohydrologic Model* (DTN: LL000509012312.002, DTN: LL000509112312.003, and DTN: LL000509212312.004) to compute thermal response sensitivities to various parameters. The LDTH submodel, L4C4, was extracted from the MSTHM and used in all of the 2D thermal-hydrologic sensitivity analyses contained in this report. The L4C4 LDTH submodel was selected because of its location relative to the center of the repository. The DDT submodel, L4C3, was extracted from the MSTHM and used in all of the 3D thermal (conduction-only) sensitivity analyses included in this report. The L4C3 DDT model was selected primarily because it is the only DDT model in the MSTHM, but it should be noted that its location is very close to the location of the LDTH submodel, L4C4, which is a benefit for comparison purposes. Submodels were selected from the MSTHM because of the goal of analyzing the sensitivity of drift-scale thermal-hydrologic responses, which is the scale of the MSTHM. These submodels are appropriate for their application in this calculation report and used within their bounds.

5. CALCULATION

A two-dimensional 2D LDTH submodel and a 3D DDT submodel described in the *Multiscale Thermohydrologic Model* (CRWMS M&O 2000f, section 6.3 and 6.5; DTN: LL000509012312.002; DTN: LL000509112312.003; and DTN: LL00050909212312.004) were modified to perform sensitivity calculations. The LDTH submodel that was selected from the 31 LDTH submodels in the MSTHM was L4C4 (coordinates: E170501, N233808). The DDT submodel, titled L4C3 (coordinates: E170718, N233796), has a relatively close proximity to the location of the L4C4 LDTH submodel.

A description of the design parameter specific modifications made to the selected submodels is described at the beginning of each subsection in this calculation. A modification that was made to the selected LDTH model used for all of the 2D thermal-hydrologic analyses in this calculation is the refinement of host-rock finite difference nodes. The host-rock node refinements that were made have little to no impact on the in-drift measured parameters and could only add accuracy to the quarter-pillar values that were extracted. The motivation for the refinement of the host-rock nodes was to assist in graphical presentation of thermal contour lines.

The LDTH model location selected has the following characteristics of interest (further details of the model can be found in the *Multiscale Thermohydrologic Model* AMR (CRWMS M&O 2000f, section 6.3):

1) Relatively close to the geometric center of the Site Recommendation (SR) reference repository layout (CRWMS M&O 2000d, Figure 2-8).

2) Repository horizon is located approximately 395 meters below the ground surface, and 343 meters above the water table. This elevation puts the repository horizon at approximately 1074 meters above sea level. (DTN: LL000509112312.003, DTN: LL000509212312.004, and DTN: LL000509012312.002)

3) The repository horizon is located in the Topopah Springs welded tuff unit (TSw35) with approximately 58 meters of TSw35 above the repository horizon and 54 meters of TSw35 below the repository horizon. (DTN: LL000509112312.003, DTN: LL000509212312.004, and DTN: LL000509012312.002)

4) The mean infiltration conditions have a surface infiltration rates of 10.1 mm/yr during the first 600 years of emplacement (present day climate), 28.9 mm/yr from year 600 to year 2000 (monsoonal climate), and 42 mm/yr from year 2000 on (glacial transition climate). (DTN: LL000509112312.003)

5) The low infiltration conditions have a surface infiltration rates of 0.0 mm/yr during the first 600 years of emplacement (present day climate), 10.1 mm/yr from year 600 to year 2000 (monsoonal climate), and 1.99 mm/yr from year 2000 on (glacial transition

climate). (DTN: LL000509012312.002)

6) The high infiltration conditions have a surface infiltration rates of 24.3 mm/yr during the first 600 years of emplacement (present day climate), 47.6 mm/yr from year 600 to year 2000 (monsoonal climate), and 82.0 mm/yr from year 2000 on (glacial transition climate). (DTN: LL000509212312.004)

7) The ground surface temperature is fixed at 15.9 C, and the water table temperature is fixed at 32.5 C. (DTN: LL000509112312.003, DTN: LL000509212312.004, and DTN: LL000509012312.002)

8) The thermal conductivity of the invert elements are a two layered system. The lower layer only assumes ballast material is present so the thermal conductivity is 0.15W/m-K in that layer of nodes. The upper layer of invert nodes assume that steel support structure is present and this is accounted for with a thermal conductivity of 1.52W/m-K in that layer of nodes. (DTN: LL000509112312.003, DTN: LL000509212312.004, and DTN: LL000509012312.002)

It should be noted that the three infiltration conditions are meant to capture the full range of infiltration rates expected at the Yucca Mountain Site. The statistical weightings in the TSPA-SR for the low, mean, and high infiltration cases are 0.17, 0.48, and 0.35, respectively (CRWMS M&O 2000a, section 6.3). In other words, for a given location in the TSPA, model there is a 17% chance that the low infiltration case will be selected, a 48% chance that the mean infiltration case will be selected, and a 35% chance that the high infiltration case will be selected in each TSPA-SR realization. Each of the three infiltration conditions have a unique hydrologic property set assigned to it that was calibrated to match measured borehole data while imposing the respective infiltration boundary condition.

For ease of comparison a standard set of thermal-hydrologic performance parameters will be extracted in each sensitivity section that contains a tabulated summary of results . The performance parameters chosen for comparison purposes are:

Waste Package

- Peak temperature
  - Used primarily for comparison between repository layouts. Cladding integrity could be compromised if temperatures rise to 300°C.
- Years until temperature is less than or equal to 115°C
  - Used as a rough estimate for the possible initiation of canister corrosion, based on saturated pressure at this temperature.
- Years until temperature is less than or equal to 80°C
  - Used as a comparison between various designs.

Drift Wall Crown

- Peak temperature
  - Used to determine if the host rock temperature is elevated above boiling and can be used to

comparatively judge how much of the host rock is elevated above boiling temperatures, i.e. a design with a higher drift wall peak temperature would boil a greater volume of water than a design with a lower drift wall peak temperature.
  - Higher host rock temperatures are also expected to result in greater thermal-hydrologic-chemical (THC) and thermal-hydrologic-mechanical (THM) effects which should be considered when comparing design parameter differences. Greater THC or THM effects would increase the uncertainty associated with the prediction of long term thermal-hydrologic behavior.
- Years until temperature is less than or equal to 96°C
  - Used as a comparison between repository layouts with above boiling host rock. Water into the emplacement drifts from infiltration or condensate is expected to return when the local host rock temperature falls below boiling.

Pillar Conditions
- Peak temperature at the quarter pillar position (25% of pillar ~ 21.5m from drift center)
  - Useful in determining if more than 50% of pillar exceeds boiling at the peak.

These parameters are by no means comprehensive of all the parameters with bearings on system performance, but they do provide a good point from which to compare multiple scenarios. Also, the performance parameters are presented in several locations of the near field in order to capture how apparently simple design changes can simultaneously create positive and negative impacts on performance. Other parameters of interest that are not explicitly discussed or presented in this document they can be extracted from the input and output deck data submittal DTN: MO0008SPATHS03.001 and MO0103MWDTHS.001.

5.1 SENSITIVITY TO PRECLOSURE (VENTILATION) DURATION

This section presents the dependence of the thermal hydrologic performance of the repository to the duration of the ventilated preclosure period. For all models in this sensitivity analysis the preclosure ventilation is assumed to have a heat extraction efficiency of 70% (Assumption 3.4), Figure 5.1-1 shows the waste fuel decay heat curves used in the models both with and without ventilation.

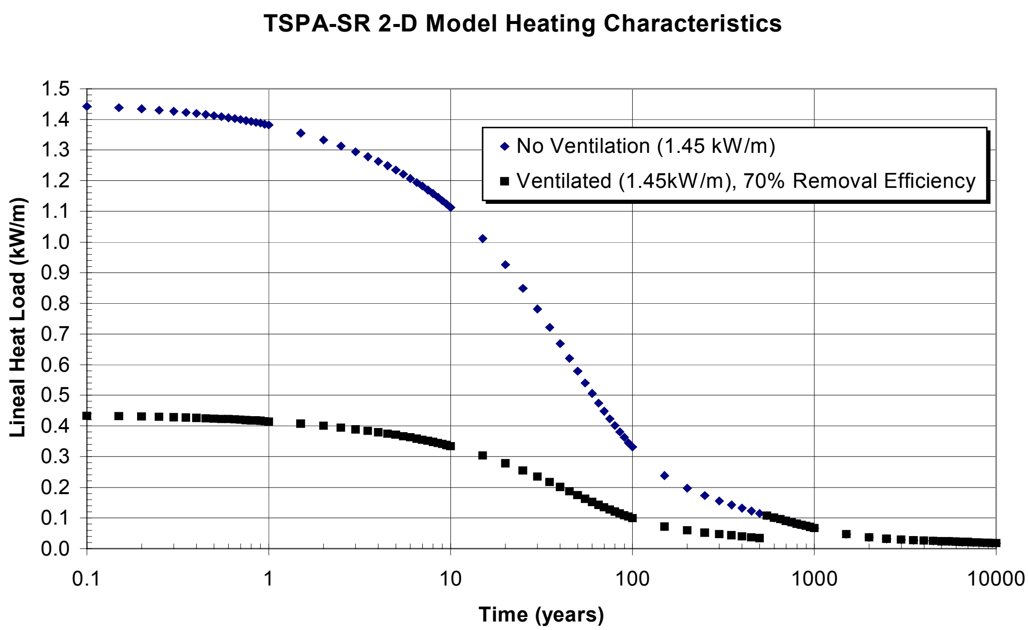

Figure 5.1-1 - Decay Heat curve used in all 2D, thermal-hydrologic sensivity analyses.

Figure 5.1-1 shows the heat output curve followed by the 2D TSPA-SR models, and the 2D models in this calculation, as provided in the report "Heat Decay Data and Repository Footprint for Thermal-Hydrologic and Conduction Only Models for the TSPA-SR" (CRWMS M&O 2000c, Figure 1; and DTN: SNT05071897001.004, filenames: "avgdhlw.txt" and "nrctor4pck.txt"). During the ventilated portion of a given model, the thermal output is reduced by 70% and is equivalent to the "Ventilated" curve shown in Figure 5.1-1. When ventilation is not present in a simulation, i.e. postclosure, the "No Ventilation" curve from Figure 5.1-1 is used. No lag time is assumed in switching from a ventilated preclosure period to a non-ventilated postclosure period, the transition from one heat output curve to the other is considered to happen instantaneously. In Table 5.1-1 a listing of the lineal heat loadings at closure as well as the summation of the heat delivered to the host rock during preclosure is presented. The full lineal heat loading values that are given for each of the preclosure periods show the level of lineal heating that the emplacement drift ramps up to when ventilation ceases at closure. This "ramping" of lineal heat loads is roughly how the LDTH model was modified and executed for this sensitivity analysis. A preclosure model was executed with 70% of the heat removed from the input heat curve, at selected closure times restart files were created. Post-closure models were then started using the preclosure restart files and 100% of the remaining lineal heat input curve.

The rows in Table 5.1-1 that contain the summation of heat delivered during the various preclosure periods can be used to show the difference in ventilated versus non-ventilated total heat delivered to the host rock. Ventilation has a particularly large impact on the heat that goes into the host rock during the early years of emplacement. Note from Table 5.1-1 that the total heat removed from the system after 50 years of ventilation is 76% greater that the heat removed from the system after only 23 years of ventilation. But if we roughly double the ventilation period again it is observed that 100 years of ventilation only removes 48% more heat than 50 years of ventilation removes from the system. Yet another comparison can be made between the 27 year period of ventilation that occurs between the 23 year and 50 year closure times and the 25 year period of ventilation that occurs between the 100 year and 125 year closure times. Between the closure times of 23 years and 50 years an additional 426 GJ/m is removed from the system, but between the closure times of 100 years and 125 years only an additional 170 GJ/m is removed from the system.

The effectiveness of ventilation to remove thermal energy diminishes as the ventilation times increase, but the last row of the Table 5.1-1 gives an estimate of how long those additional years of ventilation will affect results. After ventilation ceases the total energy of the system grows at approximately the same rate as the non-ventilated system, a small difference in the energy added to the ventilated versus non-ventilated system will occur due to the affect of the constant temperature boundary conditions. The ventilated and non-ventilated systems will proceed to maintain the energy difference created during the ventilation period over the course of the postclosure period. Note that as the energy levels of the ventilated and non-ventilated systems continue to grow, the energy removed during ventilation becomes an increasingly smaller fraction of the total system energy. An arbitrarily selected ventilated system to non-ventilated system energy difference of 10% was used for comparison purposes in order to estimate how long the effects of ventilation would be noticeable. It is noteworthy that as the power supplied by the waste decay heat diminishes during ventilation so does its ability to make up the difference after ventilation stops. This is due to the shallowness of the decay heat power curve at later time periods. So, from initial emplacement, ventilating for 50 years removes 985 GJ/m from the system and the difference between the ventilated and non-ventilated systems will become unnoticeably small after just over 5000 years. Interestingly enough, ventilating from 100 years to 125 years only removes an additional 170 GJ/m from the system, but the total system energy difference will require approximately 4000 years (18000-14000=4000) in order to make up the energy difference created by that particular 25 year period of ventilation.

Table 5.1-2 provides a summary of selected thermal hydrologic performance parameters for comparison purposes.

Table 5.1-1 – Lineal Heat loadings at select closure periods using a 70% effective heat removal rate during ventilated preclosure. 1.45kW/m initial decay heat curve.

	Years of Ventilation After Initial Emplacement						
	0	15	23	26	50	100	125
Full Lineal Heat Loading (kW/m)	1.450	1.012	0.8797	0.8354	0.5786	0.3313	0.2849
30% of Lineal Heat Loading (kW/m)	0.4327	0.3035	0.2639	0.2506	0.1736	0.0994	0.0855
Total heat delivered during non-ventilated preclosure (GJ/m)	0	561	799	881	1407	2092	2335
Total heat delivered during 70% efficient ventilated preclosure (GJ/m)	0	168	240	264	422	628	701
Years until Vent total heat is within 10% of non-Vent total heat	0	410	975	1300	5000	14,000	18,000

DTN: MO0008SPATHS03.001

Table 5.1-2 – Summary of thermal hydrologic performance parameters showing the drift-scale sensitivity to ventilation. 1.45kW/m LDTH model used for all simulations.

Performance Parameter	Infiltration Flux Case	Years of Ventilation (70% effective heat removal)					
		0	**15**	**23**	**50**	**100**	**125**
WP Peak Temperature (Celsius)	Low	313	255	229	172	129	117
	Mean	**298**	**238**	**214**	**157**	**110**	**101**
	High	288	231	207	151	107	99
Years Until WP > 115°C	Low	1450	1250	1150	900	580	380
	Mean	**650**	**575**	**500**	**300**	**0**	**0**
	High	550	450	380	240	0	0
Years Until WP > 80°C	Low	5550	5400	5150	5000	4600	4500
	Mean	**3400**	**3250**	**3200**	**2900**	**2500**	**2400**
	High	2600	2450	2400	2250	2000	1900
DW Peak Temperature (Celsius)	Low	284	232	210	160	121	111
	Mean	**268**	**215**	**195**	**145**	**103**	**96**
	High	258	208	188	138	99	93
Years Until DW > 96°C	Low	2850	2500	2300	2000	1800	1675
	Mean	**1650**	**1450**	**1350**	**975**	**620**	**0**
	High	1400	1200	1100	800	340	0
¼ Pillar Peak Temperature (Celsius)	Low	113	104	102	97	92	90
	Mean	**99**	**95**	**93**	**88**	**82**	**81**
	High	96	93	91	85	80	78

DTN: MO0008SPATHS03.001

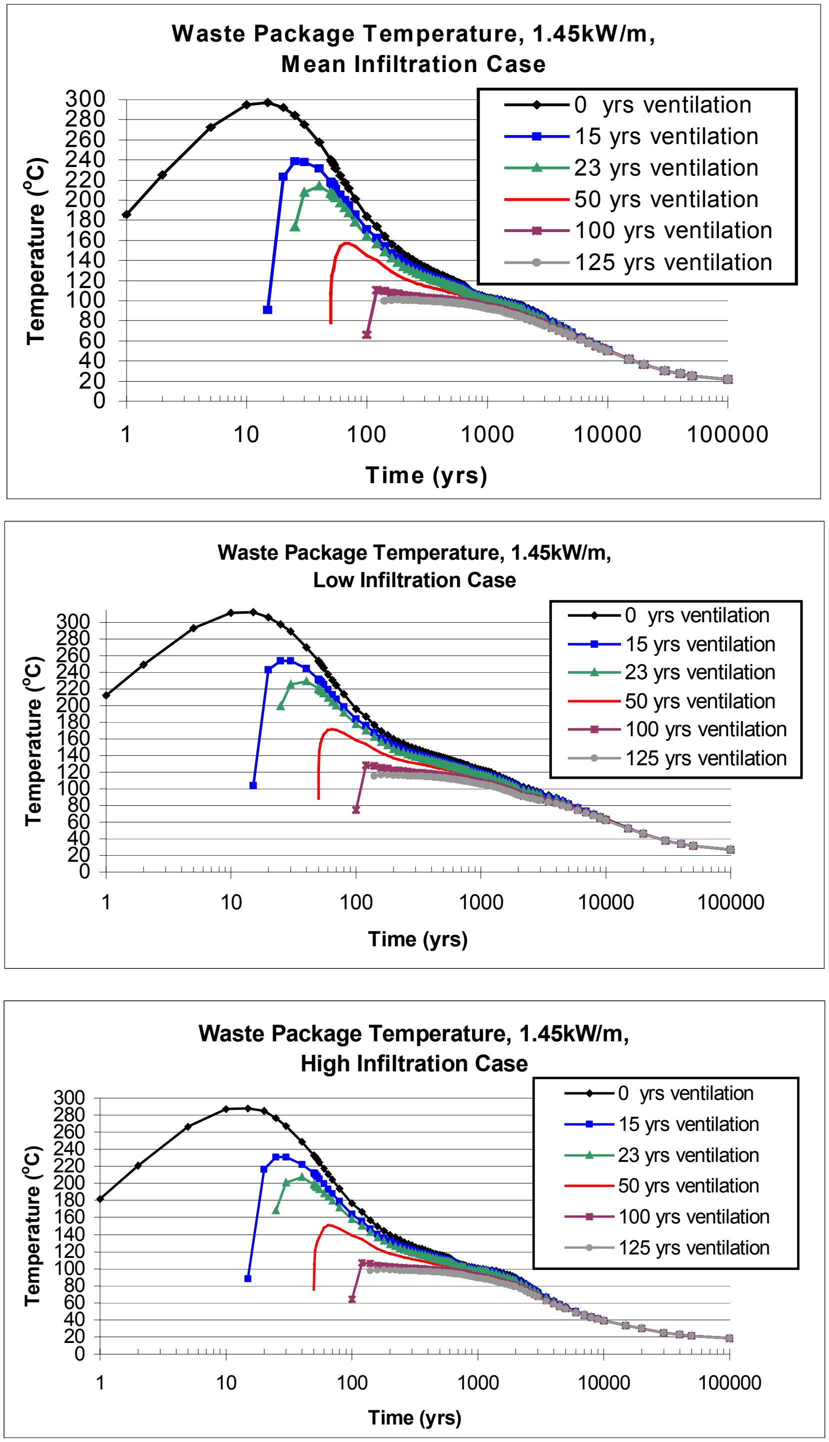

DTN: MO0008SPATHS03.001, file: ventilation_145_*_Twp.xls

Figure 5.1-2a, b, c (top to bottom) – Comparison of waste package temperature time-histories. 1.45 kW/m lineal heat loading with varying ventilation durations.

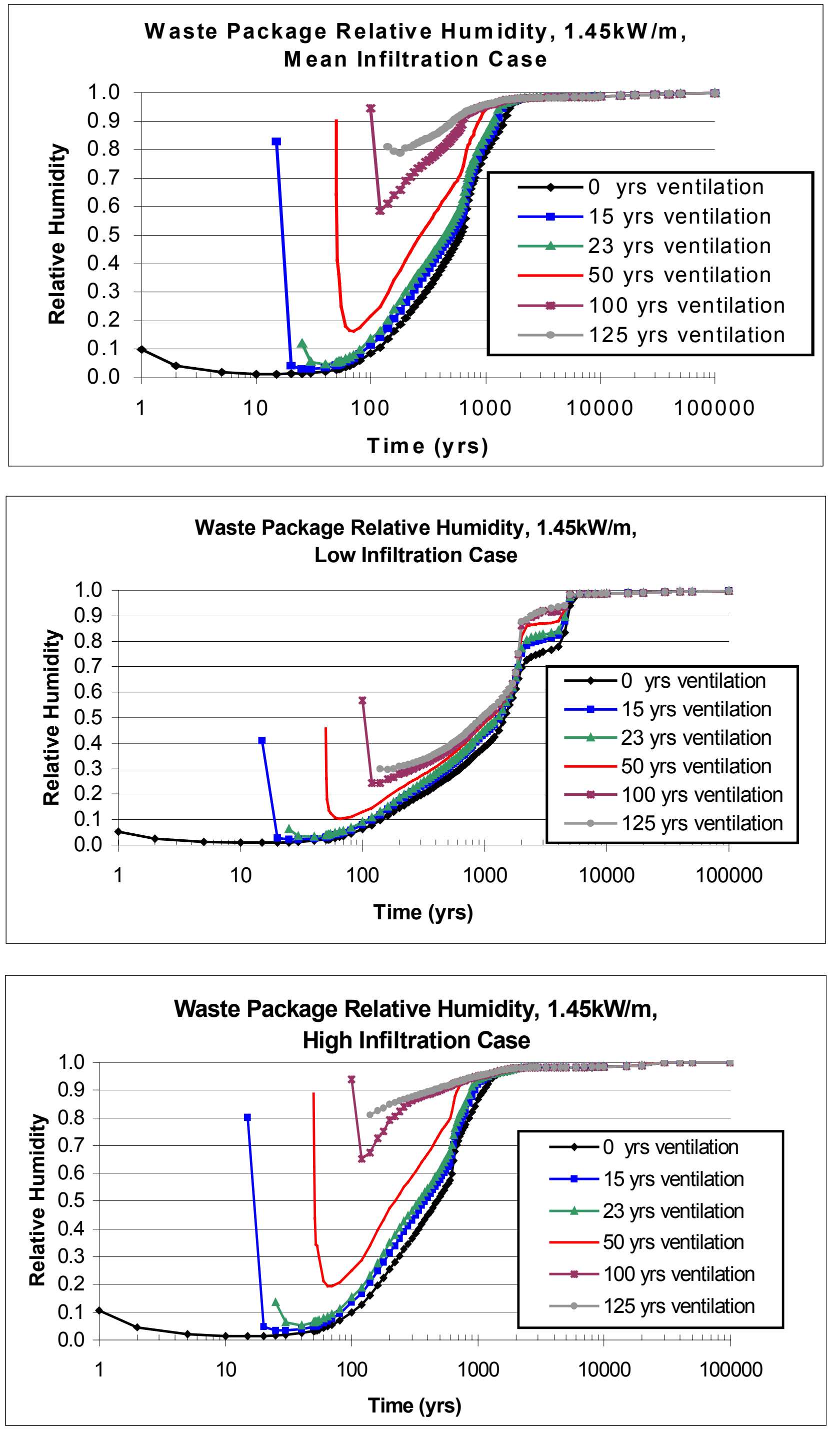

DTN: MO0008SPATHS03.001, file: ventilation_145_*_RHwp.xls

Figure 5.1-3a, b, c (top to bottom) – Comparison of waste package relative humidity time-histories. 1.45 kW/m lineal heat loading with varying ventilation durations.

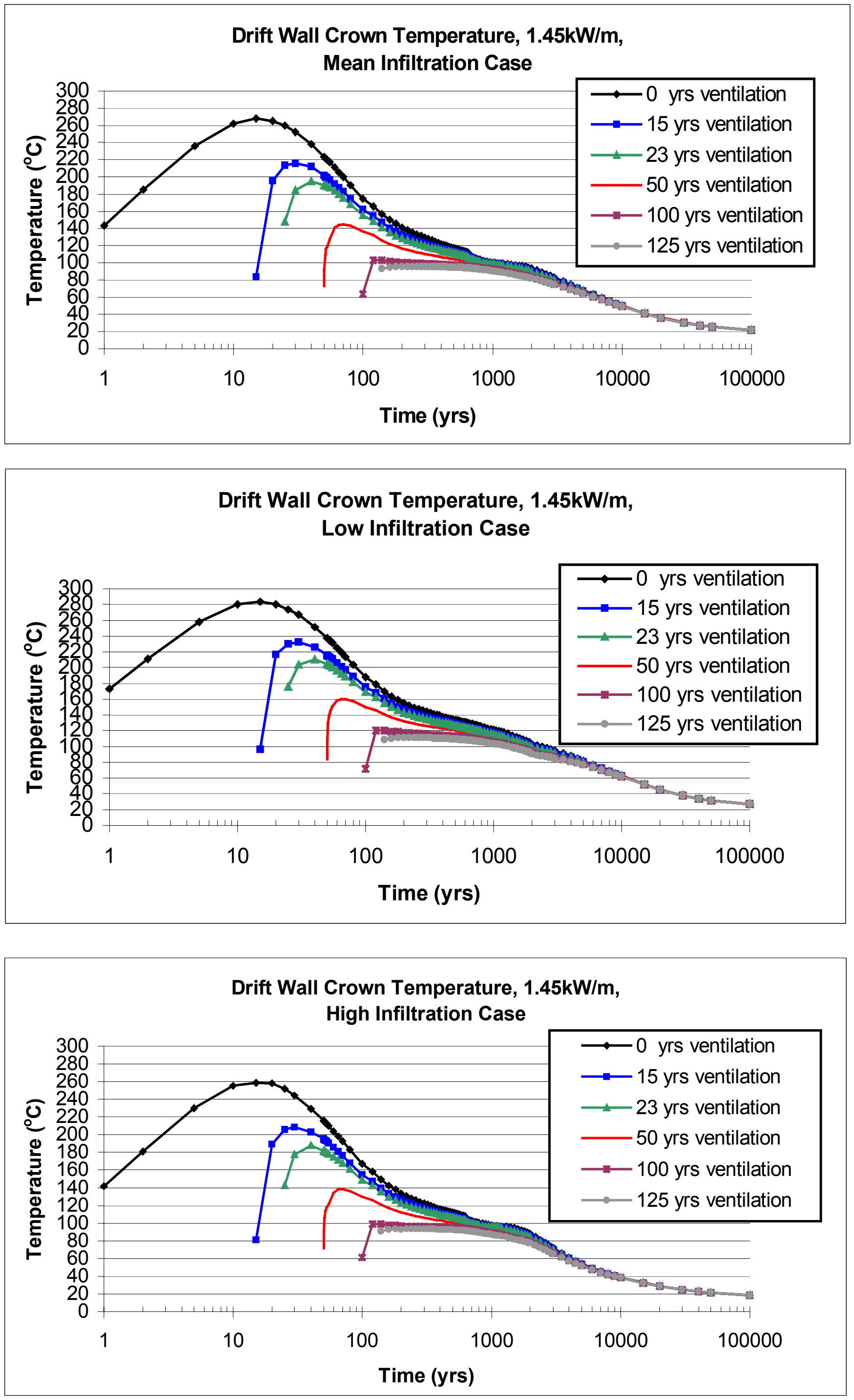

DTN: MO0008SPATHS03.001, file: ventilation_145_*_Tdw.xls

Figure 5.1-4a, b, c (top to bottom) – Comparison of the drift wall temperature time-histories, 1.45 kW/m lineal heat loading with varying ventilation durations.

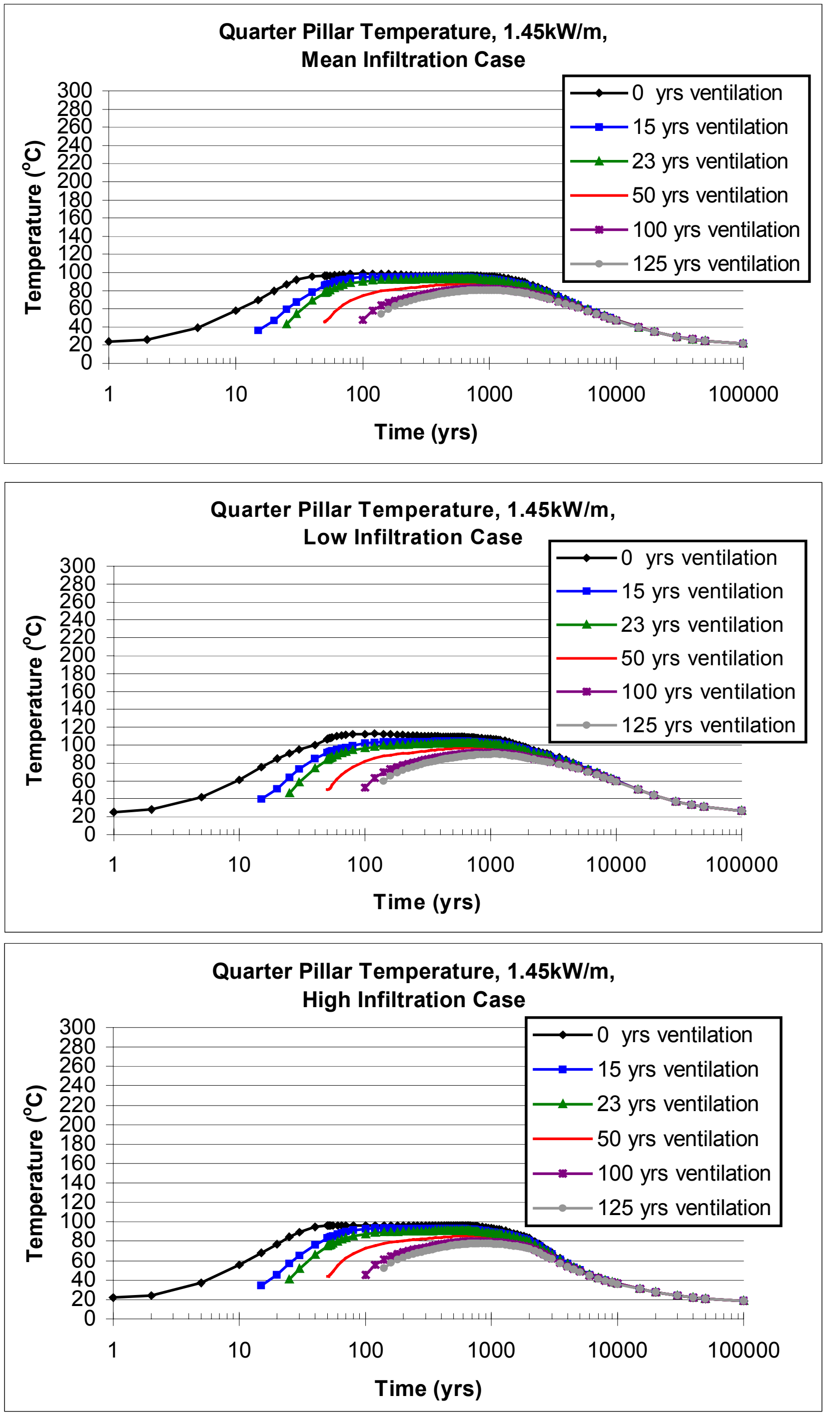

DTN: MO0008SPATHS03.001, file: ventilation_145_*_plotspillar.xls

Figure 5.1-5a, b, c (top to bottom) – Comparison of the quarter pillar temperature time-histories, 1.45 kW/m lineal heat loading with varying ventilation durations.

5.2 SENSITIVITY TO VENTILATION EFFICIENCY

The sensitivity of the SR reference design to preclosure ventilation heat removal performance was examined by modeling three different preclosure cases, one with a 50% ventilation efficiency assumption, one with a 65% ventilation efficiency assumption and one with a 70% ventilation efficiency assumption. Postclosure thermal-hydrologic performance differences are presented in Figures 5.2b and 5.2c.

Figure 5.2-1 shows the decay heat curves used in the SR reference 2-D drift-scale simulations assuming 0% efficient ventilation (no ventilation), 50% efficient ventilation, 65% efficient ventilation, and 70% efficient ventilation. The lineal heat load shown in figure 5.2-1 is derived from information provided in the calculation report "Heat Decay Data and Repository Footprint for Thermal-Hydrologic and Conduction-Only Models for TSPA-SR" (CRWMS M&O 2000c, Figure 1); and DTN: SNT05071897001.004, filenames: "avgdhlw.txt" and "nrctor4pck.txt". This figure provides modified lineal heat loadings during the preclosure ventilation period (specified here as 50 years). After 50 years the ventilation is stopped, the repository is closed, and full power repository heating resumes.

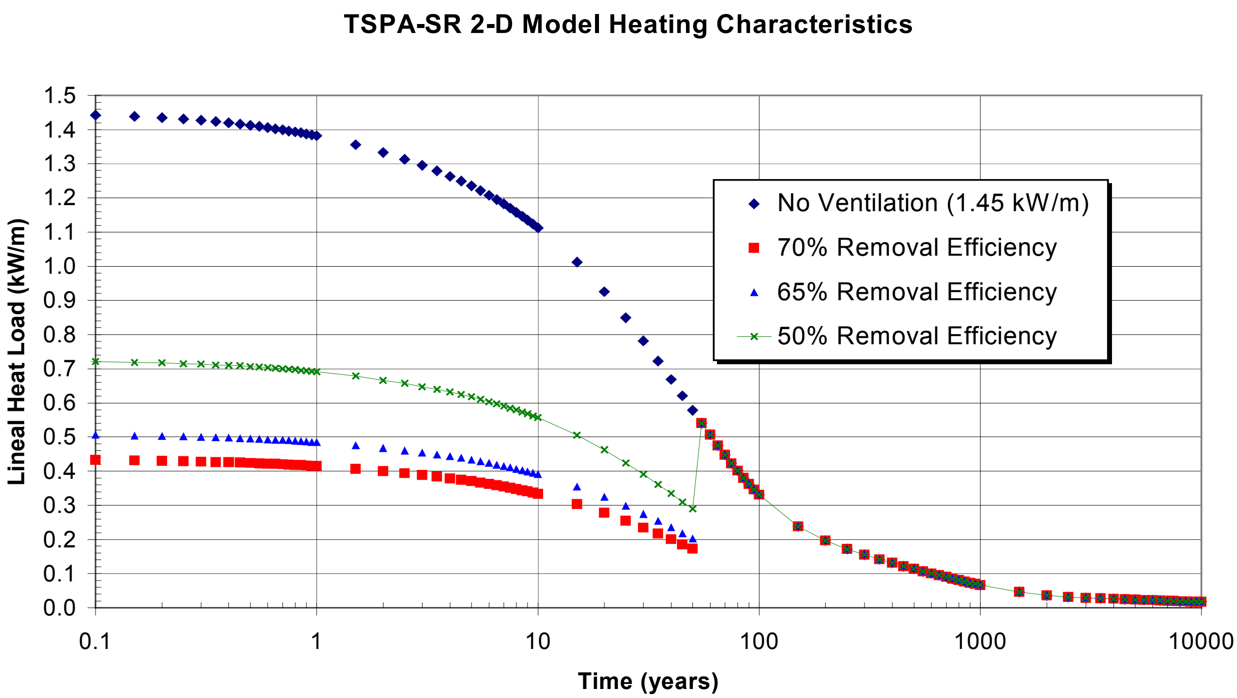

Figure 5.2-1 – Lineal heat loading curves with 0%, 50%, 65% and 70% ventilation heat removal efficiencies shown. 1.45kW/m initial heat output loading curve used in all examples.

Although specifically shown for 50 years, the heat removal curve shown in figure 5.2-1 can be modified for a ventilation process of any specified time duration. The LADS models removed 50%, assuming a flow rate of 10 m^3/s, of the waste package heat over a period of 50 years (CRWMS M&O 1999a, table O-6). The LADS preclosure heat removal efficiency required about 5 to 10 m^3/s of air flow through the repository drifts. For TSPA-SR models, the heat removal efficiency is specified to be approximately 70% heat removed during a 50 year preclosure period, this requires a ventilation rate of approximately 10 to 15 m^3/s per emplacement drift (CRWMS M&O 2000k, section 6.5 and 7.).

Figure 5.2-2 shows the temperature histories for the waste packages for all three of the ventilation efficiencies and for the two different preclosure periods of 26 years and 50 years. The two ventilation durations were examined so that the two extremes of the repository footprint could be examined. When the first emplacement drift (North end of the repository) has been ventilated for 50 years, the repository will be closed and ventilation will cease. For this scenario the last emplacement drift (South end) will experience significantly less ventilation than the emplacement drifts filled first. In this example, the total repository emplacement time is approximated to require 24 years leaving 26 years of ventilation before closure for the Southern emplacement drifts. Figure 5.2-3 shows the waste package relative humidity histories for each of the three ventilation efficiencies during the two preclosure durations of 26 years and 50 years.

Tables 5.2-1 and 5.2-2 are included to simplify comparisons with Table 5.1-1.

Table 5.2-1 - Lineal Heat loadings at select closure periods using a 65% effective heat removal rate during ventilated preclosure. 1.45kW/m initial decay heat curve.

	Years After Initial Emplacement						
	0	15	23	26	50	100	125
Full Lineal Heat Loading (kW/m)	1.450	1.012	0.8797	0.8354	0.5786	0.3313	0.2849
35% of Lineal Heat Loading (kW/m)	0.5076	0.3541	0.3079	0.2924	0.2025	0.1159	0.0997
Total heat delivered during non-ventilated preclosure (GJ/m)	0	561	799	881	1407	2092	2335
Total heat delivered during 65% efficient ventilated preclosure (GJ/m)	0	196	280	308	492	732	817
Years until Vent total heat is within 10% of non-Vent total heat	0	350	800	1000	4000	12,000	15,000

DTN: MO0008SPATHS03.001

Table 5.2-2 - Lineal Heat loadings at select closure periods using a 50% effective heat removal rate during ventilated preclosure. 1.45kW/m initial decay heat curve.

	Years After Initial Emplacement						
	0	15	23	26	50	100	125
Full Lineal Heat Loading (kW/m)	1.450	1.012	0.8797	0.8354	0.5786	0.3313	0.2849
50% of Lineal Heat Loading (kW/m)	0.7252	0.6779	0.4399	0.4177	0.2893	0.1656	0.1424
Total heat delivered during non-ventilated preclosure (GJ/m)	0	561	799	881	1407	2092	2335
Total heat delivered during 50% efficient ventilated preclosure (GJ/m)	0	281	400	441	704	1046	1168
Years until vent total heat is within 10% of non-vent total heat	0	190	430	550	1900	5900	7750

DTN: MO0008SPATHS03.001

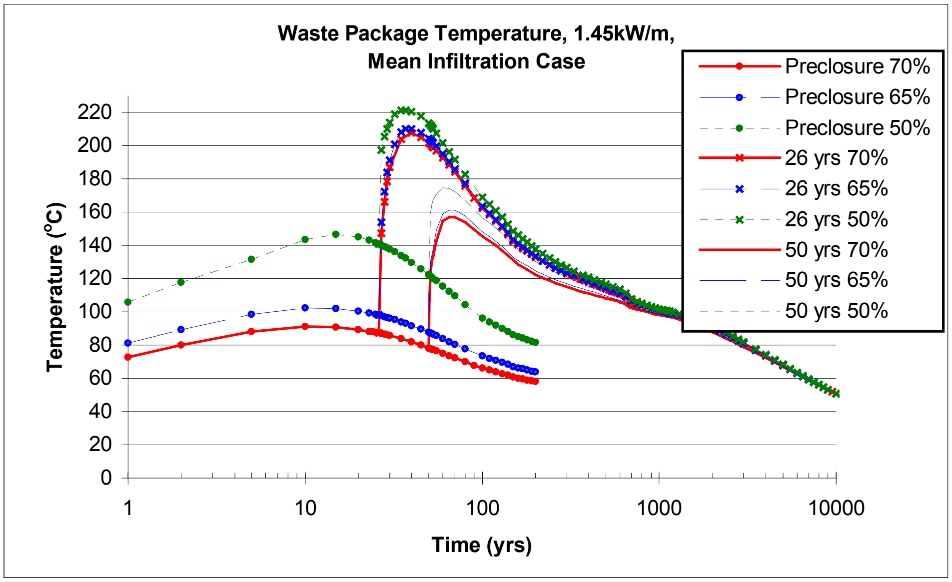

DTN: MO0008SPATHS03.001

Figure 5.2-2 – Comparison of 50%, 65%, and 70% ventilation efficiency cases during preclosure on waste package temperature history. Modified preclosure ventilation effeciency only, 1.45kW/m, mean infiltration, 26 years and 50 years of ventilation.

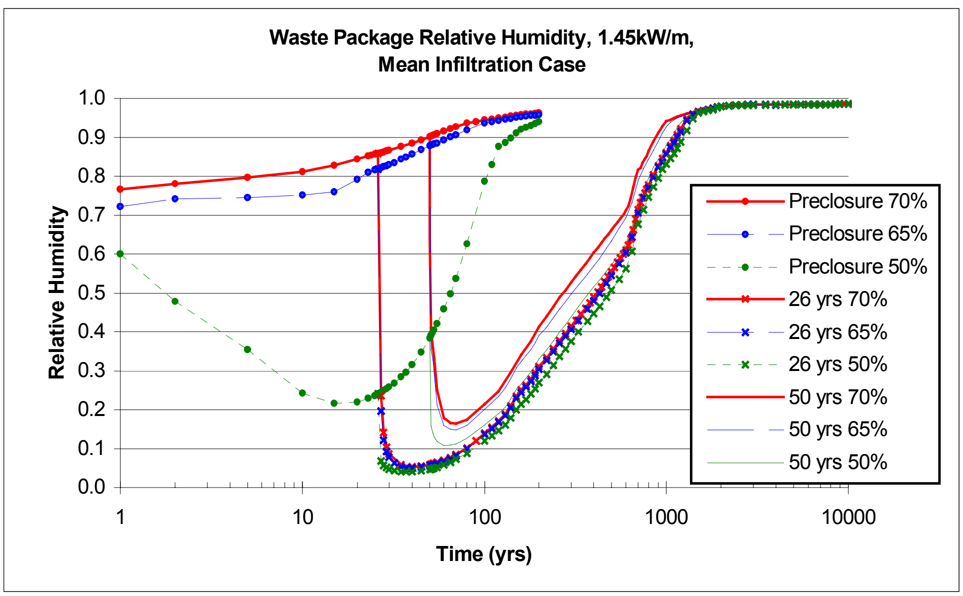

DTN: MO0008SPATHS03.001

Figure 5.2-3 – Comparison of 50%, 65%, and 70% ventilation efficiency cases during preclosure on waste package relative humidity history. Modified preclosure ventilation efficiency only, 1.45kW/m, mean infiltration, 26 years and 50 years of ventilation.

5.3 DESIGN CHARACTERISTIC COMPARISON

In the SR Design Baseline (Stroupe 2000, table on page 2) a range of design parameters was designated. The lineal heat loading for the SR design was specified to be between 0.90kW/m and 1.60kW/m. The ventilated preclosure period was defined to be between 15 and 300 years. Calculations were performed to illustrate the sensitivity of the thermal hydrologic response to the adjustment of these design parameters.

In this set of simulations, the two bounding lineal loadings of 0.90kW/m and 1.60kW/m were examined using the 2D NUFT LDTH models. Also, for this study the lower limit of ventilation duration simulated was 0 years and the upper limit of ventilation duration simulated was 100 years for each of the lineal loading. The 0 years of ventilation scenario was included in the basic set of ventilation scenarios modeled in order to capture the lower limit of the ventilation design possibilities. One of the reasons 100 years of ventilation was used in the basic set of design possibilities versus 300 years was the reduced integrated heat removal effectiveness past 100 years, see Tables 5.2-1 and 5.2-2. So even though ventilating the drifts for more than 100 years is beneficial to thermal-hydrological responses it requires considerably more ventilation in later years in order to achieve appreciable response differences. The use of 100 years of ventilation as the basic set upper threshold was chosen in order to do a more detailed examination in the ventilated preclosure years when the thermal hydrological responses are most sensitive.

Table 5.3-1 summarizes the thermal-hydrologic response of the repository system when using the upper and lower bounds of the ventilation and lineal loading design parameters. Figures 5.3-1, 5.3-2, and 5.3-3 show some of the in-drift temperature responses of the waste package and drift wall. These figures show that in the first 1000 years the system is highly sensitive to both ventilation time and lineal loading. In later years, 1000 years and beyond, the system is still sensitive to lineal loading but is gradually becoming insensitive to ventilation duration differences. Figures 5.3-4a, b, and c show the temperature response at the quarter pillar point (roughly 20 meters from the center of the emplacement drift). The plots of the quarter pillar temperature response show a higher sensitivity to lineal loading than to ventilation. The in-pillar thermal response of the system is sensitive to the ventilation duration parameter during the first 1000 years of emplacement, but is relatively insensitive to the parameter in later years.

Table 5.3-1- Summary of thermal hydrologic performance parameters showing the drift-scale sensitivity to the extremes of the design options ventilation duration and lineal heat loading.

Performance Parameter	Infiltration Flux Case	Years of Ventilation (70% effective heat removal)			
		0		100	
		Lineal Heat Loading		Lineal Heat Loading	
		0.90 kW/m	1.60 kW/m	0.90 kW/m	1.60 kW/m
WP Peak Temperature (Celsius)	Low	197	344	88	140
	Mean	**183**	**329**	**77**	**125**
	High	176	321	75	118
Years Until WP > 115°C	Low	160	1800	0	1100
	Mean	**110**	**680**	**0**	**300**
	High	95	620	0	190
Years Until WP > 80°C	Low	1550	6600	600	6000
	Mean	**740**	**4250**	**0**	**3400**
	High	600	3000	0	2450
DW Peak Temperature (Celsius)	Low	180	311	83	131
	Mean	**164**	**296**	**73**	**116**
	High	157	288	71	110
Years Until DW > 96°C	Low	400	3800	0	2450
	Mean	**170**	**2250**	**0**	**1250**
	High	150	1950	0	950
¼ Pillar Peak Temperature (Celsius)	Low	81	120	67	98
	Mean	**74**	**103**	**60**	**89**
	High	73	100	58	86

DTN: MO0008SPATHS03.001

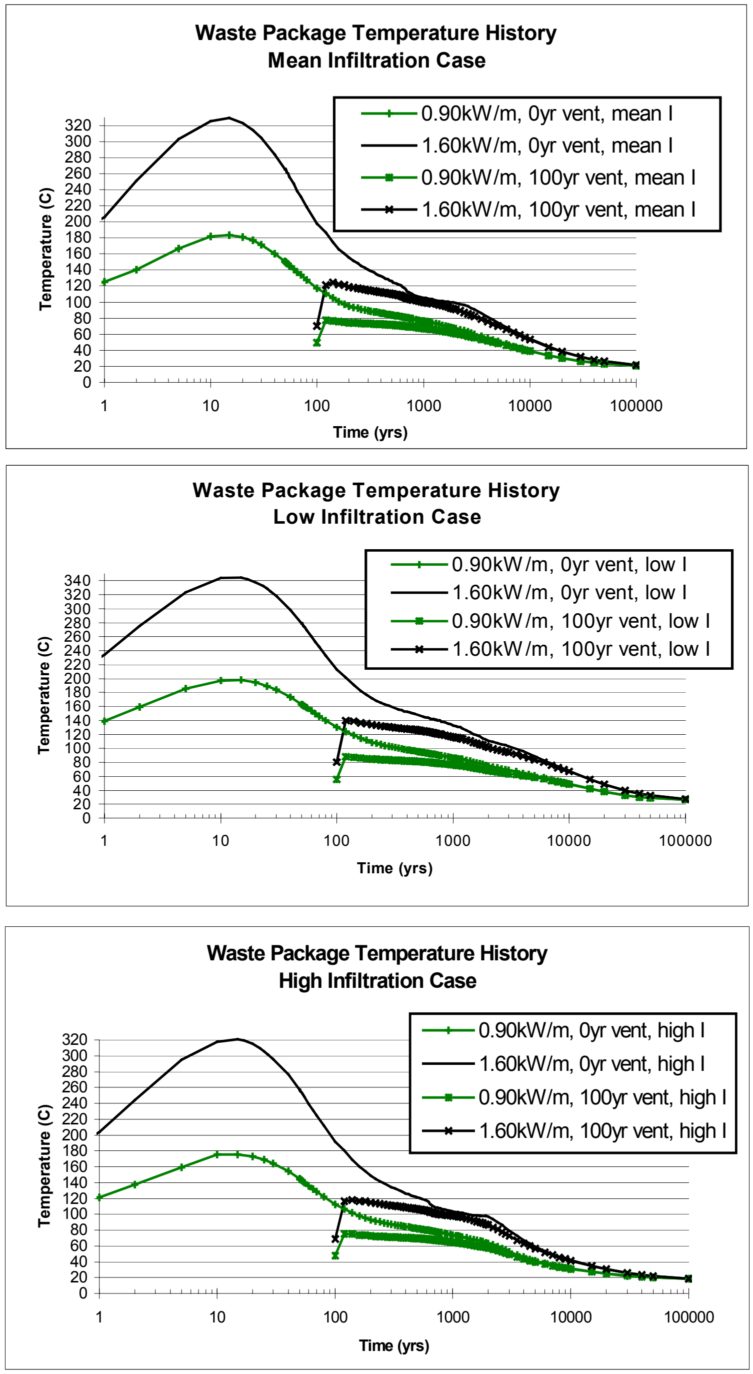

DTN: MO0008SPATHS03.001

Figure 5.3-1a, b, and c (top to bottom) – Waste package temperature response curves illustrating the sensitivity of these thermal hydrologic dependent parameters with respect to ventilation time and lineal heat loading.

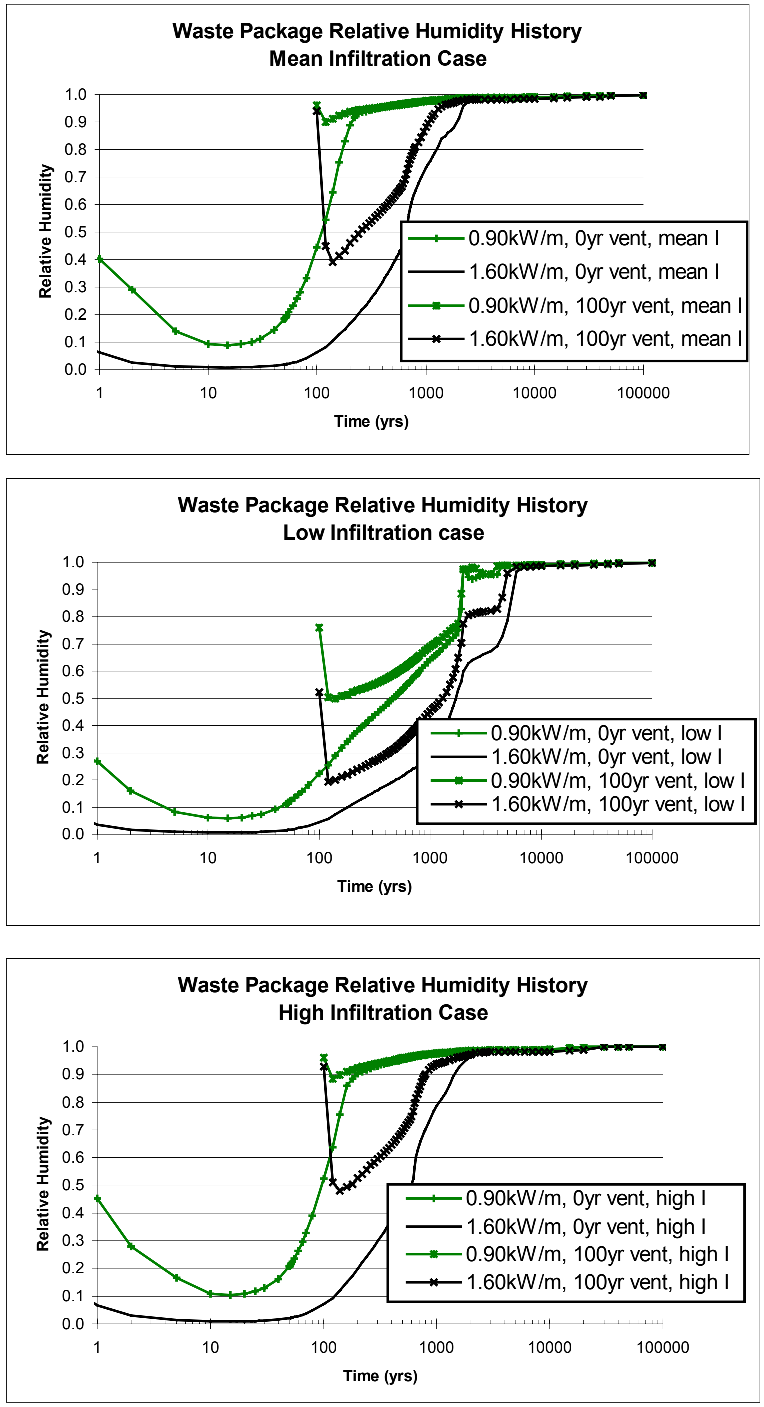

DTN: MO0008SPATHS03.001

Figure 5.3-2 a, b, c (top to bottom) – Waste package relative humidity response curves illustrating the sensitivity of these thermal hydrologic dependent parameters with respect to ventilation time and lineal heat loading.

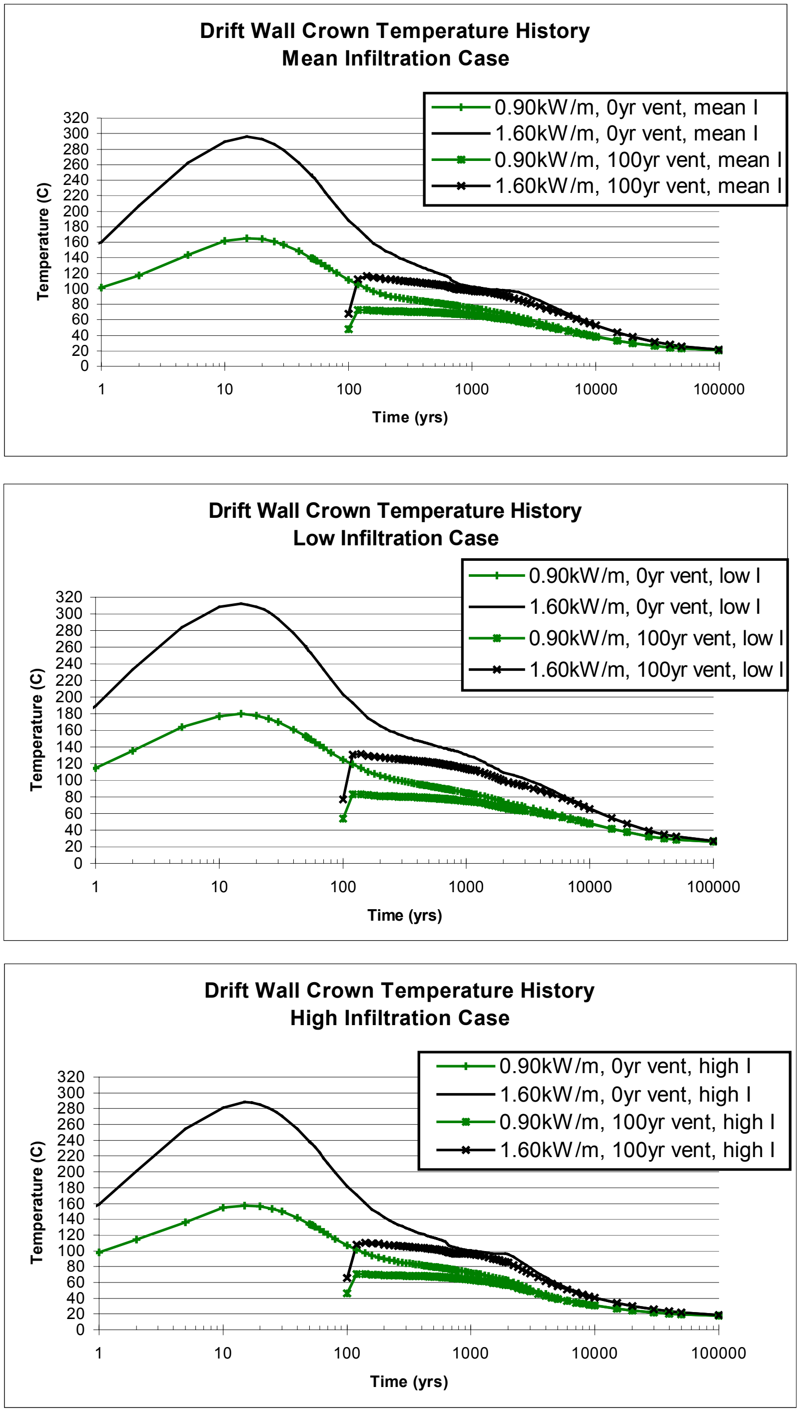

DTN: MO0008SPATHS03.001

Figure 5.3-3a, b, c (top to bottom) – Drift wall temperature response range for the design parameter range of 0.90kW/m to 1.60kW/m and 0 years of ventilation to 100 years of ventilation.

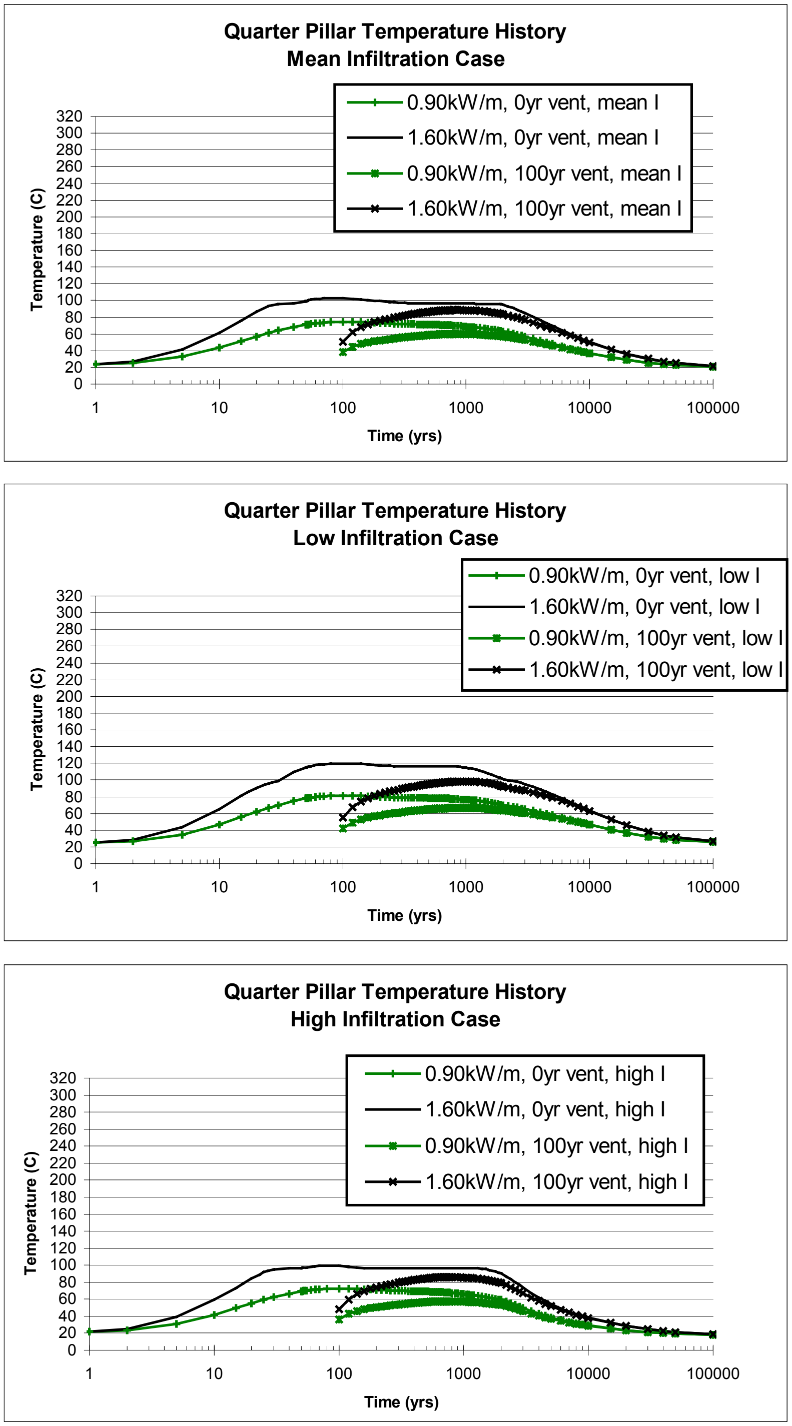

DTN: MO0008SPATHS03.001

Figure 5.3-4a, b, c (top to bottom) – Quarter pillar temperature response range for the design parameter range of 0.90kW/m to 1.60kW/m and 0 years of ventilation to 100 years of ventilation.

5.4 SENSITIVITY TO INFILTRATION

For this sensitivity analysis the bounding infiltration rates and associated property sets were applied to the SR reference case model. The TSPA-SR reference case model has an initial lineal heat loading of 1.45 kW/m, a 50 year ventilated preclosure period, and 70% heat removal efficiency during the ventilation period (CRWMS M&O 2000k, section 7.; Stroupe 2000, table on page 2).

The TSPA-SR reference case model uses an infiltration rate referred to as the mean climate infiltration rate. The mean climate infiltration rate varies spatially over the surface of the repository site. At the location modeled in this study the surface infiltration rates is 10.1 mm/yr during the first 600 years of emplacement (present day climate), 28.9 mm/yr from year 600 to year 2000 (monsoonal climate), and 42 mm/yr from year 2000 on (glacial transition climate).

The mean infiltration rate case has an upper and lower bound that will simply be referred to as the high and low infiltration rate cases. The low infiltration case assumes that the surface infiltration rate is 0.0 mm/yr during the first 600 years of emplacement (present day climate), 10.1 mm/yr from year 600 to year 2000 (monsoonal climate), and 1.99 mm/yr from year 2000 on (glacial transition climate). And, the high infiltration case assumes that the surface infiltration rates is 24.3 mm/yr during the first 600 years of emplacement (present day climate), 47.6 mm/yr from year 600 to year 2000 (monsoonal climate), and 82.0 mm/yr from year 2000 on (glacial transition climate). All infiltration rate cases have a set of rock hydrologic properties that are calibrated specifically for the applied infiltration rate of that case. A description of how the low, mean and high infiltration rates were generated is provided in the *Simulation of Net Infiltration for Modern and Potential Future Climates* AMR (USGS 2000, section 6.). The development of the hydrologic property sets is described in the *Calibrated Properties Model* AMR (CRWMS M&O 2000b, sections 6.1 & 6.2).

The three infiltration conditions are intended to capture the full range of infiltration rates expected at the Yucca Mountain Site. The statistical weightings in the TSPA-SR for the low, mean, and high infiltration cases are 0.17, 0.48, and 0.35, respectively (CRWMS M&O 2000a, section 6.3). In other words, for a given location there is a 17% chance that the low infiltration case will be selected, a 48% chance that the mean infiltration case will be selected, and a 35% chance that the high infiltration case will be selected in each of the TSPA-SR realizations.

Table 5.4-1 summarizes some of the performance parameters of interest. The mean infiltration rate property set (48% chance of TSPA model selection) and the high infiltration rate property set (35% chance of TSPA model selection) have relatively similar thermal hydrologic responses, regardless of initial lineal heat loading. The low infiltration rate property set (17% chance of TSPA model selection) predicts notably different thermal hydrologic responses then the mean and high infiltration rate property sets. The low infiltration property set cases predicted “hotter” thermal hydrologic responses than the mean and high infiltration property set cases at all initial lineal heat loadings. The figures provided in this section (Figures 5.4-1 through 5.4-4) further illustrate the short term and long term sensitivity of the thermal hydrologic response predictions to the low infiltration rate property set.

Table 5.4-1 - Summary of thermal hydrologic performance parameters showing the drift-scale sensitivity to the surface infiltration rate assumptions.

Performance Parameter	Initial Lineal Loading[a] (kW/m)	Surface Infiltration Flux Case		
		Low	**Mean**	**High**
WP Peak Temperature (Celsius)	0.90 1.25 **1.45**	114 151 172	99 136 **157**	97 129 151
Years Until WP > 115°C	0.90 1.25 **1.45**	0 320 900	0 150 **300**	0 125 240
Years Until WP > 80°C	0.90 1.25 **1.45**	950 3250 5000	250 1850 **2900**	200 1500 2250
DW Peak Temperature (Celsius)	0.90 1.25 **1.45**	106 140 160	92 125 **145**	90 119 138
Years Until DW > 96°C	0.90 1.25 **1.45**	140 1275 2000	0 320 **975**	0 240 800
¼ Pillar Peak Temperature (Celsius)	0.90 1.25 **1.45**	70 87 97	63 79 **88**	61 77 85

DTN: MO0008SPATHS03.001

NOTE: [a]The initial lineal heat loadings (kW/m) are achieved by increasing the waste package to waste package spacing only, the drift to drift spacing is held constant at 81 meters.

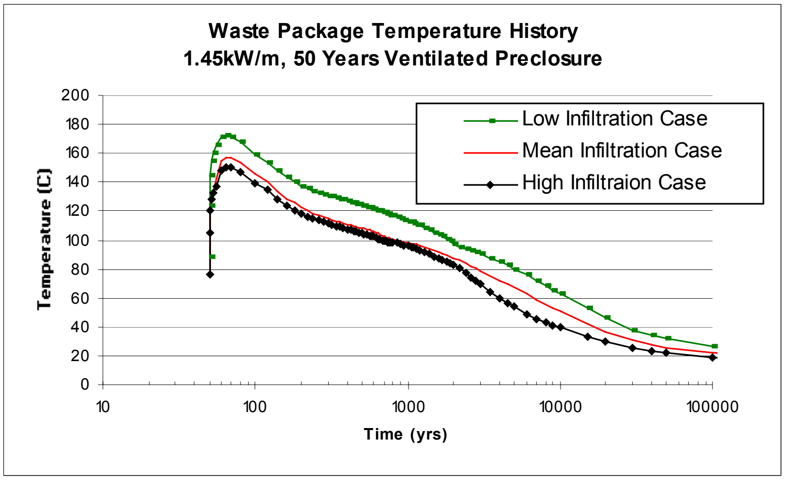

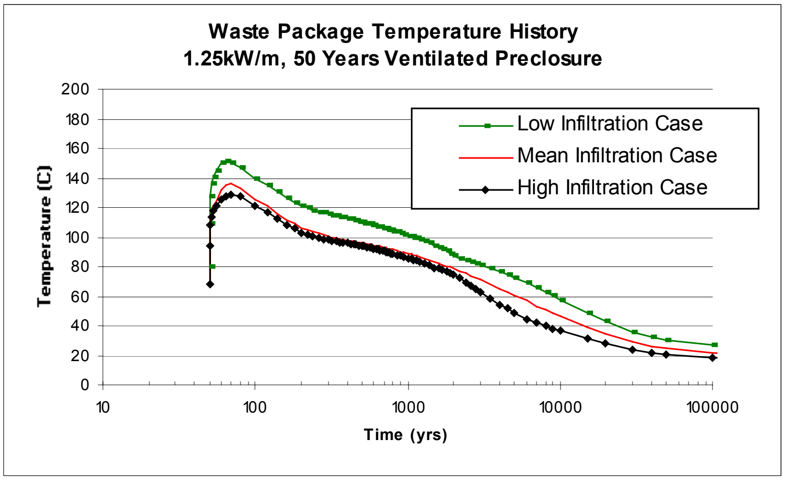

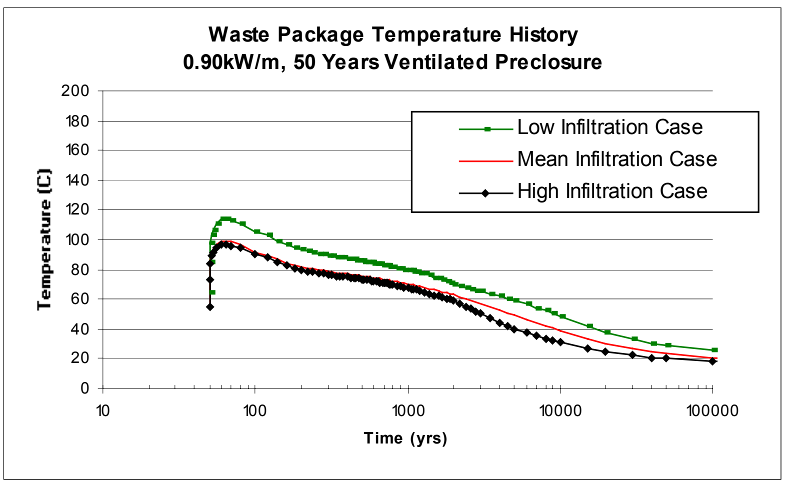

DTN: MO0008SPATHS03.001

Figure 5.4-1a, b, c (top to bottom) – Waste package temperature sensitivity to infiltration rate and initial lineal heat load.

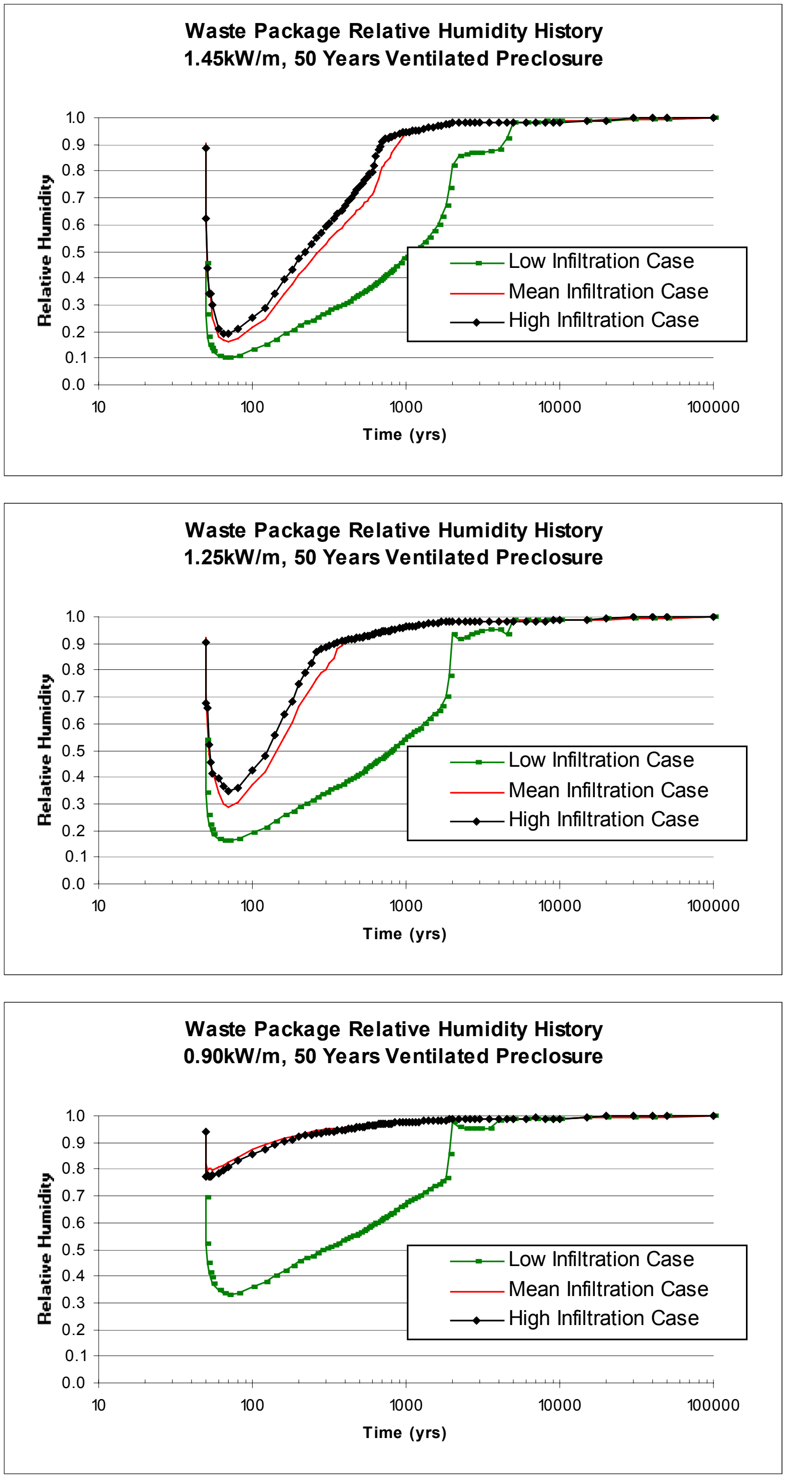

DTN: MO0008SPATHS03.001

Figure 5.4-2a, b, c (top to bottom) – Waste package relative humidity sensitivity to infiltration rate and initial lineal heat load.

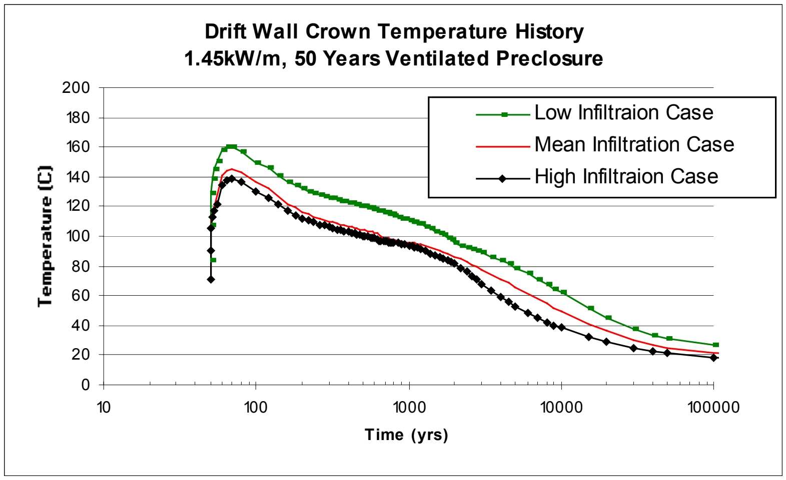

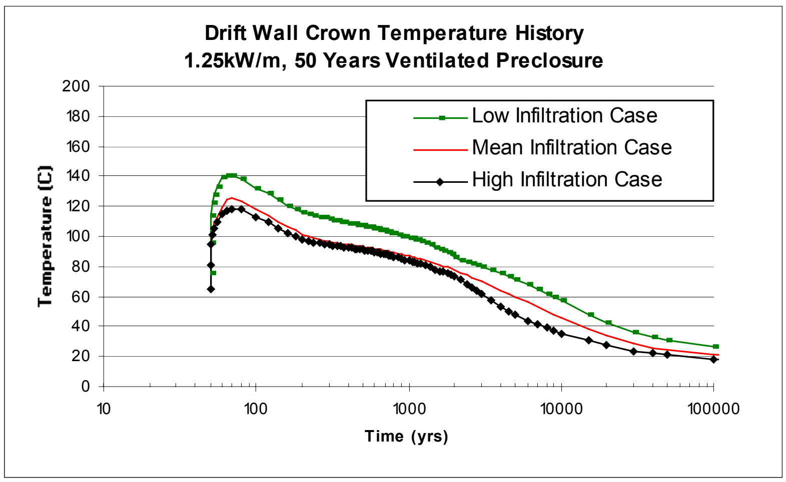

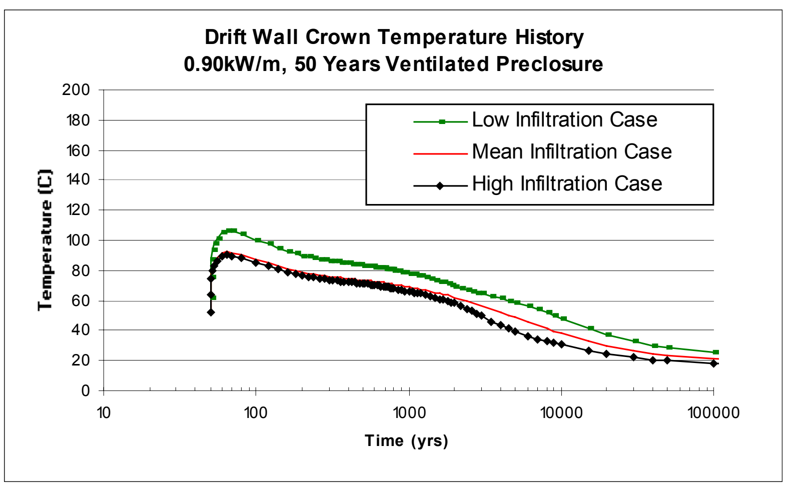

DTN: MO0008SPATHS03.001

Figure 5.4-3a, b, c (top to bottom) – Drift wall temperature sensitivity to infiltration rate and initial lineal heat load.

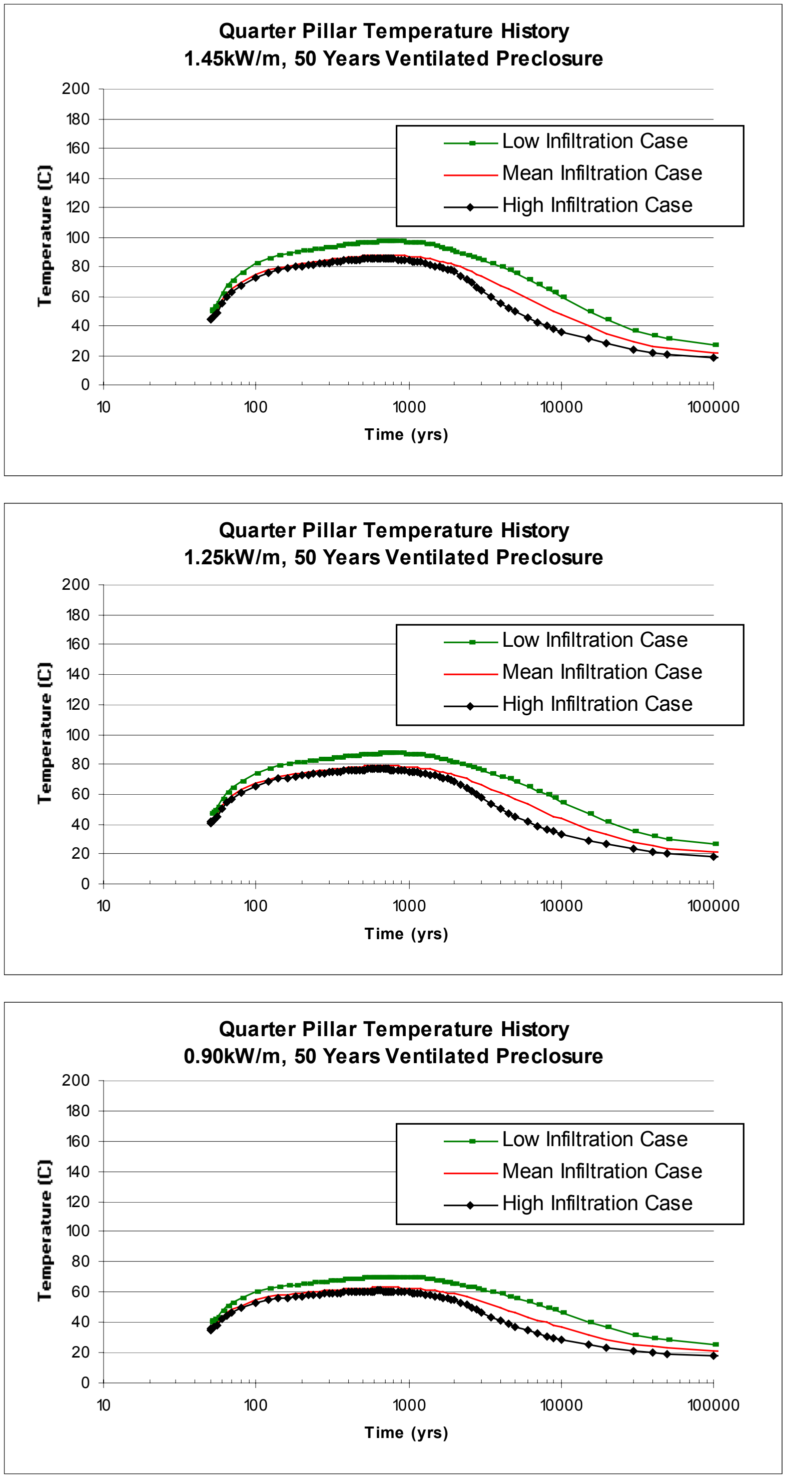

DTN: MO0008SPATHS03.001

Figure 5.4-4a, b, c (top to bottom) – Quarter pillar temperature sensitivity to infiltration rate and initial lineal heat load.

5.5 SENSITIVITY TO INVERT THERMAL CONDUCTIVITY

For this analysis three comparative simulations based on the SR Reference design without backfill were used (CRWMS 2000f, section 6.3). The only difference between the comparative simulations was the adjustment of the thermal conductivity of the invert elements from 0.15 W/m-K to 0.66 W/m-K, including the SR reference case which used multiple conductivity values. The invert modeled for the SR reference case used a two layer system where the lower layer was assumed to be ballast material only with a thermal conductivity of 0.15 W/m-K, and the top layer was assumed to have steel inserts that raised the thermal conductivity to 1.52 W/m-K.

As can be seen in Figure 5.5-1 and 5.5-2 the waste package and invert temperatures are essentially insensitive over the range of thermal conductivities value examined. It should be noted that there are two key details of the repository design which lend to this relative insensitivity. First, the thickest portion of the invert is only 0.606 meters (CRWMS M&O 2000i, figure 2), incresing the thickness of the invert would increase the in-drift thermal hydrologic response sensitivity to the invert thermal conductivity. Second, without a low conductivity backfill to focus the waste decay heat toward the invert elements, the thermal power will radiate from the waste packages to the drift walls rather than conduct through the invert. This sensitivity parameter should be reevaluated if backfill is introduced into the SR reference design.

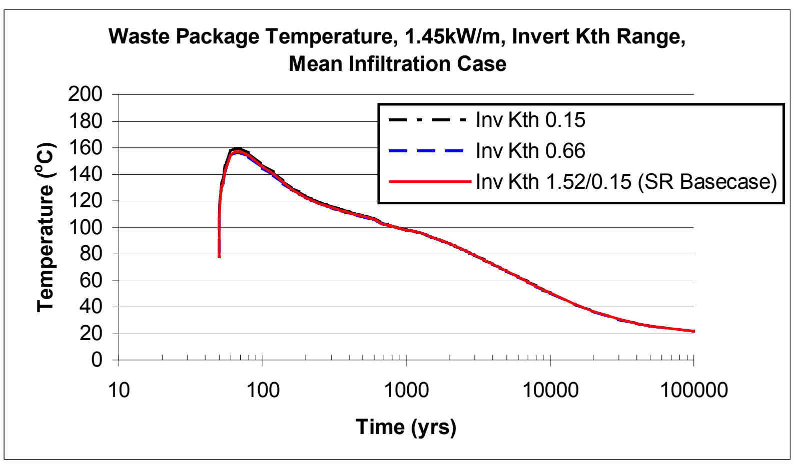

DTN: MO0008SPATHS03.001

Figure 5.5-1 – Waste package temperature sensitivity to invert thermal conductivity. Non-backfilled, 2D, 1.45kW/m, 50 year preclosure, drift-scale simulation results.

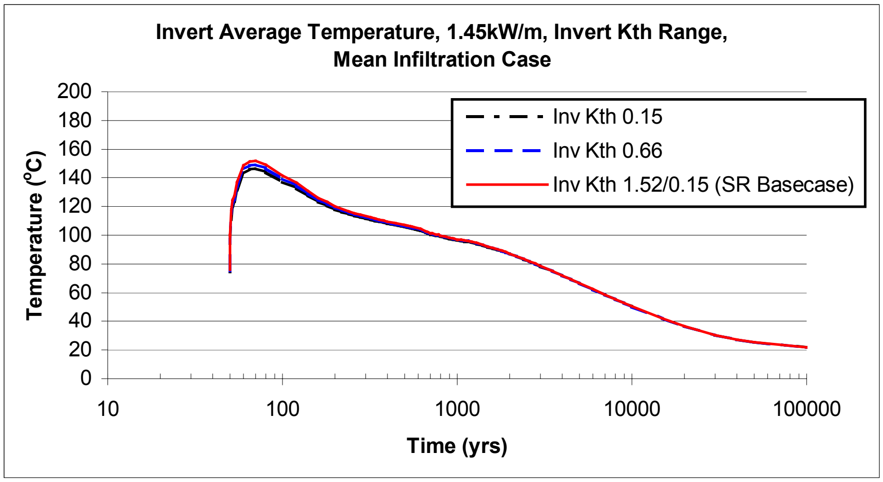

DTN: MO0008SPATHS03.001

Figure 5.5-2 – Invert temperature sensitivity to variations in invert thermal conductivity. Non-backfilled, 2D, 1.45 kW/m, 50 year preclosure, drift-scale simulation results.

5.6 COMPARISON OF BACKFILLED VERSUS NON-BACKFILLED DRIFTS

A comparison of the SR Repository Design (CRWMS M&O 2000d) with and without backfill will be performed in this section. The in-drift components of the SR design are thermally sensitive to the presence of backfill and the thermal conductivity of the backfill used, 0.33 W/m-K for this comparison. In contrast, this portion of the study will show that the sensitivity of the repository host rock to the presence of backfill or not is quite low and limited in extent. For the backfilled model presented in this section the backfill thermal-hydrologic properties, physical dimensions and characteristics that are described in the ICN 00 of the *Multiscale Thermohydrologic Model* AMR (CRWMS M&O 2000e, section 6.3) is used in the LDTH model that is used throughout this calculation report.

Figure 5.6-1 shows the temperature history of the drift wall crown (highest point in drift) model element. Figure 5.6-1 shows that the backfilled and non-backfilled models have a predicted drift wall crown temperature difference of 20 °C at the peak temperature time, between 65 and 75 years after first emplacement. Two hundred years after first emplacement the crown drift wall temperature difference is down to 10 °C. After 600 years of emplacement the drift wall temperature difference between the two scenarios is less than 5 °C. And, at approximately 950 years of emplacement the drift wall temperatures predicted for the two designs converge and are essentially the same for the rest of the simulated period.

Figure 5.6-2 shows the predicted behavior for liquid saturation at the drift wall crown in both the backfilled and non-backfilled designs. Both saturation histories follow a similar path with the only notable difference being that of the time of the beginning of resaturation. The backfilled design starts to resaturate around the 500th year of emplacement while the non-backfilled design resaturates around the 700th year. A similar trend can be observed in the side drift wall to mid-pillar profile plots contained in Figures 5.6-7a through 5.6-7f. Another parameter of interest to geochemical models, Figure 5.6-3 shows that the relative humidity history at the side drift wall in both models. Minor differences are observed in early emplacement years and those differences dissapate in a relatively short period.

Figure 5.6-4 shows the temperature history for a point in the host rock only 4.15 meters from the side drift wall. It is observed from the near field plots contained in this section that after 4 to 6 meters into the host rock the thermal hydrologic differences observed between the backfilled and non-backfilled designs diminish and are nearly undetectable. The "near-field", host rock, thermal hydrologic response differences that are observed can primarily be attributed to the difference in heat capacity of air versus the heat capacity of the backfill material. Since more energy goes into heating the backfill, less energy is available to transfer into the host rock.

Figures 5.6-5 and 5.6-6 show the in-drift differences between the backfilled and non-backfilled designs, both waste package temperature and relative humidity are presented. During the first 1000 years the in-drift differences between these two designs are quite significant, containing both positive and negative performance impacts. However, in a general observation, after 1000 years the in-drift differences between the two designs converge and the differences become insignificant shortly thereafter.

The differences in the host rock between these two designs are negligible after only a few meters. Figures 5.6-7a through 5.6-7f illustrate the relatively small differences between the temperature and saturation profiles predicted between the side drift wall and the midpillar.

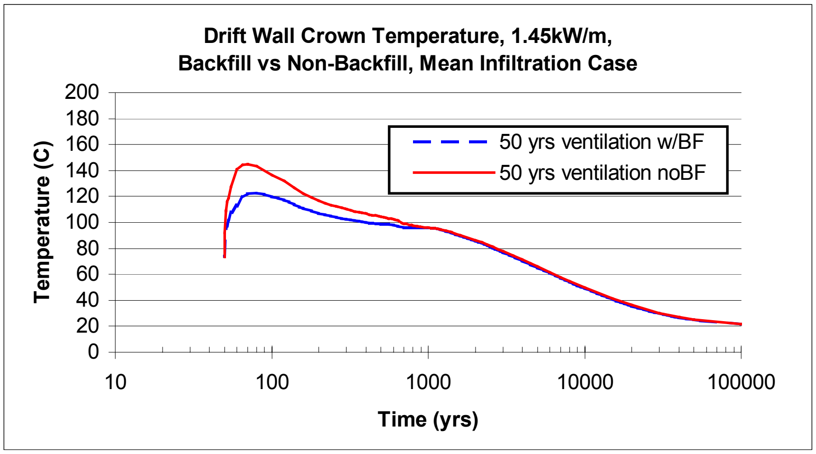

DTN: MO0008SPATHS03.001

Figure 5.6-1 – Comparison of Drift Wall Crown (highest point) temperatures. Backfilled versus Non-backfilled layouts, 1.45kW/m, 50 years ventilation.

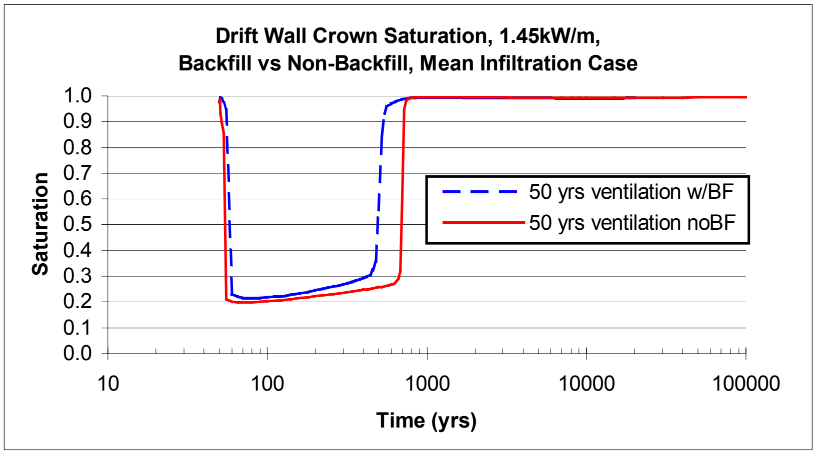

DTN: MO0008SPATHS03.001

Figure 5.6-2 – Comparison of Liquid Saturation values at the drift wall crown. Backfilled versus Non-backfilled layouts, 1.45kW/m, 50 years ventilation.

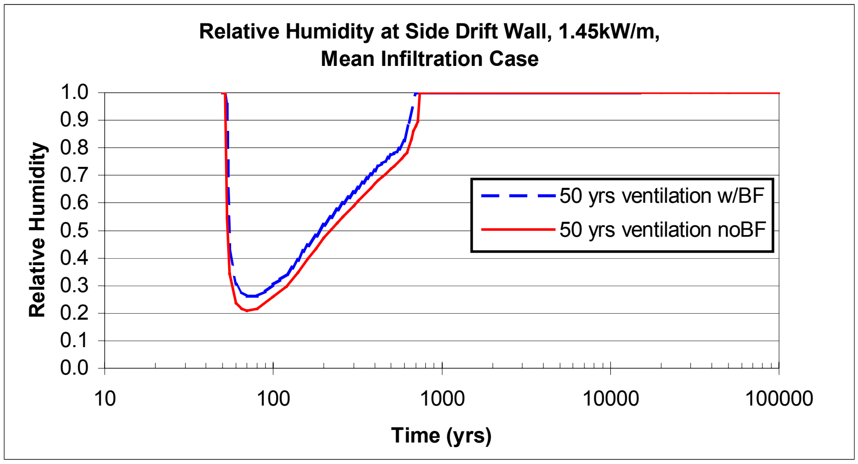

DTN: MO0008SPATHS03.001

Figure 5.6-3 – Comparison of emplacement drift's side wall Relative Humidity. Backfilled versus Non-backfilled layouts, 1.45kW/m, 50 years ventilation.

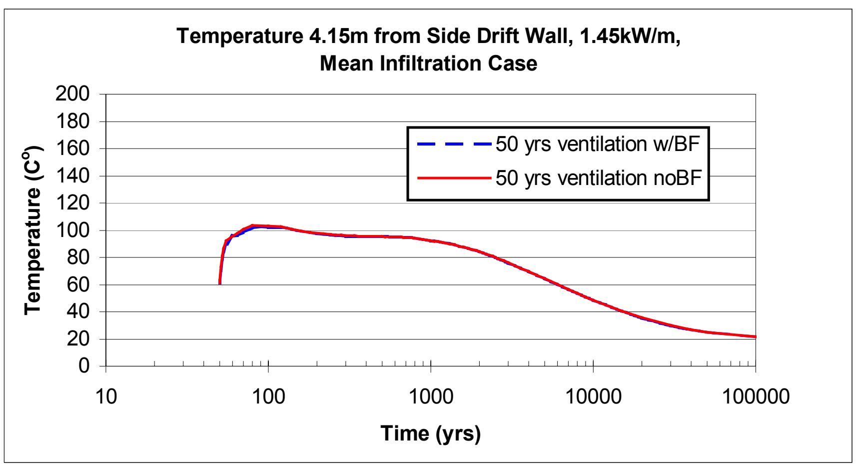

DTN: MO0008SPATHS03.001

Figure 5.6-4 – Comparison of temperature at a point 4.15 meters from the emplacement drift wall. Backfilled versus Non-backfilled layouts, 1.45kW/m, 50 years ventilation.

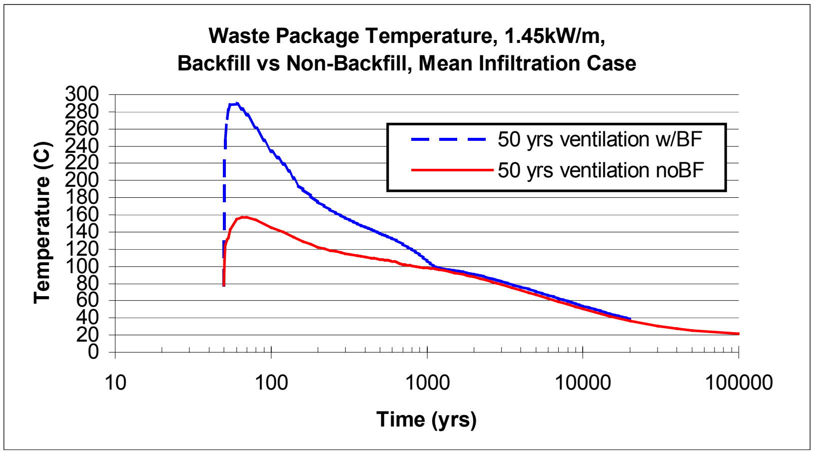

DTN: MO0008SPATHS03.001

Figure 5.6-5 – Comparison of Waste Package temperatures. Backfilled versus Non-backfilled layouts, 1.45kW/m, 50 years ventilation.

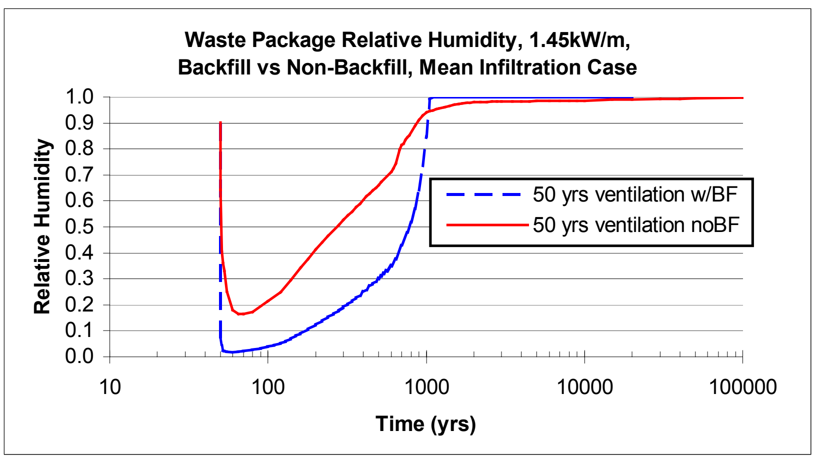

DTN: MO0008SPATHS03.001

Figure 5.6-6 – Comparison of Waste Package relative humidities. Backfilled versus Non-backfilled layouts, 1.45kW/m, 50 years ventilation.

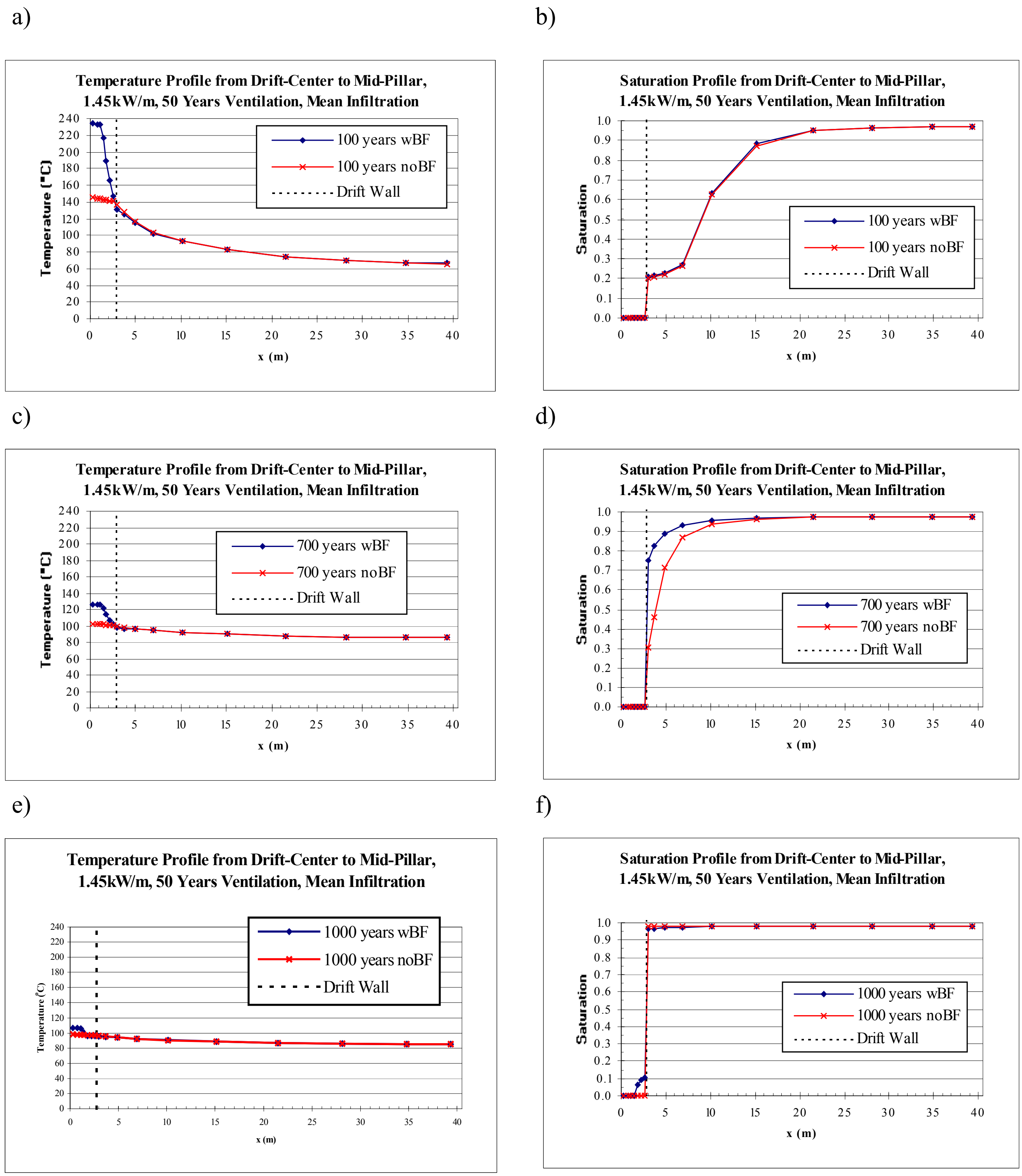

DTN: MO0008SPATHS03.001

Figure 5.6-7a, b, c, d, e, f – drift wall to mid-pillar Temperature and Saturation profiles for 100 years, 700 years, and 1000 years after emplacement. Backfilled versus Non-backfilled layouts, 1.45 kW/m, 50 years ventilation.

5.7 SENSITIVITY TO AREAL MASS LOADING

Two methods of adjusting the areal mass loading in the repository will be investigated in this section. Section 5.7.1 will adjust the actual lineal power levels through waste package to waste package spacing, and section 5.7.2 will effectively adjust to spatially equivalent loadings through drift-to-drift spacing adjustments. Since the LDTH models used are 2D, the waste package to waste package spacing adjustment is accomplished by decreasing the power input to the model while holding the drift-to-drift distance constant. The drift-to-drift spacing is a physical parameter in the 2D models so it was adjusted directly.

5.7.1 Adjustment of Areal Mass Loading by In-Drift Package Spacing

The SR reference layout design calls for a 50 year ventilated preclosure period, a lineal loading of 1.45kW/m, and a constant drift to drift spacing of 81 meters (Stroupe 2000, page 2; CRWMS M&O 1999a, Table O-6). The ventilation is assumed to remove 70% of the thermal power emitted during the preclosure ventilation period (assumption 3.4). While holding the drift to drift distance contant the lineal loading for this design can be adjusted through waste package in-drift spacing. The lineal loading of the model was adjusted through the range of 0.90kW/m to 1.60kW/m by increasing or decreasing the power output to reflect the increase or decrease in waste package to waste package spacing, while holding the drift to drift spacing constant at 81 meters.

The adjustment to the power output is done by applying a simple scale factor to the original model, in this case 1.45kW/m. A scaling factor of 0.621 is applied to the power curve in order to simulate a 0.90kW/m loading (0.90/1.45 = 0.621). The scaling factors applied to the power curve in order to achieve loadings of 1.25kW/m and 1.60kW/m were 0.862 and 1.103, respectively.

Table 5.7-1 summarizes the thermal parameter results for the four lineal loadings examined. Results from simulations with all three infiltration property sets are included for completeness. The Figures 5.7-1 through 5.7-4 show some of the thermal-hydrological response histories for the waste package, drift wall and quarter pillar.

Table 5.7-1- Summary of drift-scale thermal hydrologic parameters for analysis of the waste package spacing sensitivity.

Performance Parameter	Infiltration Flux case	Lineal Heat Loading			
		1.60 kW/m	**1.45 kW/m**	**1.25 kW/m**	**0.90 kW/m**
WP Peak Temperature (Celsius)	Low	188	172	151	114
	Mean	174	**157**	136	99
	High	167	151	129	97
Years Until WP > 115°C	Low	1400	900	320	0
	Mean	620	**300**	150	0
	High	480	240	125	0
Years Until WP > 80°C	Low	6100	5000	3250	950
	Mean	3600	**2900**	1850	250
	High	2700	2250	1500	200
DW Peak Temperature (Celsius)	Low	175	160	140	106
	Mean	161	**145**	125	92
	High	153	138	119	90
Years Until DW > 96°C	Low	3000	2000	1250	140
	Mean	1650	**1000**	325	0
	High	1400	850	240	0
¼ Pillar Peak Temperature (Celsius)	Low	104	97	87	70
	Mean	95	**88**	79	63
	High	92	86	77	61

DTN: MO0008SPATHS03.001

NOTE: Initial Lineal Heat loading adjusted by increasing or decreasing the waste package to waste package spacing only, the drift to drift spacing is held constant at 81 meters.

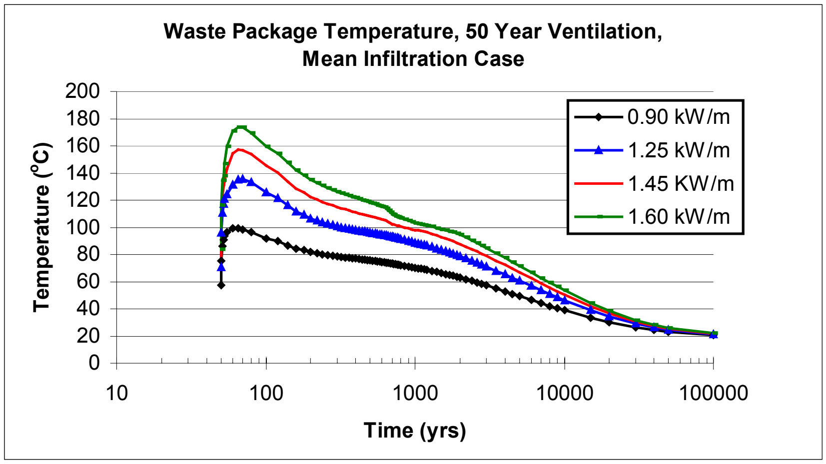

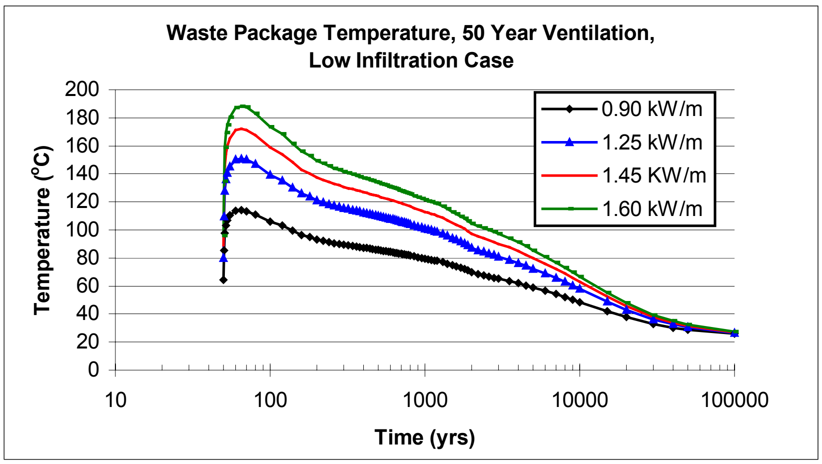

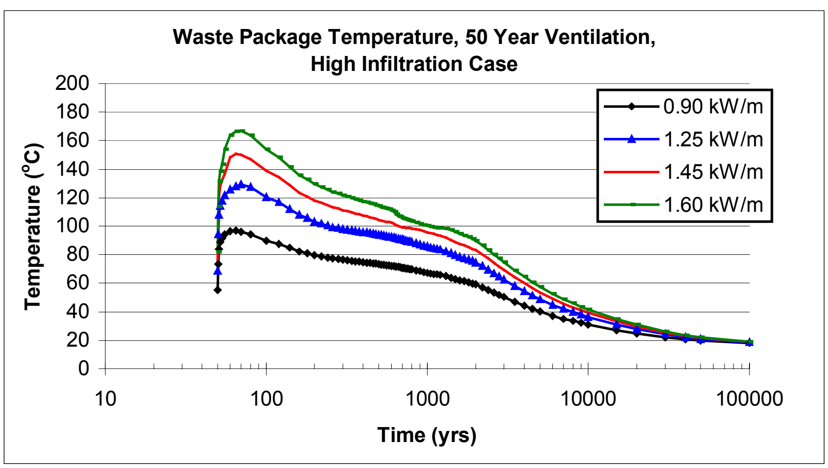

DTN: MO0008SPATHS03.001

Figure 5.7-1a, b, c (top to bottom) – Waste Package Temperature comparisons through the range of lineal heat loads. Thermal-hydrologic, 2D, drift-scale model. Lineal heat loading achieved by adjusting the waste package to waste package spacing while keeping drift to drift spacing constant at 81 meters.

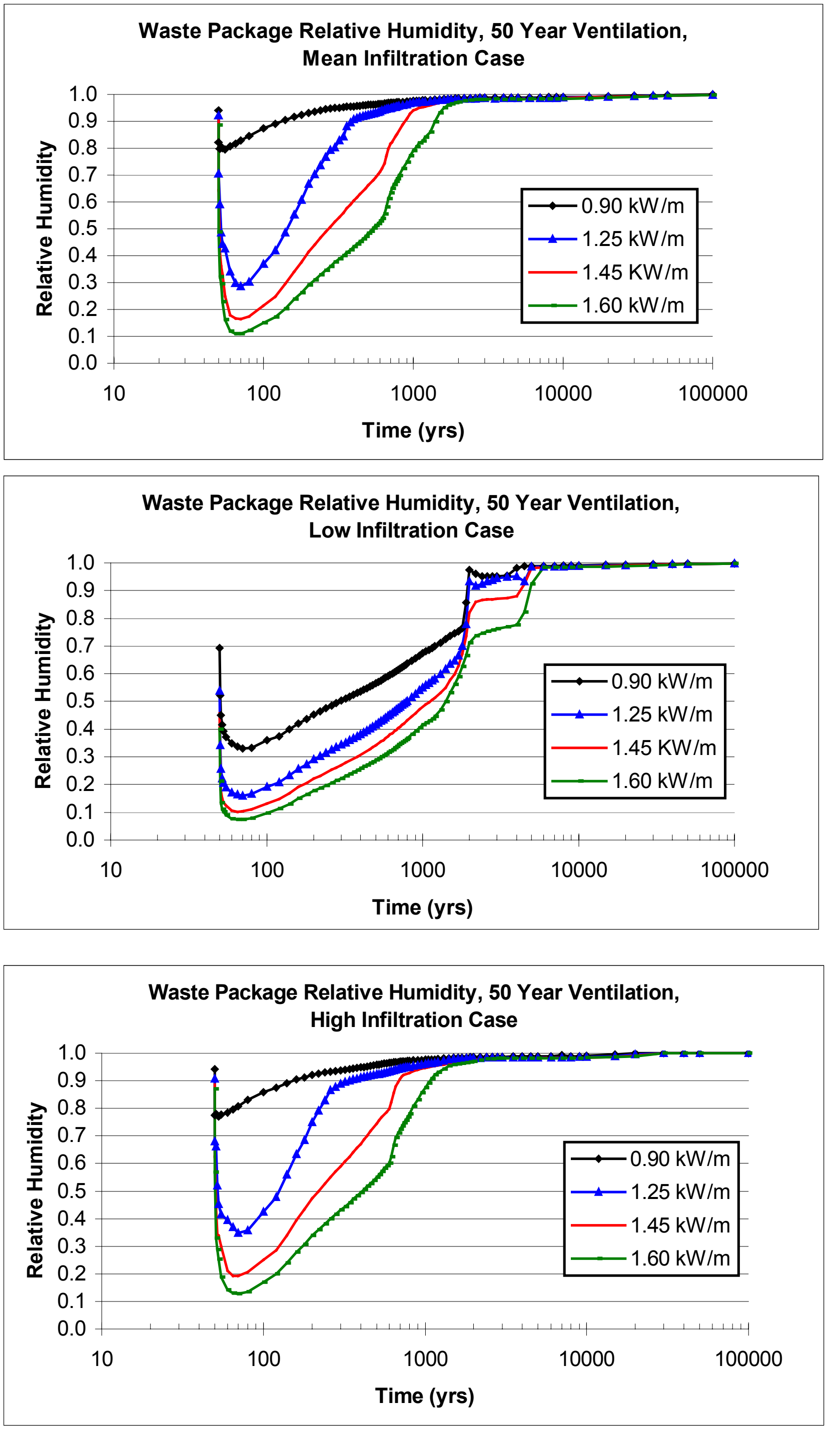

DTN: MO0008SPATHS03.001

Figure 5.7-2a, b, c (top to bottom) – Waste Package Relative Humidity comparisons through the range of lineal heat loadings. Thermal-hydrologic, 2D drift-scale model. Lineal heat loading achieved by adjusting the waste package to waste package spacing, the drift to drift spacing was held constant at 81 meters.

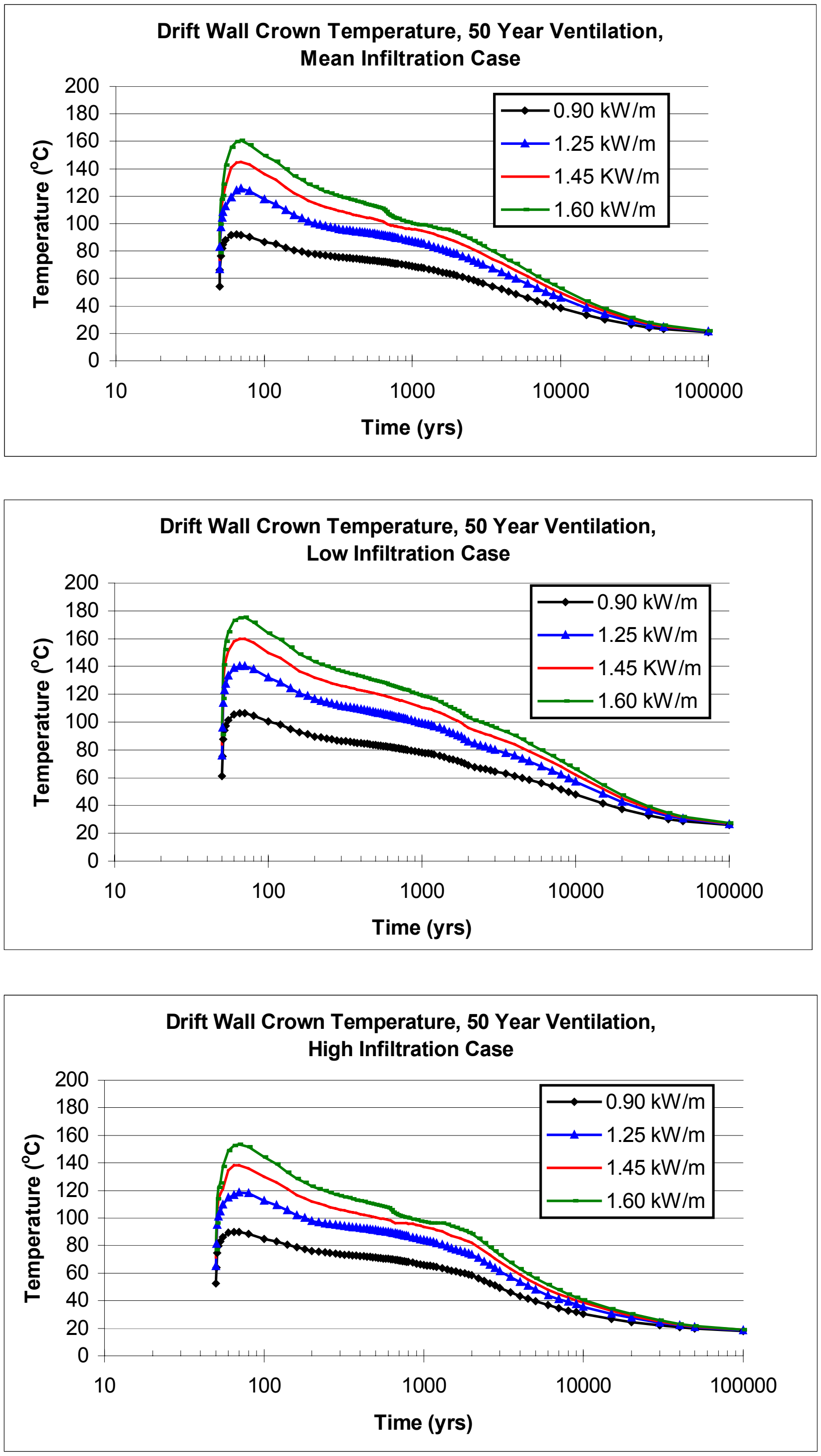

DTN: MO0008SPATHS03.001

Figure 5.7-3a, b, c (top to bottom) – Drift Wall temperature comparison through the range of lineal heat loadings. Thermal-hydrologic, 2D drift-scale model. Lineal heat loading achieved by adjusting the waste package to waste package spacing, the drift to drift spacing was held constant at 81 meters.

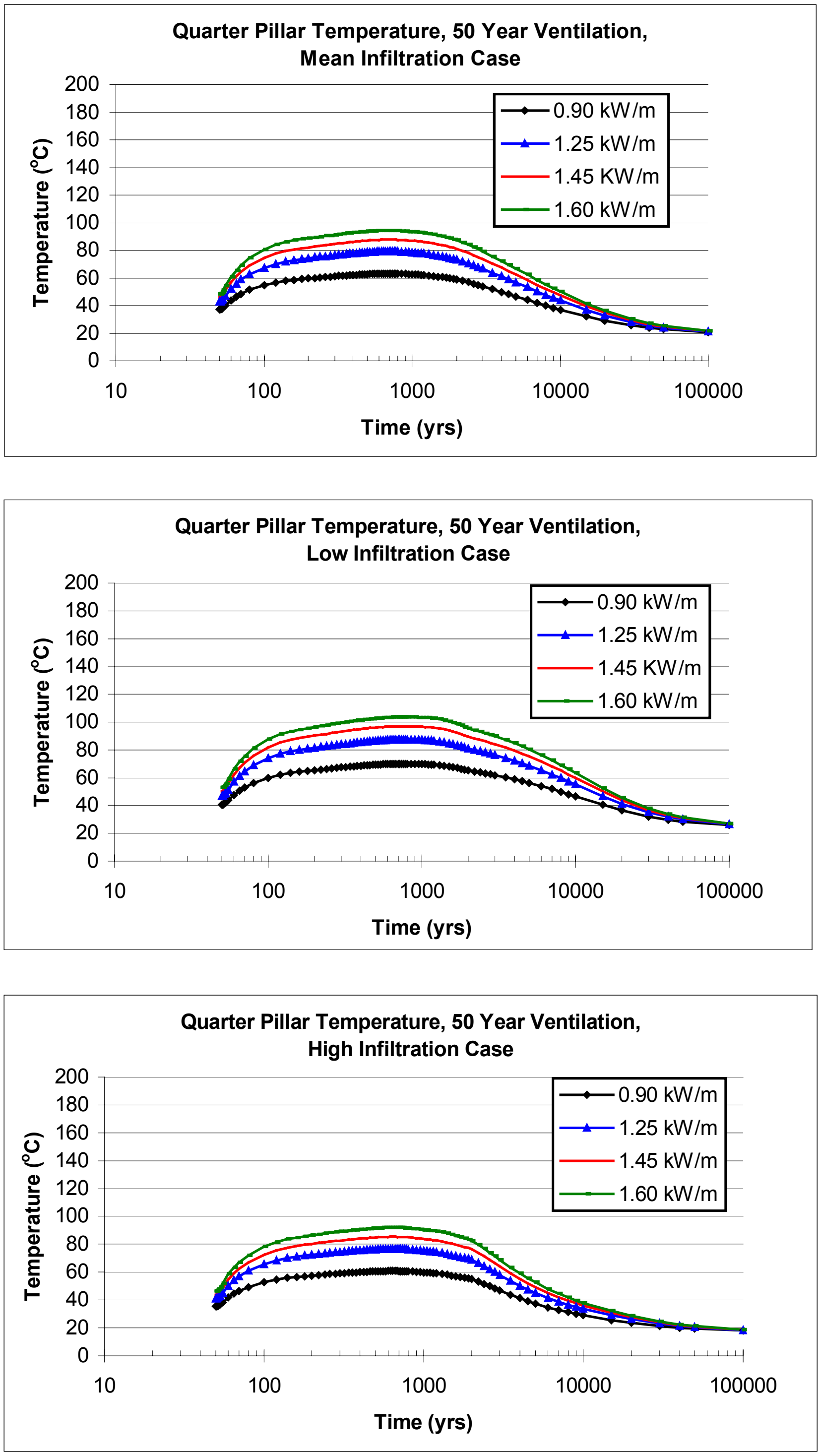

DTN: MO0008SPATHS03.001

Figure 5.7-4a, b, c (top to bottom) – Quarter pillar temperature history comparison through the range of lineal heat loadings. Thermal-hydrologic, 2D drift-scale model. The drift-to-drift spacing was held constant at 81 meters.

5.7.2 Adjustment of Areal Mass Loading by Drift to Drift Spacing

The adjustment of the areal mass loading of the repository can be achieved by adjusting the drift to drift spacing, instead of the waste package to waste package spacing. Figures 5.7-5 and 5.7-6 show the affect on the waste package temperature and relative humidity response when the effective lineal loading is achieved by adjusting drift-to-drift spacings of the SR Reference design case (50 year ventilated preclosure, 1.45 kW/m, 0.1 meter gaps between waste packages held constant). Even though the actual lineal power in each scenario is the same as the 1.45kW/m SR reference design scenario the spatial area per kilowatt is adjusted to effectively match the total repository power loading of a lower, or higher, lineal loading case where the waste package spacing was adjusted. The results are presented in the effective lineal loading format for ease of comparison.

The drift-to-drift adjusted effective lineal loading changes were achieved by modifying the drift-scale, 2D, 1.45kW/m, LDTH model that was used throughout this sensitivity study. The 1.60kW/m loading was achieved by decreasing the pillar width from 81 meters to 73.4 meters (81m*(1.45/1.60)=73.4m). The 1.25kW/m and 0.90kW/m loadings were achieved by increasing the pillar width to 93.96 meters and 130.5 meters, respectively.

Because the in-drift thermal hydrological peaks occur relatively soon after closure all of the scenarios have similar short term (~80 years) parameter responses. This short term similarity is due to the identical in-drift power output levels and the considerable lag time before the thermal energy levels in the pillar rise to where thermal communication between drifts begins to occur. By the 200th year of emplacement thermal communication between drifts is starting to occur and the differences between the effective lineal loading scenarios are beginning to show. Since the power output levels in the drifts are identical, the differences in thermal reponse histories observed are primarily due to the heat capacity of the host rock and the increased, or decreased, amount of pillar available.

After 5000 years of emplacement the power output levels in the drifts have diminished to levels that are not significantly different from the levels observed in similarly loaded drifts where the waste package to waste package spacing was adjusted instead of the drift-to-drift spacing. So in the later years of emplacement, when the entire repository is cooling down, the power output levels in the drift-to-drift adjusted drifts are not high enough to drive the in-drift thermal response levels higher, or lower, than the equivalent waste package to waste package adjusted drift layouts. Comparing Figure 5.7-5 with Figure 5.7-1a it is observed that after year 5000 the differences in the drift-to-drift adjusted layouts to the waste package to waste package adjusted layouts are negligible. At the drift wall this convergence of thermal-hydrological response histories occurs after only 3000 years of emplacement, see Figures 5.7-7 and Figure 5.7-3a.

The temperatures at the quarter pillar are not directly comparable since there is varying distances from the drift center used to describe the quarter pillar point in drift-to-drift adjusted designs. The quarter pillar temperature values in Figure 5.7-8 are presented for information purposes only. Though not directly comparable, it is interesting to note how similar the quarter pillar temperature histories are between the two lineal loading layout types, see Figure 5.7-8 and 5.7-4a.

Note that no other results in this report will be derived from thermally loaded models that incorporate the drift-to-drift adjustment technique; this is the only section of this report that will present these comparisons.

Table 5.7-2 – Summary of thermal hydrologic performance parameters showing the drift-scale sensitivity to the adjustment of the drift to drift spacings.

Performance Parameter	Infiltration Flux Case	Initial Effective Lineal Heat Loading[a]			
		Dx~1.60 kW/m	**1.45 kW/m**	**Dx~1.25 kW/m**	**Dx~0.90 kW/m**
WP Peak Temperature (Celsius)	Low **Mean** High	159	**157**	154	151
Years Until WP > 115°C	Low **Mean** High	500	**300**	200	150
Years Until WP > 80°C	Low **Mean** High	3200	**3000**	2100	850
DW Peak Temperature (Celsius)	Low **Mean** High	147	**145**	142	139
Years Until DW > 96°C	Low **Mean** High	1550	**1000**	520	210
¼ Pillar Peak Temperature (Celsius)	Low **Mean** High	94	**88**	80	63

DTN: MO0008SPATHS03.001

NOTE: [a]Initial effective lineal heat loading derived by increasing or decreasing the drift to drift spacing, waste package to waste package spacing held constant at 0.1 meters, actual in-drift power equivalent to the 1.45kW/m case.

Table 5.7-3 – Summary of thermal hydrologic performance parameters showing the drift-scale sensitivity to the lineal loading parameter, comparing the two methods of adjusting the effective lineal heat load of the repository.

Performance Parameter	Infiltration Flux Case/ (power loading method)	Effective Lineal Heat Loading			
		Dx~1.60 kW/m	**1.45 kW/m**	**Dx~1.25 kW/m**	**Dx~0.90 kW/m**
WP Peak Temperature (Celsius)	Mean / (drift-to-drift adjust)	159	157	154	151
	Mean / (WP-to-WP adjust)	174	**157**	136	99
Years Until WP > 115°C	Mean / (drift-to-drift adjust)	500	300	200	150
	Mean / (WP-to-WP adjust)	625	**300**	150	0
Years Until WP > 80°C	Mean / (drift-to-drift adjust)	3200	3000	2100	850
	Mean / (WP-to-WP adjust)	3600	**3000**	1900	250
DW Peak Temperature (Celsius)	Mean / (drift-to-drift adjust)	147	145	142	139
	Mean / (WP-to-WP adjust)	160	**145**	125	92
Years Until DW > 96°C	Mean / (drift-to-drift adjust)	1550	1000	520	210
	Mean / (WP-to-WP adjust)	1650	**1000**	325	0
¼ Pillar Peak Temperature (Celsius)	Mean / (drift-to-drift adjust)	94	88	80	63
	Mean / (WP-to-WP adjust)	95	**88**	79	63

DTN: MO0008SPATHS03.001

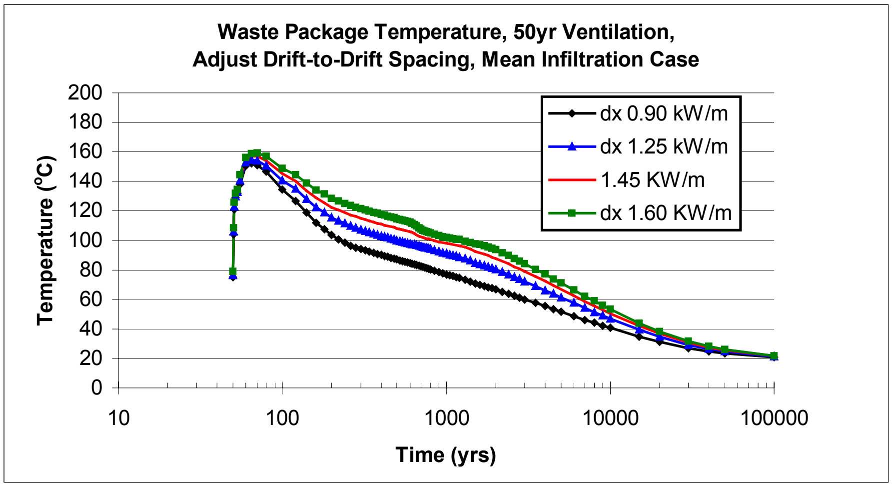

DTN: MO0008SPATHS03.001

Figure 5.7-5 – Comparison of drift-to-drift space adjusted thermal loading models, waste package temperature comparison. Thermal-hydrologic, 2D drift-scale model. Waste package to waste package spacing was constant at 0.1 meters.

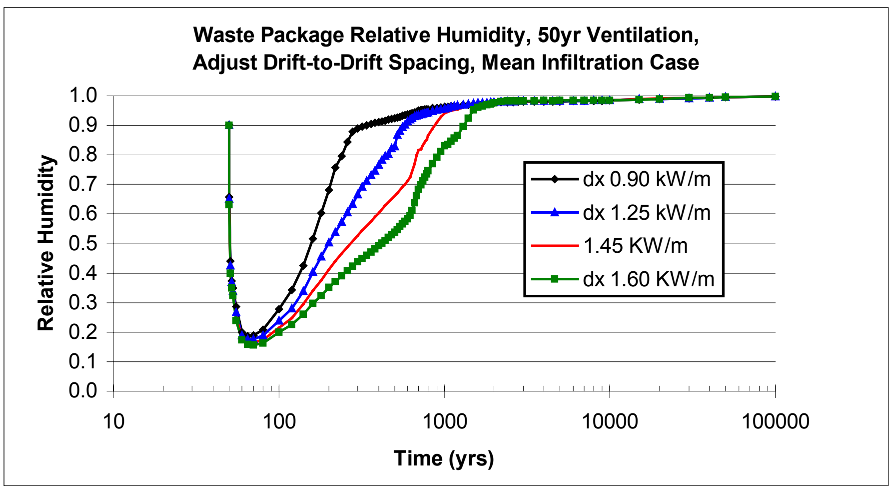

DTN: MO0008SPATHS03.001

Figure 5.7-6 – Comparison of drift-to-drift spacing adjusted thermal loading models, waste package relative humidity histories. Thermal-hydrologic, 2D drift-scale model. Waste package to waste package spacing was constant at 0.1 meters.

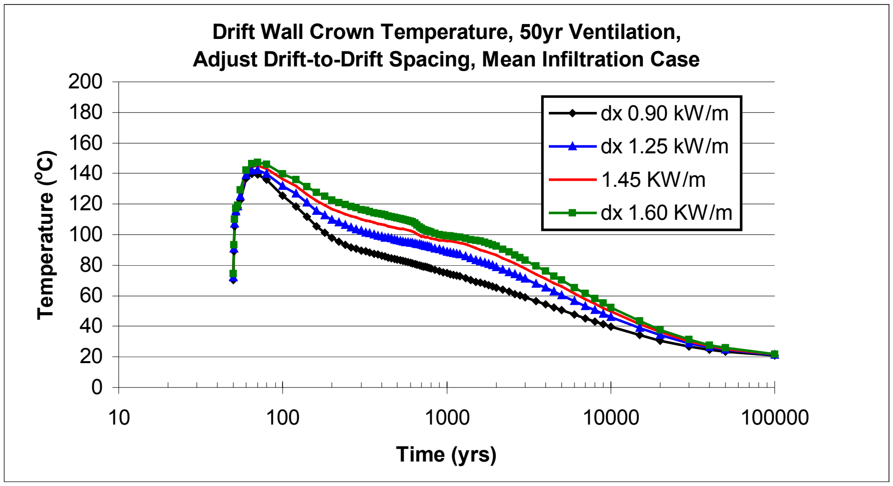

DTN: MO0008SPATHS03.001

Figure 5.7-7 – Comparison of drift-to-drift spacing adjusted thermal loading models, Drift Wall Crown temperature histories. Thermal-hydrologic, 2D drift-scale model. Waste package to waste package spacing constant at 0.1 meters.

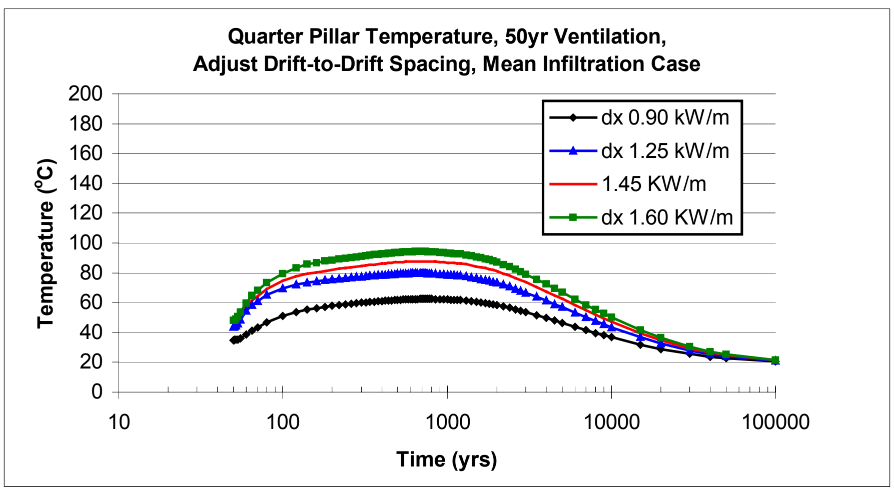

DTN: MO0008SPATHS03.001

Figure 5.7-8 – Comparison of drift-to-drift spacing adjusted thermal loading models, quarter pillar temperature histories. Thermal-hydrologic, 2D drift-scale model. Waste package to waste package spacing constant at 0.1 meters.

5.8 RANGE ASSOCIATED WITH THERMAL RESPONSE CURVES

Results presented throughout this document have been 2D representations of the repository emplacement drifts. The 2D emplacement drift representation is limited in that it simulates a smeared average waste package thermal-hydrologic response. In the actual repository there will be package to package differences in thermal response that cannot be captured by the 2D representation of the emplacement drift. In this section, a 3D thermal conduction-only model will be used to approximate the temperature range of response that should be considered when interpreting results from the LDTH models.

Unfortunately, performing the sensitivities in this calculation report with a thermal-hydrologic 3D representation of a drift section was not possible due to computational limitations and the highly non-linear nature of the dual permeability conceptual model. A decoupled, thermal conduction-only, 3D representation of a discrete drift emplacement section can be modeled in order gain an understanding of the range of response associated with 2D representations of the same drift section. But because the 3D model is a thermal conduction-only representation of the thermal response it cannot be directly compared with the 2D thermal-hydrologic representations. One indirect, but fair, comparison that can be useful between the DDT and LDTH models is that of the temperature difference between the waste package and drift wall. Such comparisons are included in Figures 5.8-3a, b, and c.

The DDT submodel described in the *Multiscale Thermohydrology Model* AMR (CRWMS M&O 2000f, section 6.5) was selected in order to run the thermal response range simulations presented in this section. The model selected was extracted from the non-backfilled multiscale model data submittal DTN: LL000509112312.003. The multiscale DDT submodel, the idealized drift segment, used in this calculation is illustrated in Figure 5.8-1. Two modifications were made to the submodel in order to perform the simulations required for this sensitivity analysis: 1) The 0.1 meter spacing between the waste packages which included thermal radiation connections were replaced with additional rows of effective thermal conductivity elements, and 2) the thermal radiation connections from the waste package surface to the dripshield underside were removed and replaced with effective thermal conductivity properties between those two surfaces. Since the additional rows of elements between the modeled waste packages used an effective thermal conductivity they could be adjusted for the various lineal heat loadings of interest to this study.

A description of the waste packages in the DDT representative drift segment is given in Table 5.8-1 (CRWMS M&O 2000c, Table 6). It is an idealized representation of the waste packages that may populate the repository but does not represent a perfectly “average” section of the repository. The waste package selections (for a three-dimensional drift-scale model) are based on the total number of a particular waste type in the repository. As an example, the fraction of the total 21-PWRs in the repository is 4279/9965 = 0.4294. In the idealized 7-waste package model, the fraction of this type is 3/7 ≈ 0.4286. Since the idealized segment does not contain 9965 waste packages, it is not possible to exactly represent any given type or include those types that are few in number in the entire repository waste stream (e.g., to include a 12-PWR in an idealized segment would require a 32 waste package model since they only comprise 1.6% of the total inventory).

In Table 5.8-1 it is noted that this “idealized” emplacement drift layout contains five CSNF waste packages and 2 non-CSNF waste packages. For the purpose of this calculation, the SR reference DDT model was modified by increasing, or decreasing, the waste package to waste package spacing until the desired lineal heat load was achieved. Because of the selected package lengths and heat ouputs of those packages, the highest lineal loading that was possible was 1.57kW/m which corresponds to a package to package spacing of 0.0 meters. Because of the selected packages in the submodel the lineal loading associated with the SR reference design package to package spacing of 0.1 meters is approximately 1.54 kW/m which is higher than the total repository average of 1.45 kW/m. In order to achieve a lineal loading of 1.45 kW/m with the selected waste packages, the package to package spacing was increased to 0.42 meters. See Table 5.8-2 for a listing of waste package to waste package spacings and their associated lineal loadings in the selected DDT submodel.

In Figures 5.8-2a, b, c, and d the DDT model predicted temperature histories for four different linear loading layouts are presented. Each figure shows three temperature histories, one for a PWR waste package, one for a BWR package, and one for a defense waste package. The PWR2 waste package shown in each figure is one of the hotter 21PWR packages that would be expected in the repository, while the HLW1 waste package is one of the cooler waste packages expected to be in the repository. The BWR1 waste package shown in each figure is roughly the average waste package with an average thermal response history to be expected for the repository.

The waste package to drift wall temperature differences from the 0.90kW/m, 1.25kW/m, and 1.45kW/m DDT models are compared against the equivalent LDTH model temperature differences in Figures 5.8-3a, b, and c. Note that the 0.90kW/m LDTH model is significantly below the average BWR1 temeprature difference curve. The differences observed in the lower lineal heat load model, 0.90kW/m, shows how smearing the thermal energy along the drift begins to create unrealistically cooler thermal response curves in the 2D simulations. In essence the 0.90kW/m, 2D LDTH model is no longer representative of the average thermal response of that repository scenario; it becomes representative of a cooler package in the 0.90kW/m layout. The thermal balance is still correct and accurately representative of the average thermal activity in the host rock, but in-drift thermal response is more represenative of a below average waste package instead of average. Also, since the 2D host rock thermal balance is correct then it is assumable that the thermal responses of the host rock would behave similarly with the host rock of the 3D models, i.e. the host rock in a 2D model loaded at 0.90kW/m will behave similarly with the host rock in a 3D model loaded at 0.90kW/m. Differences between 2D and 3D models become more apparent inside the drift, but by using the host rock as a common point of reference lends to a fair comparison between 2D and 3D models. This is why the temperature difference between the waste package and the drift wall is a good reference to show the 3D range of in-drift thermal responses to be expected when analyzing average 2D simulation results. Theoretically, in a perfectly line loaded emplacement (no gaps between waste package ends) the 2D model response would be equivalent to the average response in the 3D model. By introducing increasingly larger waste package to waste package gaps the 2D response will begin to behave more and more as a below average 3D model waste package response.

Table 5.8-1 - Representative Drift Segment (CRWMS M&O 2000c, Table 6)

Waste Package Type		Fraction of Total in Repository	Length (m)	Fraction of Total in Model	# in Model	Length (m) w/0.1m gaps	Initial Heat Generation Rate (kW)	Initial Heat Generation Rate (kW)	Mass (MTU)
21-PWR	Absorber	0.429	5.305	0.429	3	15.915 + 0.3	11.334	11.334 x 3	27.149
	Control Rods	0.009	5.305	0.000	0	0.000	2.371	0	0.0
12-PWR	Long	0.016	5.791	0.000	0	0.000	9.540	0	0.0
44-BWR	Absorber	0.290	5.275	0.290	2	10.550 + 0.2	7.135	7.135 x 2	15.575
24-BWR	Thick Plates	0.001	5.245	0.000	0	0.000	0.491	0	0.0
5-DHLW		0.125	3.730	0.214	1.5	5.595 + 0.15	4.058	4.058 x 1.5	NA
5-DHLW	Long	0.042	5.357	0.000	0	0.000	0.000	0	NA
Naval	Combined	0.029	5.888	0.000	0	0.000	0.000	0	NA
DOE/other		0.060	5.570	0.071	0.5	2.785 + 0.05	0.793	0.793 x 0.5	NA
				1.000	7	35.545		54.7555	42.724

NA – not applicable

Table 5.8-2 – WP-to-WP Spacings associated with the 7 package drift section as described in Figure 5.8-1 and Table 5.8-1.

WP-to-WP Gap (m)	Conversion to Lineal Heat Loading (Total kW / Total section length)	Lineal Heat Loading (kW/m)
0.01	54.7555 kW / (34.845+0.07)	1.57
0.10	54.7555 kW / (34.845+0.70)	1.54
0.42	54.7555 kW / (34.845+2.94)	1.45
1.28	54.7555 kW / (34.845+8.96)	1.25
2.85	54.7555 kW / (34.845+19.95)	1.00
3.70	54.7555 kW / (34.845+25.90)	0.90

DTN: MO0008SPATHS03.001

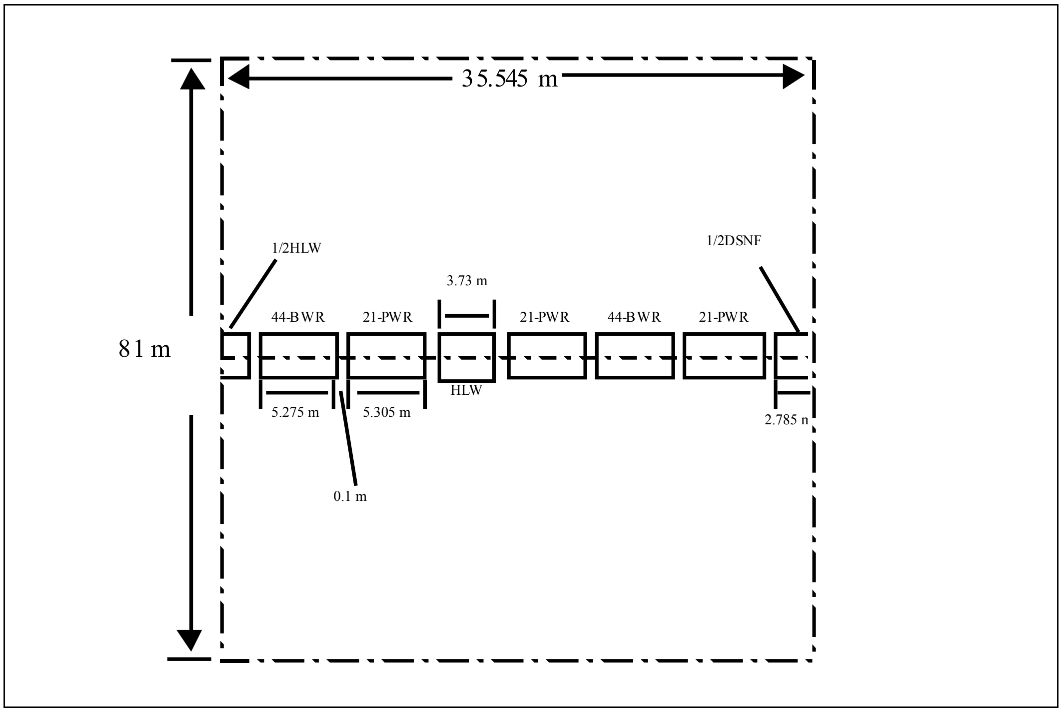

Figure 5.8-1 – Representative drift segment in the MSTHM DDT submodel (not to scale). Package to package spacing of 0.1 meters shown. (CRWMS 2000c, figure 3)

a)

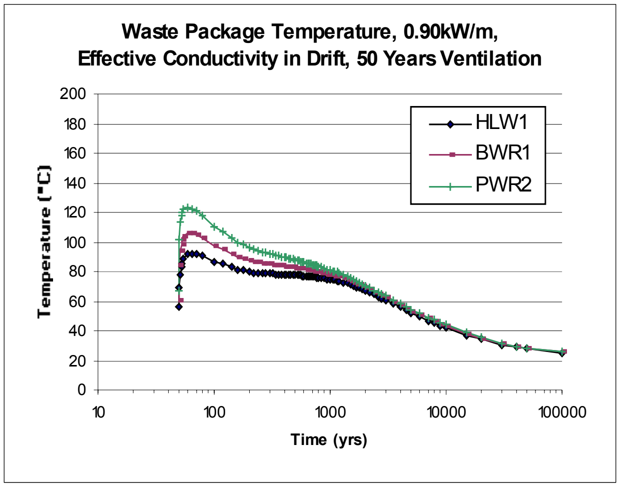

b)

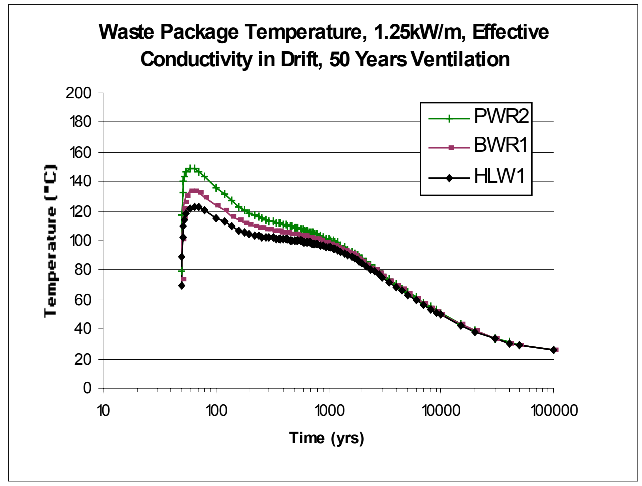

c)

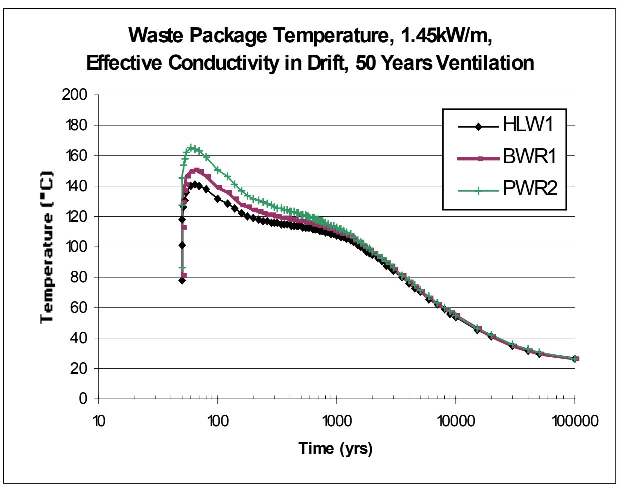

d)

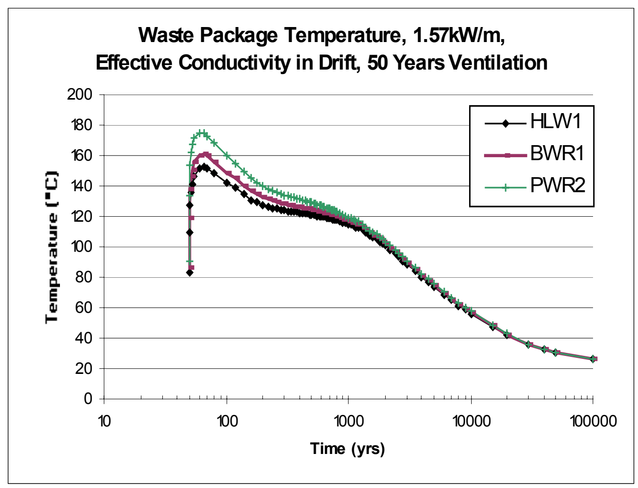

DTN: MO0008SPATHS03.001

Figure 5.8-2a, b, c, d – Discrete drift sections' upper and lower bounds for the waste package temperature history. Lineal heat loading achieved by adjusting the waste package to waste package spacing, the drift to drift spacing of 81 meters is held constant. 50 year preclosure assumed.

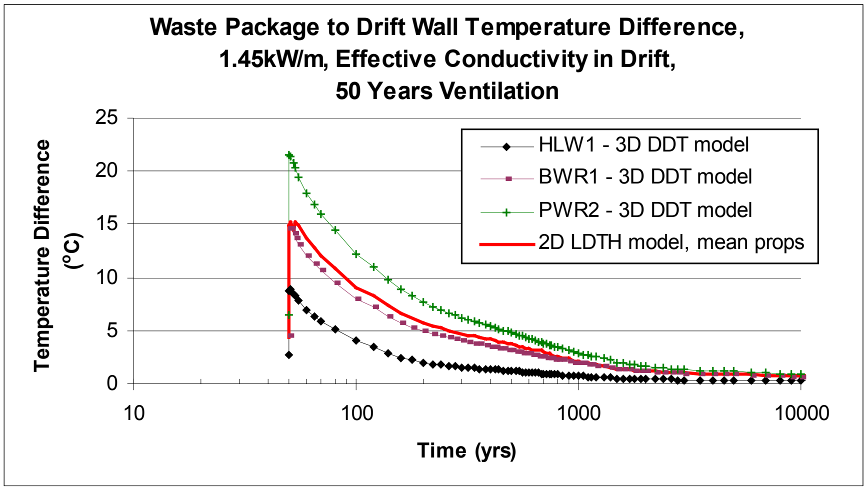

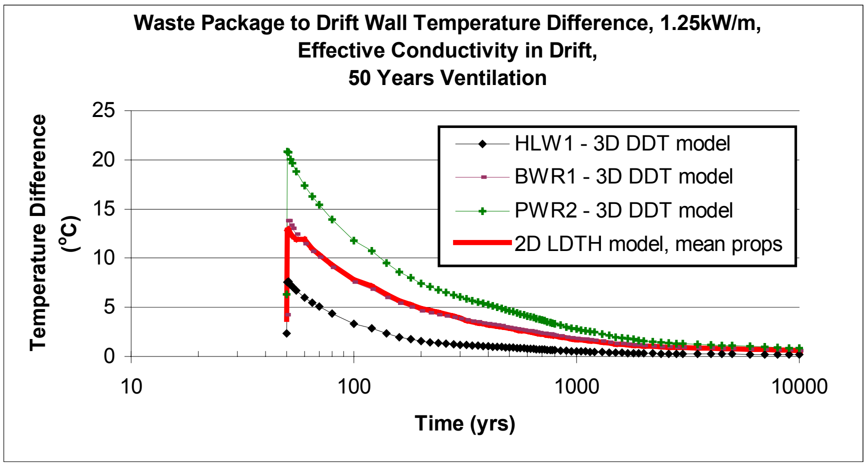

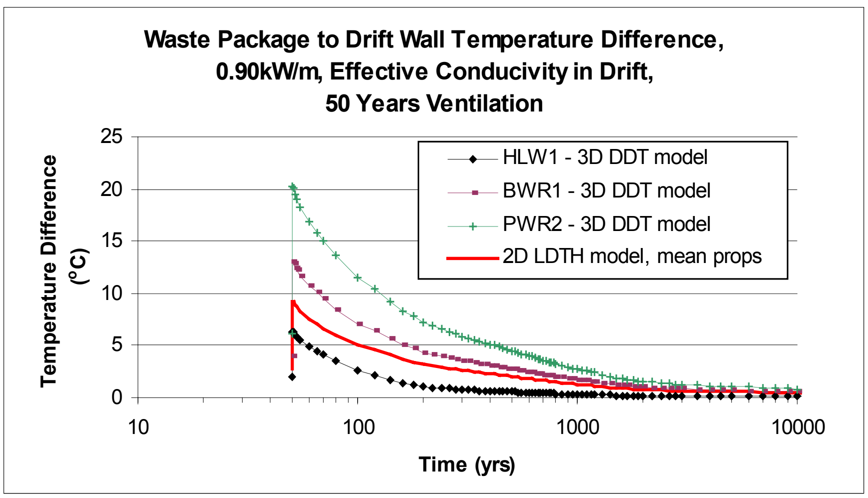

DTN: MO0008SPATHS03.001

Figure 5.8-3a, b, c (top to bottom) – Temperature difference history, LDTH results overlaid comparable DDT results. Temperature difference taken from the waste package surface to the neighboring drift wall element. 50 year preclosure.

5.9 LOWER TEMPERATURE OPERATION MODE SCENARIOS

Different lower temperature operating mode scenarios are introduced in the thermal hydrologic sensitivity calculation in order to develop an operational mode in which the waste package surface temperature after closure remains at or below 85°C for the majority of the waste package population. Four methods are studied to better understand over what range of design parameters are needed to maintain waste package temperatures below 85°C. The four scenarios documented in this section are; the increased waste package spacing scenario, the pre-emplacement fuel-aging scenario, the increased drift spacing scenario, and the Environmental Impact Statement (EIS) low thermal load (small drift spacing and large waste package spacing) scenario. All of the sensitivity studies were performed by modifying either the geometry and/or the heat input into the L4C4 LDTH submodel.

For the increased waste package spacing scenario, the waste package types, number, and drift-to-drift spacing (81 meters) remain the same as those in the current SR Reference Design (CRWMS M&O 2000d). Reduction in the peak post-closure waste package surface temperature is achieved by reducing the areal mass loading (by increasing the waste package spacing) and by increasing the pre-closure active ventilation duration. The areal mass loading of this operational mode is reduced from the current SR Reference Design value of 60 MTU/acre (CRWMS M&O 2000c) to approximately 28 MTU/acre. The waste package spacing required in order to achieve the operational areal mass loading is approximately 6 meters. It is assumed that each emplacement drift will be ventilated for 100 years after it is loaded and that, as before, 70% of the energy is removed by the ventilation. As stated in the section 5.8, the 2D LDTH model somewhat underestimates the temperature values compared to the 3D DDT model under the low linear heat loading of 0.90 kW/m. The under-prediction of low linear heat loading should be considered in this scenario.

The pre-emplacement fuel-aging scenario achieves low waste package temperatures by increasing the spacing between waste packages, by delaying the emplacement of waste by some fixed amount of time, and by extending the pre-closure ventilation time. The effective age of the emplaced waste stream may be increased by as much as 30 years by managing the waste stream used to load waste packages before they are emplaced and allowing young fuel assemblies to age in storage at an above ground fuel handling facility. This management of the waste fuel stream will likely increase the amount of time required to emplace the waste fuel into the repository by at least 30 years. From figure 5.1-1, the heat decay curve drops from 1.45 kW/m down to 0.78 kW/m after 30 years or a reduction of 46% of the lineal heat load at emplacement. The scenario of the aging of the fuel prior to emplacement is implemented into the LDTH model by simply adjusting the model to treat year 30 of the thermal output curves as year 0 of the simulation. This 30 year offset between the time represented in the model and the time on the thermal output curve from which waste package thermal output is derived is maintained throughout the simulation. The waste package types, number, and drift-to-drift spacing (81 meters) remain the same as those in the current SR Reference Design (CRWMS M&O 2000d). The areal mass loading of this operational mode is approximately 40 MTU/acre, or approximately 20 MTU/acre lower than the SR Reference Design value. The waste package spacing required to achieve the operational areal mass loading is slightly over 2 meters. It is assumed that each emplacement drift will be ventilated for 75 years after it is loaded. As before, 70% of the thermal load is removed by the ventilation.

The increased drift spacing scenario is simulated and presented in the thermal hydrologic sensitivity calculation. This scenario reduces the waste package temperatures by increasing the quantity of rock between drifts as well as extending the pre-closure ventilation time. The waste package types, number, and in-drift spacing (0.1 meters) remain the same as those in the current SR Reference Design (CRWMS M&O 2000d). The areal mass loading of this operational mode is approximately 40 MTU/acre. The drift to drift spacing required in order to achieve the operational areal mass loading is approximately 120 meters. It is assumed that each emplacement drift will be ventilated for 300 years after it is loaded. As before, 70% of the thermal load is removed by the ventilation.

The EIS low thermal load scenario is also simulated and presented in the thermal hydrologic sensitivity calculation. Reduction in the peak post-closure waste package surface temperature is achieved by increasing the waste package spacing by up to 19 meters while reducing drift to drift spacing to 38 meters. The areal mass loading of this operational mode is 25 MTU/acre. It is assumed that the emplacement drifts will be not be ventilated after they are loaded. As stated in the section 5.8, the 2D LDTH model somewhat underestimates the temperature values compared to the 3D DDT model under the low linear heat loading of 0.90 kW/m. The under-prediction of low linear heat loading should be considered in this scenario.

A summary of the important parameters for the lower temperature operating scenarios as well as those for the SR Reference Design is presented Table 5.9-1. All the low temperature operating mode scenarios were simulated using the mean infiltration fluxes and property sets (DTN: LL000509112312.003).

Table 5.9–1 – Summary of the lower temperature operating mode scenarios.

Scenario Description	Lineal Heat Loading (kW/m)	Areal Mass Loading (MTU/acre)	Drift Spacing (m)	Waste Package Spacing (m)	Forced Ventilation (year)	Increase of Fuel Aging (year)
Increased waste package spacing	0.70	28	81	6	100	0
Pre-emplacement fuel aging	1.00	40	81	2	75	30
Increased drift spacing	1.45	40	120	0.1	300	0
EIS low thermal load	0.30	25	38	19	0	0
SR reference design	1.45	60	81	0.1	50	0

DTN: MO0103MWDTHS03.001

The waste package and drift wall temperatures for the increased waste package spacing scenario are displayed in Figure 5.9-1. The waste package surface temperature history predicted by the LDTH model had a peak post-closure temperature of 66°C. The post-closure temperature peak of the average packages represented by the two-dimensional analysis are well under the 85°C operational threshold when using the full 100 years of 70% efficient pre-closure ventilation. By increasing the drift spacing to an areal mass loading of approximately 28 MTU/acre and allowing 100 years of preclosure ventilation, the increased waste package spacing scenario will maintain the average waste package surface temperature during post-closure under 85°C. A more detailed analysis can be performed to determine if the full 100 years of pre-closure ventilation is required to achieve the thermal goal of this operational mode (Waste package surface temperature < 85°C) or if a shorter ventilation period may be used. In addition, development of a 3D DDT model for the scenario is suggested in order to investigate the effect of temperature under-prediction from the low linear heat load LDTH model.

The waste package surface history predicted by the pre-emplacement fuel aging scenario had a peak post-closure temperature of 78°C and is displayed in Figure 9.5-2. The post-closure temperature peak of the average packages represented by the two-dimensional analysis are well under the 85°C operational threshold when using the full 75 years of pre-closure ventilation pre-closure. Increasing the effective age of the waste fuel prior to emplacement had a notable affect of the pre-closure waste package peak temperatures, reducing the pre-closure peak to approximately 52°C. In conclusion, the average waste package surface temperature during post-closure will remain under 85°C through the use of a combination of aging the waste fuel by 30 years, increasing the waste package spacing to an areal mass loading of approximately 40 MTU/acre, and allowing for at least 75 years of pre-closure ventilation. A more detailed analysis can be performed to determine if the full 75 years of pre-closure ventilation is required to achieve the thermal goal of this operational mode (Waste package surface temperature < 85°C) or if a shorter ventilation may be used.

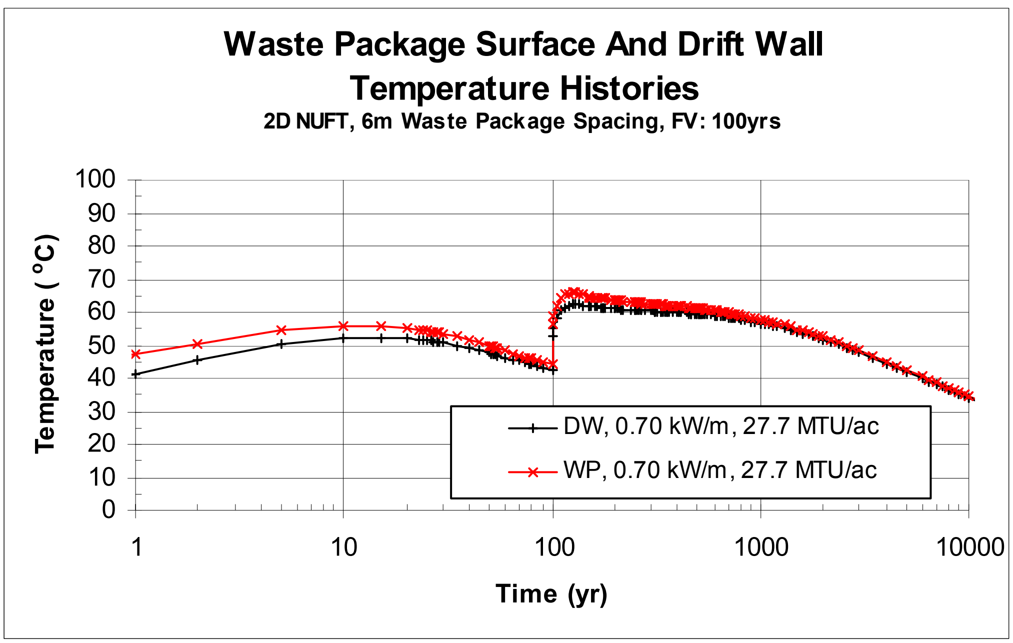

DTN: MO0103MWDTHS03.001

Figure 5.9–1 – Waste Package (WP) Surface and Drift Wall (DW) temperature history for the increased WP spacing scenario (100 years of ventilation and 6 m WP spacing).

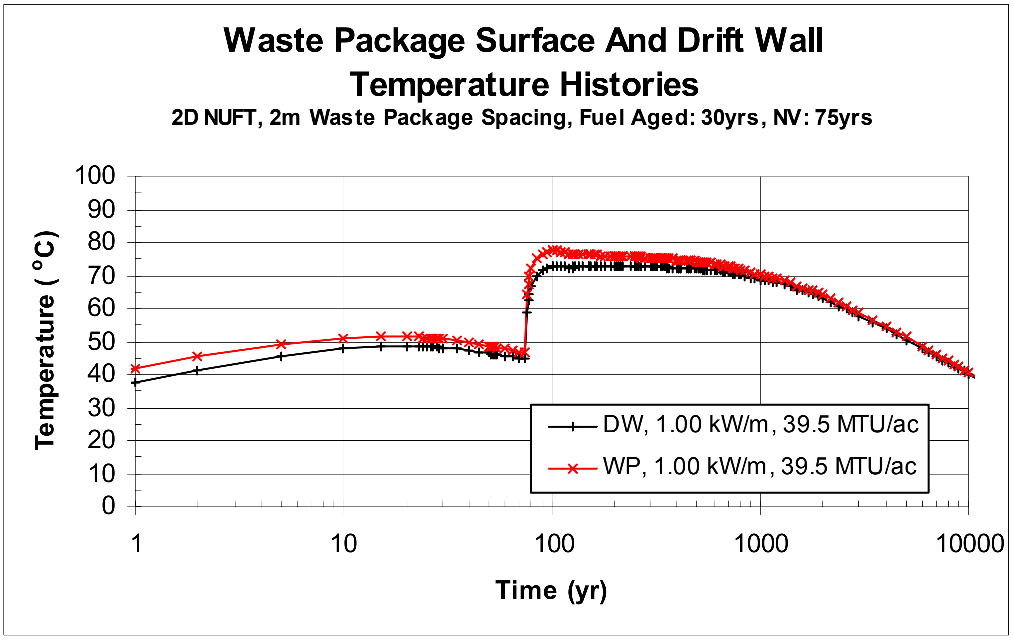

DTN: MO0103MWDTHS03.001

Figure 5.9–2 – Waste Package (WP) Surface and Drift Wall (DW) temperature history for the pre-emplacement fuel aging scenario (waste fuel aged by 30 years before emplacement followed by 75 years of ventilation).

The waste package and drift wall temperature histories for the increased drift spacing scenario are presented in Figure 5.9-3. The waste package surface temperature history predicted by the LDTH model had a peak post-closure temperature of 76°C at 440 Years. The post-closure temperature peak of the average packages represented by the two-dimensional analysis are well under the 85°C operational threshold when using the full 300 years of pre-closure ventilation pre-closure. The pre-closure temperature peak is observed to be over 85°C. Therefore, in the increased drift spacing scenario, the average waste package surface temperature during post-closure will remain under 85°C, by increasing the drift spacing to an areal mass loading of approximately 40 MTU/acre and allowing 300 years of pre-closure ventilation. A more detailed analysis can be performed to determine if the full 300 years of pre-closure ventilation is required to achieve the thermal goal of this operational mode (waste package surface temperature < 85°C) or if a shorter ventilation may be used.

The waste package and drift wall temperature histories for the EIS low thermal load scenario are displayed in Figure 5.9-4. The waste package surface temperature history predicted by the LDTH model had a peak post-closure temperature of 78°C. The pre-closure relative humidity levels during pre-closure ventilation are expected to be well below water film developing levels (~10%). In spite of 38m drift spacing, the EIS low thermal load scenario will maintain the average waste package surface temperature during post-closure under 85°C by increasing the waste package spacing to an areal mass loading of approximately 25 MTU/acre. Development of a 3D DDTH model for the scenario is suggested in order to investigate the effect of temperature under-prediction from the low linear heat load LDTH model.

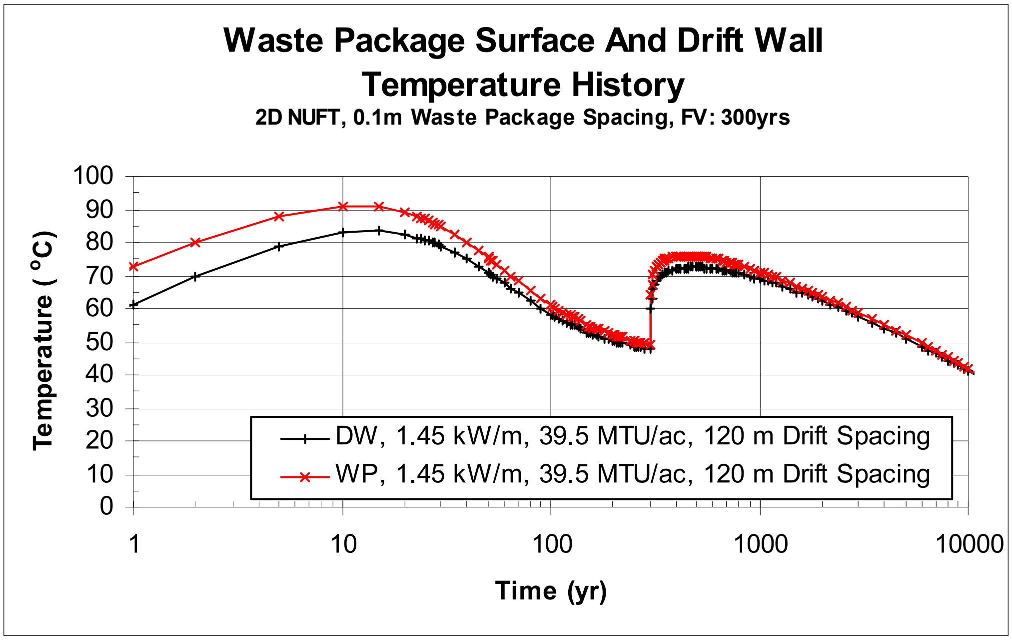

DTN: MO0103MWDTHS03.001

Figure 5.9–3 – Waste Package (WP) Surface and Drift Wall (DW) temperature history for the increased drift spacing scenario (300 years of ventilation).

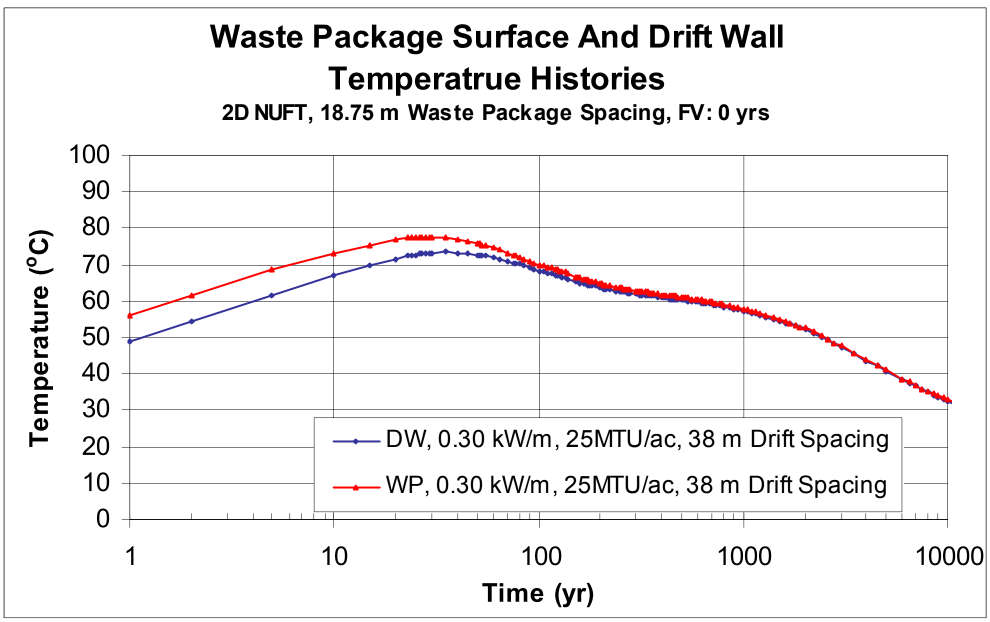

DTN: MO0103MWDTHS03.001

Figure 5.9–4 – Waste Package (WP) Surface and Drift Wall (DW) temperature history for the EIS low thermal load scenario (0 years of ventilation).

5.10 SUMMARY OF LINEAL DRIFT-SCALE THERMAL-HYDROLOGIC CASES

Because previous sections in this report have been focused on specific questions of thermal-hydrologic sensitivity, the entire set of simulations have not been presented simultaneously. This section will simply summarize key predicted thermal-hydrologic response values for the entire set of simulations.

The ventilation periods of 23 years and 125 years were not simulated for the LDTH models with lineal loadings of 1.25kW/m and 1.60kW/m, therefore there are no results to present from those scenarios in the summary tables of this section. Tables 5.9-1 through 5.9-3 present the predicted waste package performance indicator values for the majority of the scenarios simulated for this study. Tables 5.9-4 and 5.9-5 present the predicted drift wall crown performance indicator values for the majority of the scenarios simulated. And, Table 5.9-6 presents the predicted quarter pillar peak temperature values for the majority of the scenarios simulated for this study.

A summary of all of the performance indicators extracted from the complete set of 0.90kW/m lineal loaded LDTH models is presented in Table 5.9-7. The 0.90kW/m set of LDTH models was the only one that included a 75 year ventilation scenario and Table 5.9-7 presents all of the ventilation scenarios in one location. Note that because of observations in section 5.8 the 2D results for the waste package temperatures in the 0.90kW/m models could be higher than those presented here and in other portions of this calculation report.

Table 5.10-1 – Summary of waste package peak temperature as predicted by each thermal-hydrologic 2D model simulation.

Lineal Loading[a]	Infiltration Flux Case	Years of Ventilation (70% effective heat removal)					
		0	15	23	50	100	125
0.90 kW/m	Low	197	163	148	114	88	81
	Mean	**183**	**149**	**133**	**99**	**77**	**72**
	High	176	141	126	97	75	70
1.25kW/m	Low	270	221	--	151	113	--
	Mean	**255**	**207**	**--**	**136**	**98**	**--**
	High	247	199	--	129	96	--
1.45kW/m	Low	313	255	229	172	129	117
	Mean	**298**	**238**	**214**	**157**	**110**	**101**
	High	288	231	207	151	107	99
1.60kW/m	Low	344	281	--	188	140	--
	Mean	**329**	**264**	**--**	**174**	**125**	**--**
	High	321	256	--	167	118	--

DTN: MO0008SPATHS03.001

NOTE: [a]Lineal Heat loading achieved by adjusting the waste package to waste package spacing, drift to drift spacing is held constant at 81 meters for all tabulated cases.

Table 5.10-2 – Summary of time required after first emplacement before the Waste Package temperature falls to 115 °C or less as predicted by each thermal-hydrologic 2D model simulation.

Lineal Loading[a]	Infiltration Flux Case	Years of Ventilation (70% effective heat removal)					
		0	**15**	**23**	**50**	**100**	**125**
0.90 kW/m	Low	160	125	110	0	0	0
	Mean	**110**	**90**	**75**	**0**	**0**	**0**
	High	95	80	65	0	0	0
1.25kW/m	Low	780	620	--	320	0	--
	Mean	**340**	**250**	**--**	**150**	**0**	**--**
	High	280	200	--	125	0	--
1.45kW/m	Low	1450	1250	1150	900	580	380
	Mean	**650**	**575**	**500**	**300**	**0**	**0**
	High	550	450	380	240	0	0
1.60kW/m	Low	1800	1650	--	1400	1100	--
	Mean	**680**	**680**	**--**	**620**	**300**	**--**
	High	620	620	--	480	190	--

DTN: MO0008SPATHS03.001

NOTE: [a]Initial Lineal Heat loading achieved by adjusting the waste package to waste package spacing, drift to drift spacing is held constant at 81 meters for all tabulated cases.

Table 5.10-3 – Summary of time required after first emplacement before the Waste Package temperature falls to 80 °C or less as predicted by each thermal-hydrologic 2D model simulation.

Lineal Loading[a]	Infiltration Flux Case	Years of Ventilation (70% effective heat removal)					
		0	**15**	**23**	**50**	**100**	**125**
0.90 kW/m	Low	1550	1350	1275	950	600	420
	Mean	**740**	**560**	**480**	**250**	**0**	**0**
	High	600	430	360	200	0	0
1.25kW/m	Low	4100	3750	--	3250	2750	--
	Mean	**2500**	**2300**	**--**	**1850**	**1475**	**--**
	High	2000	1850	--	1500	1175	--
1.45kW/m	Low	5550	5400	5150	5000	4600	4500
	Mean	**3400**	**3250**	**3200**	**2900**	**2500**	**2400**
	High	2600	2450	2400	2250	2000	1900
1.60kW/m	Low	6600	6500	--	6100	6000	--
	Mean	**4250**	**4000**	**--**	**3600**	**3400**	**--**
	High	3000	2900	--	2700	2450	--

DTN: MO0008SPATHS03.001

NOTE: [a]Initial Lineal Heat loading achieved by adjusting the waste package to waste package spacing, drift to drift spacing is held constant at 81 meters for all tabulated cases.

Table 5.10-4 – Summary of Drift Wall peak temperature as predicted by each thermal-hydrologic 2D model simulation.

Lineal Loading[a]	Infiltration Flux Case	Years of Ventilation (70% effective heat removal) 0	15	23	50	100	125
0.90 kW/m	Low	180	149	136	106	83	78
	Mean	**164**	**134**	**120**	**92**	**73**	**69**
	High	157	127	113	90	71	67
1.25kW/m	Low	245	201	--	140	107	--
	Mean	**229**	**187**	**--**	**125**	**92**	**--**
	High	222	179	--	119	90	--
1.45kW/m	Low	284	232	210	160	121	111
	Mean	**268**	**215**	**195**	**145**	**103**	**96**
	High	258	208	188	138	99	93
1.60kW/m	Low	311	256	--	175	131	--
	Mean	**296**	**239**	**--**	**161**	**116**	**--**
	High	288	230	--	153	110	--

DTN: MO0008SPATHS03.001

NOTE: [a]Initial Lineal Heat loading achieved by adjusting the waste package to waste package spacing, drift to drift spacing is held constant at 81 meters for all tabulated cases.

Table 5.10-5 – Summary of time required after first emplacement before Drift Wall temperature falls below 96 °C as predicted by each thermal-hydrologic 2D model simulation.

Lineal Loading[a]	Infiltration Flux Case	Years of Ventilation (70% effective heat removal) 0	15	23	50	100	125
0.90 kW/m	Low	400	260	215	140	0	0
	Mean	**170**	**130**	**115**	**0**	**0**	**0**
	High	150	110	95	0	0	0
1.25kW/m	Low	1800	1600	--	1275	875	--
	Mean	**900**	**680**	**--**	**320**	**0**	**--**
	High	740	540	--	240	0	--
1.45kW/m	Low	2850	2500	2300	2000	1800	1675
	Mean	**1650**	**1450**	**1350**	**975**	**620**	**0**
	High	1400	1200	1100	800	340	0
1.60kW/m	Low	3800	3550	--	3000	2450	--
	Mean	**2250**	**2050**	**--**	**1600**	**1250**	**--**
	High	1950	1700	--	1325	950	--

DTN: MO0008SPATHS03.001

NOTE: [a]Initial Lineal Heat loading achieved by adjusting the waste package to waste package spacing, drift to drift spacing is held constant at 81 meters for all tabulated cases.

Table 5.10-6 – Summary of ¼ Pillar temperature peaks as predicted by each thermal-hydrologic 2D model simulation.

Lineal Loading[a]	Infiltration Flux Case	Years of Ventilation (70% effective heat removal) 0	15	23	50	100	125
0.90 kW/m	Low	81	75	74	70	67	65
	Mean	**74**	**68**	**67**	**63**	**60**	**59**
	High	73	66	64	61	58	56
1.25kW/m	Low	102	94	--	87	83	--
	Mean	**95**	**86**	**--**	**79**	**74**	**--**
	High	92	84	--	77	72	--
1.45kW/m	Low	113	104	102	97	92	90
	Mean	**99**	**95**	**93**	**88**	**82**	**81**
	High	96	93	91	85	80	78
1.60kW/m	Low	120	111	--	104	98	--
	Mean	**103**	**98**	**--**	**94**	**89**	**--**
	High	100	96	--	92	86	--

DTN: MO0008SPATHS03.001

NOTE: [a]Initial Lineal Heat loading achieved by adjusting the waste package to waste package spacing, drift to drift spacing is held constant at 81 meters for all tabulated cases.

Table 5.10-7 – Summary of thermal hydrologic performance parameters showing the drift-scale sensitivity to ventilation. 0.90kW/m LDTH model used for all simulations.

Performance Parameter	Infiltration Flux Case	Years of Ventilation (70% effective heat removal) 0	15	23	50	75	100	125
WP Peak Temperature (Celsius)	Low	197	163	148	114	97	88	81
	Mean	**183**	**149**	**133**	**99**	**85**	**77**	**72**
	High	176	141	126	97	83	75	70
Years Until WP > 115°C	Low	160	125	110	0	0	0	0
	Mean	**110**	**90**	**75**	**0**	**0**	**0**	**0**
	High	95	80	65	0	0	0	0
Years Until WP > 80°C	Low	1550	1350	1275	950	800	600	420
	Mean	**740**	**560**	**480**	**250**	**175**	**0**	**0**
	High	600	430	360	200	140	0	0
DW Peak Temperature (Celsius)	Low	180	149	136	106	91	83	78
	Mean	**164**	**134**	**120**	**92**	**80**	**73**	**69**
	High	157	127	113	90	78	71	67
Years Until DW > 96°C	Low	400	260	215	140	0	0	0
	Mean	**170**	**130**	**115**	**0**	**0**	**0**	**0**
	High	150	110	95	0	0	0	0
¼ Pilr Peak Temperature (Celsius)	Low	81	75	74	70	68	67	65
	Mean	**74**	**68**	**67**	**63**	**61**	**60**	**59**
	High	73	66	64	61	59	58	56

DTN: MO0008SPATHS03.001

6. RESULTS

This calculation does not contain any assumptions that need to be confirmed prior to the use of the results of the calculation.

The thermal response curves presented in this report are contained in the TDMS under the data tracking number (DTN): MO0008SPATHS03.001 and MO0103MWDTHS03.001. The data has been submitted to the TDMS according to procedure AP-SIII.3Q *Submittal and Incorporation of Data to the Technical Data Management System*. The data submitted to the TDMS are not qualified (NQ). The data DTN contains the post-processed thermal response histories as well as the input and output decks used in the NUFT 3.0s simulations required to assemble this calculation.

7. REFERENCES

7.1 AP-2.13Q, Rev. , ICN 3. *Technical Product Development Planning*. Washington, D.C.: U.S. Department of Energy, Office of Civilian Radioactive Waste Management. ACC: MOL.20000504.0305.

7.2 AP-2.21Q, Rev. 1, ICN 0, BSCN 1. *Quality Determinations and Planning for Scientific, Engineering, and Regulatory Compliance Activities*. [Washington, D.C.]: U.S. Department of Energy, Office of Civilian Radioactive Waste Management.

7.3 AP-3.12Q, Rev. 0, ICN 4. *Calculations.* Washington, D.C.: U.S. Department of Energy, Office of Civilian Radioactive Waste Management. ACC: MOL.20010404.0008.

7.4 AP-SI.1Q, Rev. 3. *Software Management*. Washington, D.C.: U.S. Department of Energy, Office of Civilian Radioactive Waste Management. ACC: MOL.20010405.0012.

7.5 AP-SIII.3Q, Rev 0, ICN 3. *Submittal and Incorporation of Data to the Technical Data Management System*. Washington, D.C.: U.S. Department of Energy, Office of Civilian Radioactive Waste Management. ACC: MOL.20000418.0808.

7.6 AP-SV.1Q, Rev. 0, ICN 2. *Control of the Electronic Management of Information*. Washington, D.C.: U.S. Department of Energy, Office of Civilian Radioactive Waste Management. ACC: MOL.20000831.0065.

7.7 CRWMS M&O 1999a. *License Application Design Selection Report*. B00000000-01717-4600-00123 REV 01 ICN 01. Las Vegas, Nevada: CRWMS M&O. ACC: MOL.19990908.0319.

7.8 CRWMS M&O 2000a. *Analysis of Infiltration Uncertainty*. ANL-NBS-HS-000027 REV 00. Las Vegas, Nevada: CRWMS M&O. ACC: MOL.20000525.0377.

7.9 CRWMS M&O 2000b. *Calibrated Properties Model*. MDL-NBS-HS-000003 REV 00. Las Vegas, Nevada: CRWMS M&O. ACC: MOL.19990721.0520.

7.10 CRWMS M&O 2000c. *Heat Decay Data and Repository Footprint for Thermal-Hydrologic and Conduction Only Models for TSPA-SR*. CAL-MGR-HS-000001 REV 00. Las Vegas, Nevada: CRWMS M&O. ACC: MOL.20000516.0007.

7.11 CRWMS M&O 2000d. *Monitored Geologic Repository: Project Description Document.* TDR-MGR-SE-000004 REV 02 ICN 01. Las Vegas, Nevada: CRWMS M&O. ACC: MOL.20010212.0296.

7.12 CRWMS M&O 2000e. *Multiscale Thermohydrologic Model*. ANL-EBS-MD-000049 REV 00 ICN 00. Las Vegas, Nevada: CRWMS M&O. ACC: MOL.20000609.0267.

7.13 CRWMS M&O 2000f. *Multiscale Thermohydrologic Model*. ANL-EBS-MD-000049 REV 00 ICN 01. Las Vegas, Nevada: CRWMS M&O. ACC: MOL.20001208.0062.

7.14 CRWMS M&O 2000g. Process Control Evaluation For Supplement V: "Performance Assessment Operations. (Reference QAP-2-0 Activity Evaluation Form. Conduct of Performance Assessment, November 9, 1999)". Las Vegas, Nevada: CRWMS M&O. ACC: MOL.20000128.0236.

7.15 CRWMS M&O 2000h. Site Recommendation Design Baseline. Technical Change Request T2000-0133. Las Vegas, Nevada: CRWMS M&O. ACC: MOL.20000503.0159.

7.16 CRWMS M&O 2000i. *Tabulated In-Drift Geometric and Thermal Properties Used in Drift-Scale Models for TSPA-SR*. CAL-EBS-HS-000002 REV00. Las Vegas, Nevada: CRWMS M&O. ACC: MOL.20000718.0219.

7.17 CRWMS M&O 2000j. *Thermal Hydrology EBS Design Sensitivity Analysis*. Development Plan TDP-EBS-HS-000004 Rev 00. Las Vegas, Nevada: CRWMS M&O. ACC: MOL.20000605.0436.

7.18 CRWMS M&O 2000k. *Ventilation Model*. ANL-EBS-MD-000030 REV 00. Las Vegas, Nevada: CRWMS M&O. ACC: MOL.20000107.0330.

7.19 LL000509112312.003. TSPA-SR Multiscale TH Results (E0120) Mean Calculations Using Drift Scale Property Set. Submittal date: 05/18/2000.

7.20 LL000509012312.002. TSPA-SR Multiscale TH Results (E0120) Lower Calculations Using Drift Scale Property Set. Submittal date: 05/18/2000.

7.21 LL000509212312.004. TSPA-SR Multiscale TH Results (E0120) Upper Calculations Using Drift Scale Property Set. Submittal date: 05/18/2000.

7.22 SNT05071897001.004. Total System Performance Assessment-Viability Assessment (TSPA-VA) Heat Loading Data. Submittal Date: 03/26/1998.

7.23 Stroupe, E.P. 2000. "Approach to Implementing the Site Recommendation Design Baseline." Interoffice correspondence from E.P. Stroupe (CRWMS M&O) to D.R. Wilkins, January 26, 2000, LV.RSO.EPS.1/00-004, with attachment. ACC: MOL.20000214.0480.

7.24 USGS (U.S. Geological Survey) 2000. *Simulation of Net Infiltration for Modern and Potential Future Climates*. ANL-NBS-HS-000032 REV 00. Denver, Colorado: U.S. Geological Survey. ACC: MOL.20000801.0004.

7.25 Wilkens,D.R. and Heath, C.A. 1999. "Direction to Transition to Enhanced Design Alternative II." Letter from D.R. Wilkins (CRWMS M&O) and C.A. Heath (CRWMS M&O) to Distribution, June 15, 1999, LV.NS.JLY.06/99-026, with enclosures, "Strategy for Baselining EDA II Requirements" and "Guidelines for Implementation of EDA II." ACC: MOL.19990622.0126, MOL.19990622.0127, MOL.19990622.0128.

7.26 YAP-SV.1Q, Rev. 0, ICN 1. *Control of the Electronic Management of Data*. Las Vegas, Nevada: Yucca Mountain Site Characterization Office. ACC: MOL.19991008.0209.

8. ATTACHMENTS

ATTACHMENT	TITLE	NUMBER OF PAGES
I	SENSITIVITY TO PRECLOSURE VENTILATION DURATION	8
II	SUMMARY OF LINEAL DRIFT-SCALE THERMAL-HYDROLOGIC PERFORMANCE PARAMETERS	3
III	BELOW BOILING DRIFT WALL DESIGN CASES	6
IV	STRUCTURE OF THE THERMAL-HYDROLOGY SENSITIVITY CALCULATION DATA SUBMITTAL	4

Attachment I

SENSITIVITY TO PRECLOSURE VENTILATION DURATION

This attachment graphically presents the sensitivity of the selected performance parameters through the full range of lineal loadings and Preclosure ventilation durations. Four performance parameters are presented in time history plots: waste package temperature, waste package relative humidity, drift wall temperature, and quarter pillar temperature. Combined with the section 5.1, the figures should aid in understanding the coupled effects of lineal loading and ventilation duration. Each of the lineal loadings examined in the calculation are presented here, 0.90kW/m, 1.25kW/m, 1.45kW/m, and 1.60kW/m. Also, each ventilation duration scenario that was simulated for the calculation is presented.

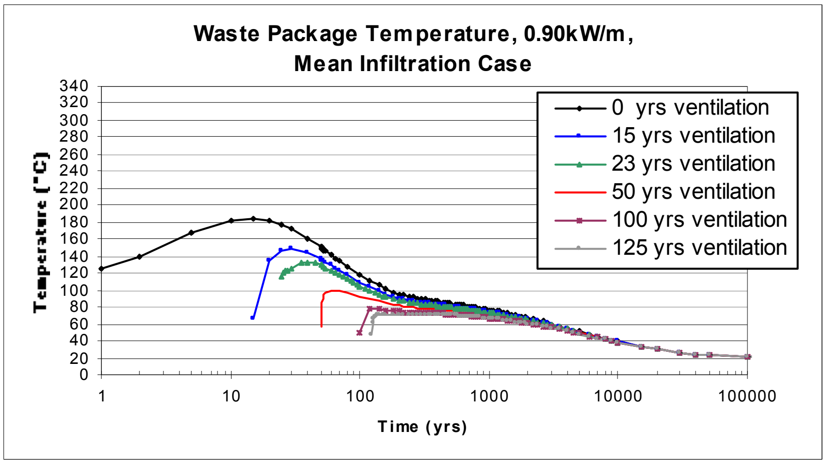

DTN: MO0008SPATHS03.001

Figure I-1. Comparison of waste package temperature time-histories. Lineal power loading of 0.90kW/m and varying ventilation durations.

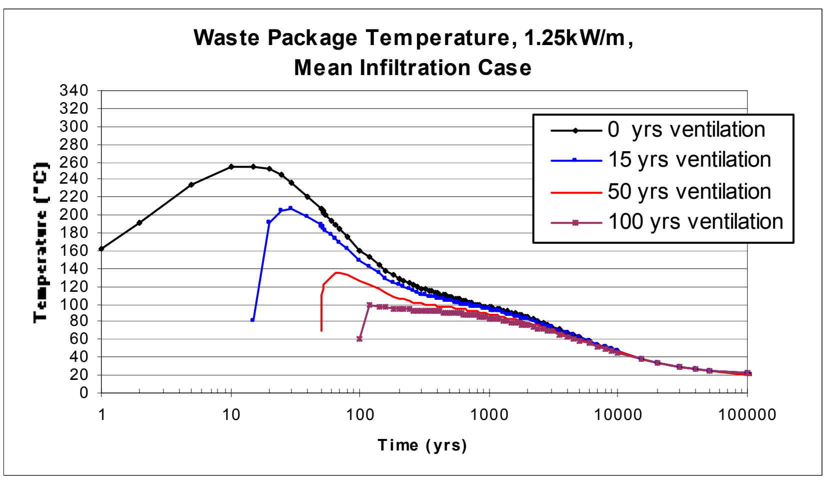

DTN: MO0008SPATHS03.001

Figure I-2. Comparison of waste package temperature time-histories. Lineal power loading of 1.25kW/m and varying ventilation durations.

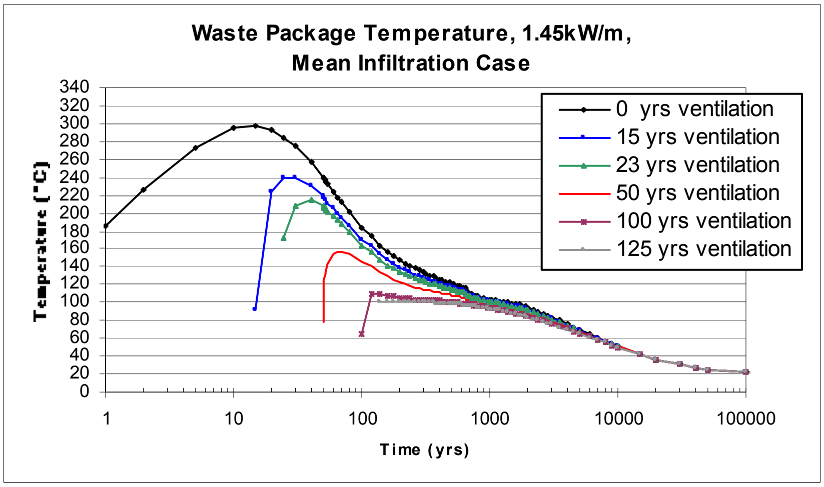

DTN: MO0008SPATHS03.001

Figure I-3. Comparison of waste package temperature time-histories. Lineal power loading of 1.45kW/m and varying ventilation durations.

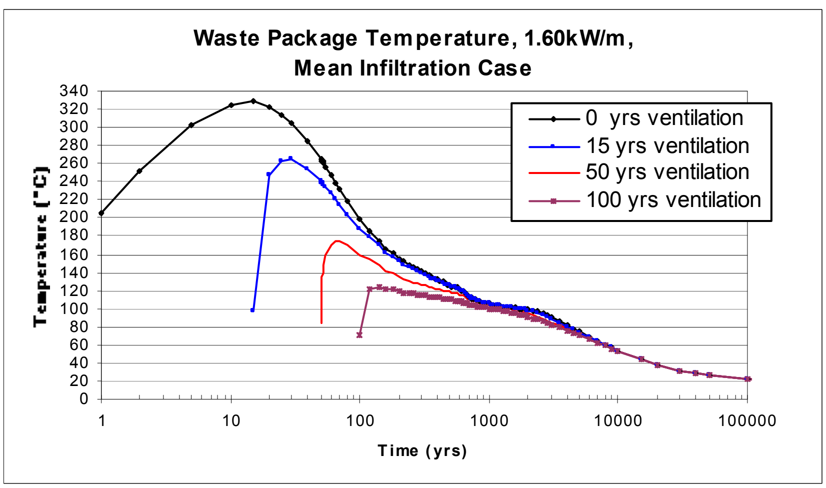

DTN: MO0008SPATHS03.001

Figure I-4. Comparison of waste package temperature time-histories. Lineal power loading of 1.60kW/m and varying ventilation durations.

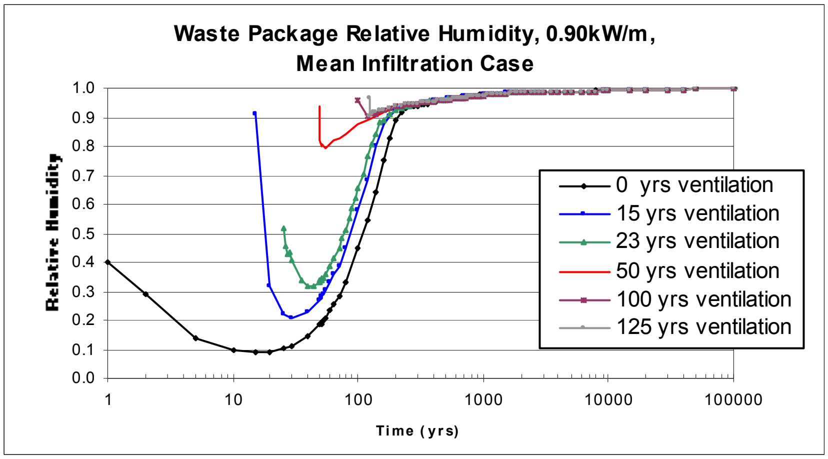

DTN: MO0008SPATHS03.001

Figure I-5. Comparison of waste package relative humidity time-histories. Lineal power loading of 0.90kW/m and varying ventilation durations.

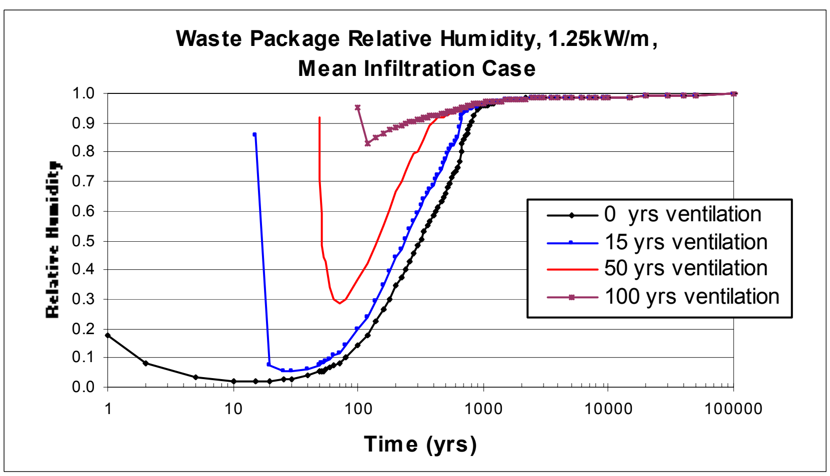

DTN: MO0008SPATHS03.001

Figure I-6. Comparison of waste package relative humidity time-histories. Lineal power loading of 1.25kW/m and varying ventilation durations.

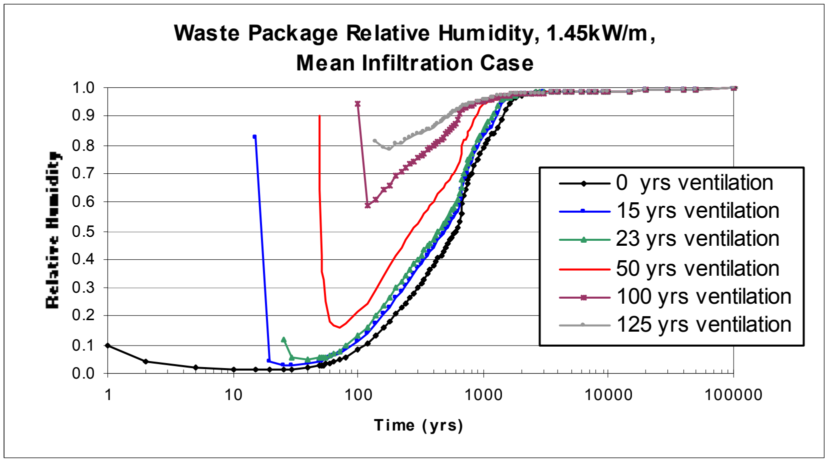

DTN: MO0008SPATHS03.001

Figure I-7. Comparison of waste package relative humidity time-histories. Lineal power loading of 1.45kW/m and varying ventilation durations.

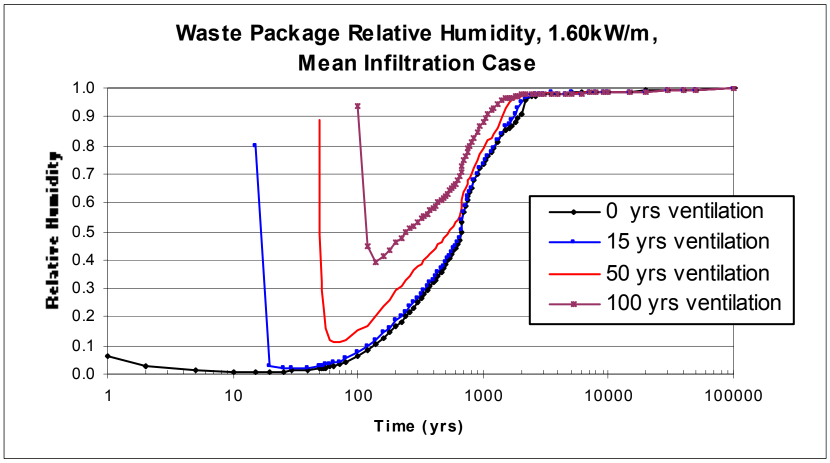

DTN: MO0008SPATHS03.001

Figure I-8. Comparison of waste package relative humidity time-histories. Lineal power loading of 1.60kW/m and varying ventilation durations.

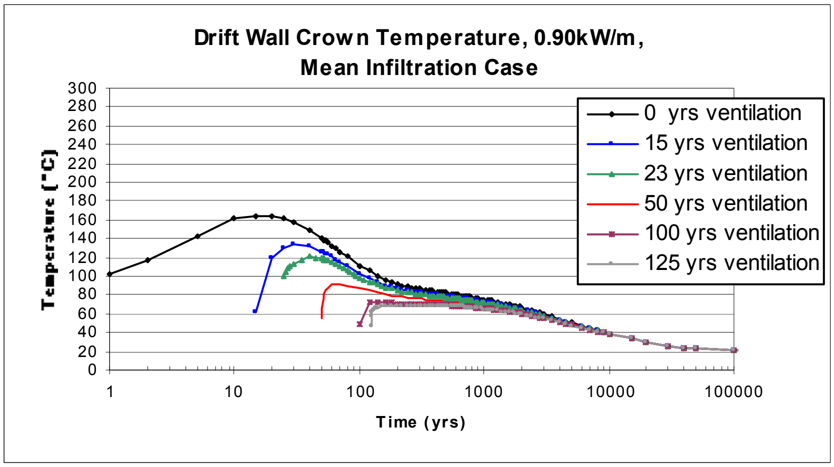

DTN: MO0008SPATHS03.001

Figure I-9. Comparison of drift wall temperature time-histories. Lineal power loading of 0.90kW/m and varying ventilation durations.

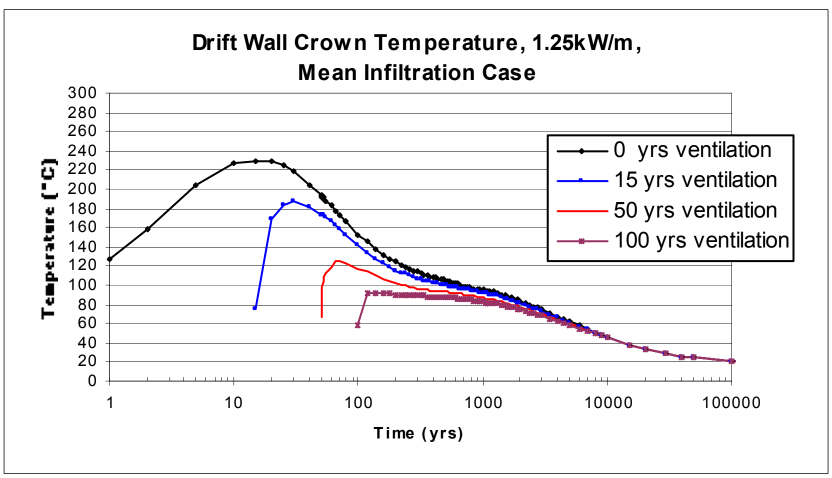

DTN: MO0008SPATHS03.001

Figure I-10. Comparison of drift wall temperature time-histories. Lineal power loading of 1.25kW/m and varying ventilation durations.

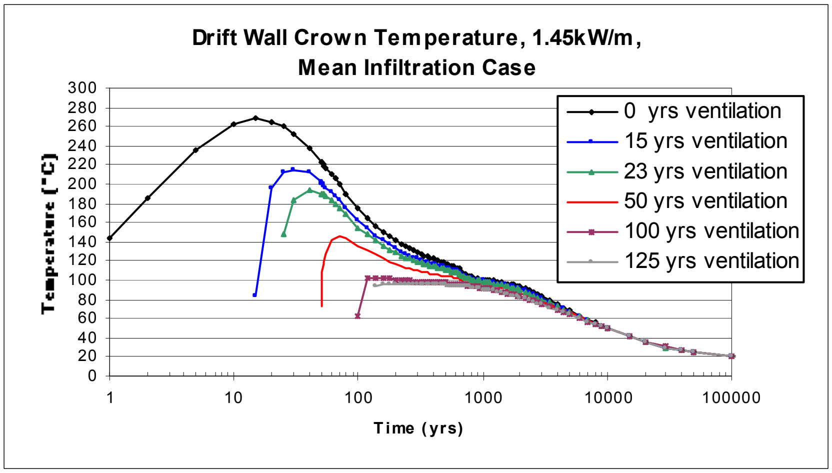

DTN: MO0008SPATHS03.001

Figure I-11. Comparison of drift wall temperature time-histories. Lineal power loading of 1.45kW/m and varying ventilation durations.

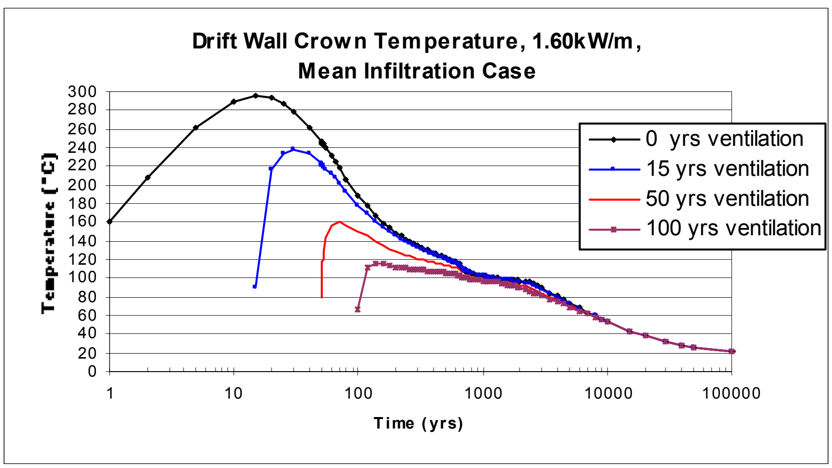

DTN: MO0008SPATHS03.001

Figure I-12. Comparison of drift wall temperature time-histories. Lineal power loading of 1.60kW/m and varying ventilation durations.

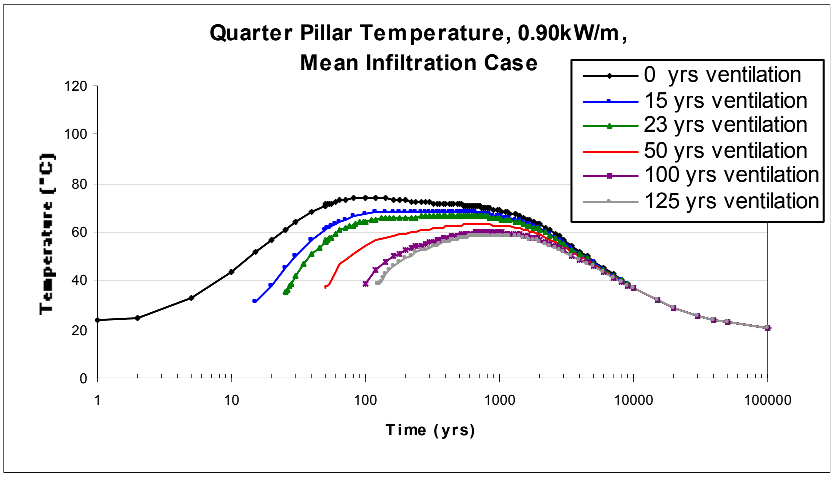

DTN: MO0008SPATHS03.001

Figure I-13. Comparison of quarter pillar temperature time-histories. Lineal power loading of 0.90kW/m and varying ventilation durations.

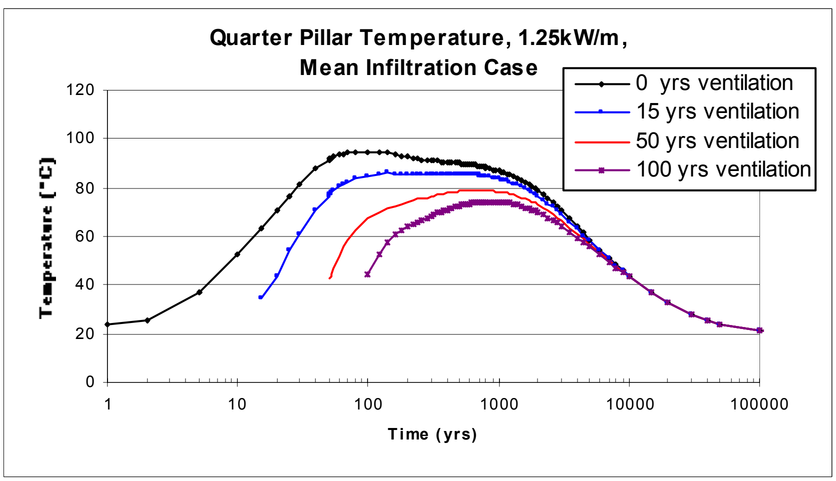

DTN: MO0008SPATHS03.001

Figure I-14. Comparison of quarter pillar temperature time-histories. Lineal power loading of 1.25kW/m and varying ventilation durations.

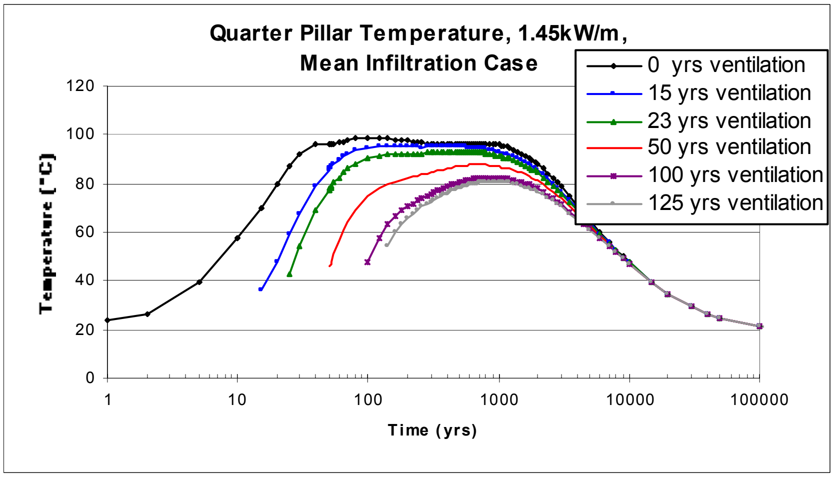

DTN: MO0008SPATHS03.001

Figure I-15. Comparison of quarter pillar temperature time-histories. Lineal power loading of 1.45kW/m and varying ventilation durations.

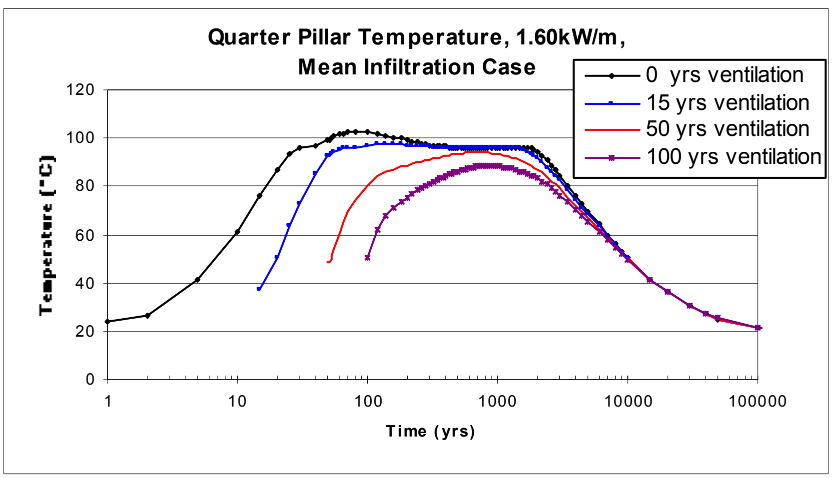

DTN: MO0008SPATHS03.001

Figure I-16. Comparison of quarter pillar temperature time-histories. Lineal power loading of 1.60kW/m and varying ventilation durations.

Attachment II

SUMMARY OF LINEAL DRIFT-SCALE THERMAL-HYDROLOGIC PERFORMANCE PARAMETERS

This attachment presents tables of performance parameters for the complete range of lineal power loadings and ventilation duration times. The four tables presented in this attachment show the lineal loadings of 0.90kW/m, 1.25kW/m, 1.45kW/m, and 1.60kW/m. Each table also presents each of the different ventilation duration times that was simulated for this sensitivity study. The tables containing the performance parameter information for the lineal loadings of 0.90kW/m (Table II-1 ~ Table 5.9-7) and 1.45kW/m (Table II-3 ~ Table 5.1-2) are repeated here for ease of comparison with the tables that were not presented previously.

Table II-1. Summary of thermal hydrologic performance parameters showing the drift-scale sensitivity to ventilation. 0.90kW/m LDTH model used for all simulations.

Performance Parameter	Infiltration Flux Case	Years of Ventilation (70% effective heat removal)						
		0	**15**	**23**	**50**	**75**	**100**	**125**
WP Peak Temperature (Celsius)	Low	197	163	148	114	97	88	81
	Mean	**183**	**149**	**133**	**99**	**85**	**77**	**72**
	High	176	141	126	97	83	75	70
WP > 115°C Time (Years)	Low	160	125	110	0	0	0	0
	Mean	**110**	**90**	**75**	**0**	**0**	**0**	**0**
	High	95	80	65	0	0	0	0
WP > 80°C Time (Years)	Low	1550	1350	1275	950	800	600	420
	Mean	**740**	**560**	**480**	**250**	**175**	**0**	**0**
	High	600	430	360	200	140	0	0
DW Peak Temperature (Celsius)	Low	180	149	136	106	91	83	78
	Mean	**164**	**134**	**120**	**92**	**80**	**73**	**69**
	High	157	127	113	90	78	71	67
DW > 96°C Time (Years)	Low	400	260	215	140	0	0	0
	Mean	**170**	**130**	**115**	**0**	**0**	**0**	**0**
	High	150	110	95	0	0	0	0
¼ Pillar Peak Temperature (Celsius)	Low	81	75	74	70	68	67	65
	Mean	**74**	**68**	**67**	**63**	**61**	**60**	**59**
	High	73	66	64	61	59	58	56

DTN: MO0008SPATHS03.001

Table II-2. Summary of thermal hydrologic performance parameters showing the drift-scale sensitivity to ventilation. 1.25kW/m LDTH model used for all simulations.

Performance Parameter	Infiltration Flux Case	Years of Ventilation (70% effective heat removal)			
		0	15	50	100
WP Peak Temperature (Celsius)	Low	270	221	151	113
	Mean	**255**	**207**	**136**	**98**
	High	247	199	129	96
WP > 115°C Time (Years)	Low	770	610	320	0
	Mean	**345**	**250**	**150**	**0**
	High	270	210	130	0
WP > 80°C Time (Years)	Low	4050	3550	3200	2700
	Mean	**2450**	**2250**	**1860**	**1500**
	High	2000	1810	1470	1200
DW Peak Temperature (Celsius)	Low	245	201	140	107
	Mean	**229**	**187**	**125**	**92**
	High	222	179	119	90
DW > 96°C Time (Years)	Low	1800	1600	1300	860
	Mean	**900**	**690**	**320**	**0**
	High	740	540	230	0
¼ Pillar Peak Temperature (Celsius)	Low	102	94	87	82
	Mean	**95**	**86**	**79**	**74**
	High	92	83	77	72

DTN: MO0008SPATHS03.001

Table II-3. Summary of thermal hydrologic performance parameters showing the drift-scale sensitivity to ventilation. 1.45kW/m LDTH model used for all simulations.

Performance Parameter	Infiltration Flux case	Years of Ventilation (70% effective heat removal)					
		0	15	23	50	100	125
WP Peak Temperature (Celsius)	Low	313	255	229	172	129	117
	Mean	**298**	**238**	**214**	**157**	**110**	**101**
	High	288	231	207	151	107	99
WP > 115°C Time (Years)	Low	1450	1250	1150	900	580	380
	Mean	**650**	**575**	**500**	**300**	**0**	**0**
	High	550	450	380	240	0	0
WP > 80°C Time (Years)	Low	5550	5400	5150	5000	4600	4500
	Mean	**3400**	**3250**	**3200**	**2900**	**2500**	**2400**
	High	2600	2450	2400	2250	2000	1900
DW Peak Temperature (Celsius)	Low	284	232	210	160	121	111
	Mean	**268**	**215**	**195**	**145**	**103**	**96**
	High	258	208	188	138	99	93
DW > 96°C Time (Years)	Low	2850	2500	2300	2000	1800	1675
	Mean	**1650**	**1450**	**1350**	**975**	**620**	**0**
	High	1400	1200	1100	800	340	0
¼ Pillar Peak Temperature (Celsius)	Low	113	104	102	97	92	90
	Mean	**99**	**95**	**93**	**88**	**82**	**81**
	High	96	93	91	85	80	78

DTN: MO0008SPATHS03.001

Table II-4. Summary of thermal hydrologic performance parameters showing the drift-scale sensitivity to ventilation. 1.60kW/m LDTH model used for all simulations.

Performance Parameter	Infiltration Flux Case	Years of Ventilation (70% effective heat removal)			
		0	**15**	**50**	**100**
WP Peak Temperature (Celsius)	Low	344	281	188	140
	Mean	**329**	**264**	**174**	**125**
	High	321	256	167	118
WP > 115°C Time (Years)	Low	1780	1660	1400	1100
	Mean	**690**	**680**	**610**	**290**
	High	630	620	470	195
WP > 80°C Time (Years)	Low	6600	6500	6200	5900
	Mean	**4300**	**4000**	**3700**	**3400**
	High	3000	2830	2620	2440
DW Peak Temperature (Celsius)	Low	312	256	175	131
	Mean	**296**	**239**	**161**	**116**
	High	288	230	153	110
DW > 96°C Time (Years)	Low	3800	3500	3000	2450
	Mean	**2250**	**2030**	**1610**	**1250**
	High	1920	1650	1330	960
¼ Pillar Peak Temperature (Celsius)	Low	120	111	104	98
	Mean	**103**	**98**	**94**	**88**
	High	100	96	92	86

DTN: MO0008SPATHS03.001

Attachment III

BELOW BOILING DRIFT WALL DESIGN CASES

This attachment presents the design cases of the thermal-hydrological sensitivity calculation that maintain drift wall temperatures below boiling. The non-boiling cases are defined by the drift wall temperature remaining under the boiling point, 96 °C at a repository elevations, after the closure of the emplacement drifts (after ventilation stops). Three different lineal loadings of 0.90kW/m, 1.25kW/m, and 1.45kW/m are presented in this attachment, in each scenario the drift-to-drift spacing is 81 meters.

Figures III-1 through III-4 present temperature and relative humidity histories of the drift wall and the waste package when only considering the mean infiltration hydrologic properties set case. The basecase design, initial lineal loading 1.45kW/m, 50 years ventilation, and the mean infiltration flux case, is included for comparison purposes. A summary of the thermal-hydrologic performance parameters shown in figures III-1 through III-4 is presented in Table III-1.

Figures III-5 through III-8 present temperature and relative humidity histories of the drift wall and the waste package when only considering the low infiltration hydrologic properties set case. The basecase design, initial lineal loading 1.45kW/m, 50 years ventilation, and the low infiltration flux case, is included for comparison purposes. A summary of the thermal-hydrologic performance parameters shown in figures III-5 through III-8 is presented in Table III-2.

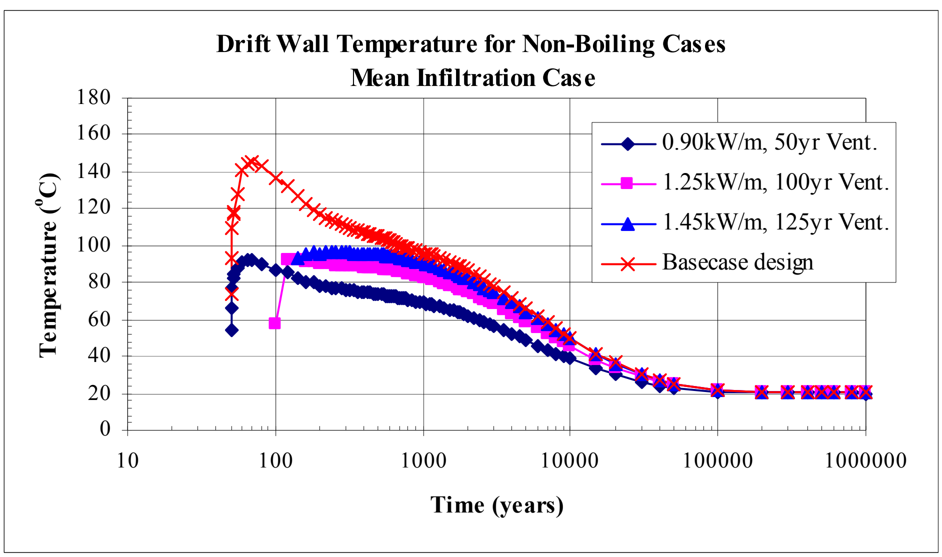

DTN: MO0008SPATHS03.001

Figure III-1. Drift wall temperature time-histories of non-boiling cases. The basecase design represents the 1.45kw/m and 50 years ventilation case.

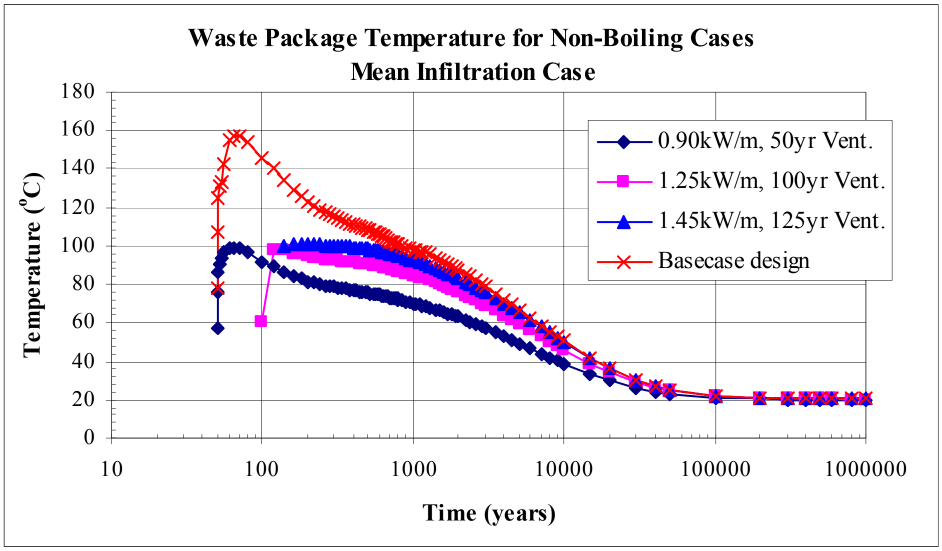

DTN: MO0008SPATHS03.001

Figure III-2. Waste package temperature time-histories of non-boiling cases. The basecase design represents the 1.45kw/m and 50 years ventilation case.

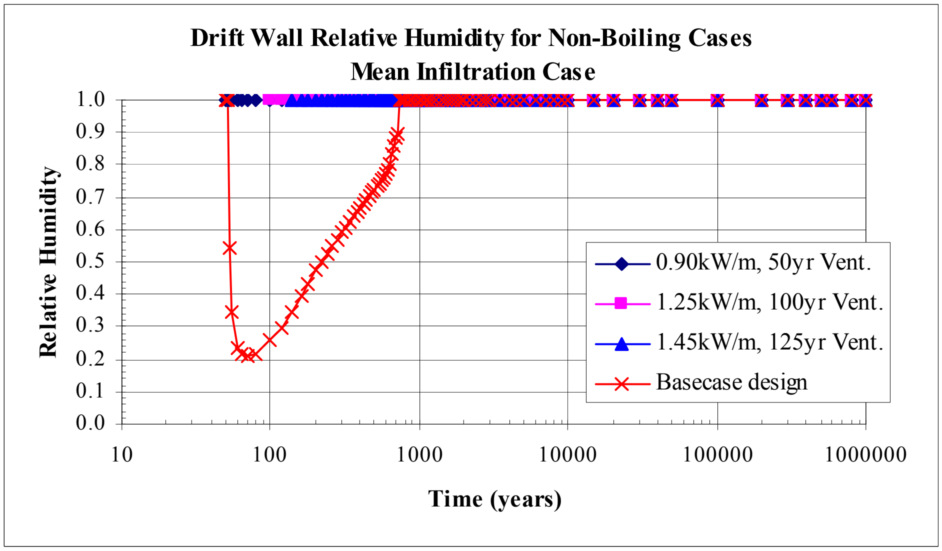

DTN: MO0008SPATHS03.001

Figure III-3. Drift wall relative humidity time-histories of non-boiling cases. The basecase design represents the 1.45kw/m and 50 years ventilation case.

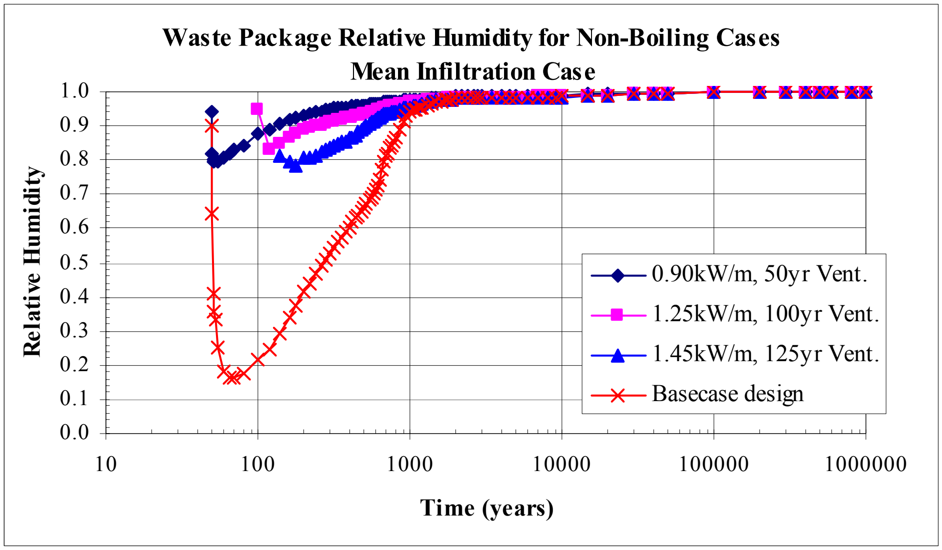

DTN: MO0008SPATHS03.001

Figure III-4. Waste package relative humidity time-histories of non-boiling cases. The basecase design represents the 1.45kw/m and 50 years ventilation case.

Table III-1. Summary of thermal hydrologic performance parameters for non-boiling cases.

Performance Parameter	Infiltration Flux Case	Linear Heat Load Years of Ventilation			
		0.90kW/m 50 yrs	1.25kW/m 100 yrs	1.45kW/m 125 yrs	1.45kW/m 50 yrs
WP Peak Temperature (Celsius)	Mean	99	98	101	157
WP > 115°C Time (Years)	Mean	0	0	0	300
WP > 80°C Time (Years)	Mean	250	1500	2400	2900
DW Peak Temperature (Celsius)	Mean	92	92	96	145
DW > 96°C Time (Years)	Mean	0	0	0	975
¼ Pilr Peak Temperature (Celsius)	Mean	63	74	81	88

DTN: MO0008SPATHS03.001

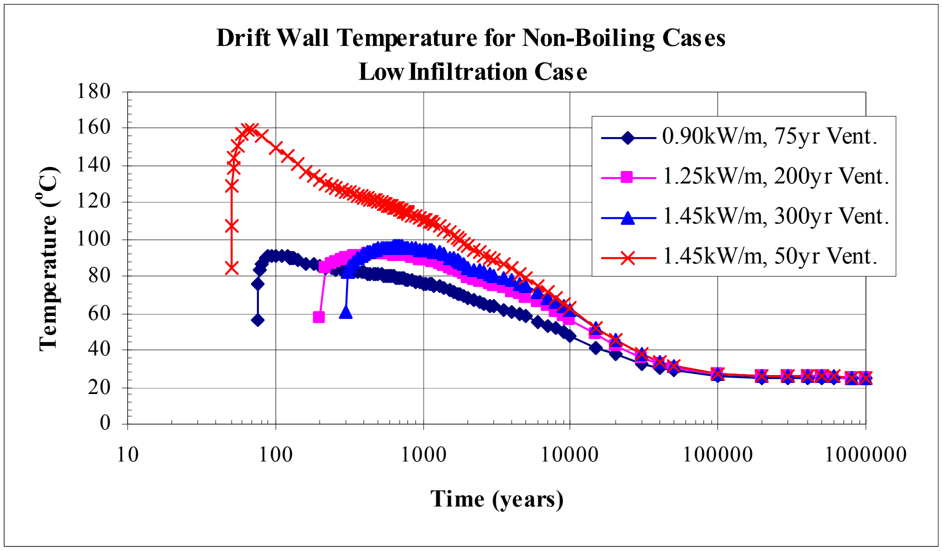

DTN: MO0008SPATHS03.001

Figure III-5. Drift wall temperature time-histories of non-boiling cases for low infiltration flux.

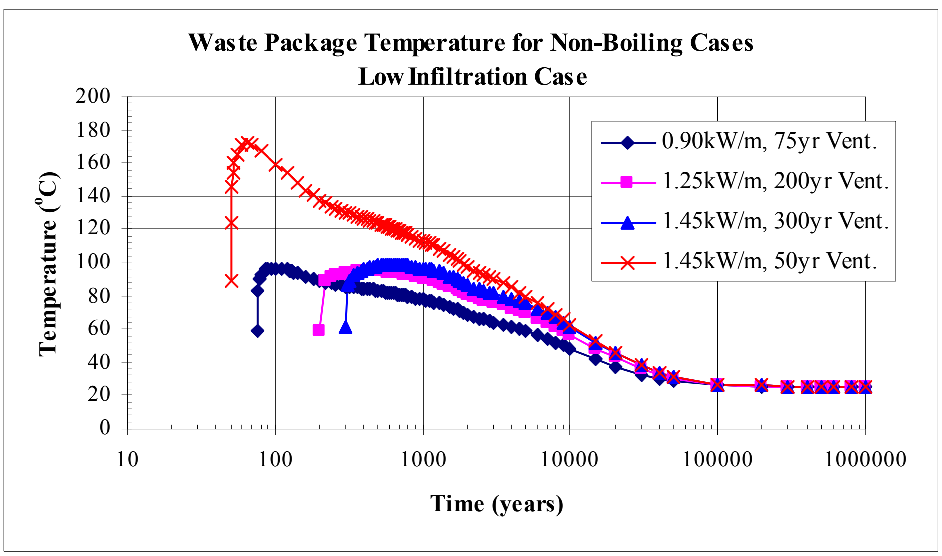

DTN: MO0008SPATHS03.001

Figure III-6. Waste package temperature time-histories of non-boiling cases for low infiltration flux.

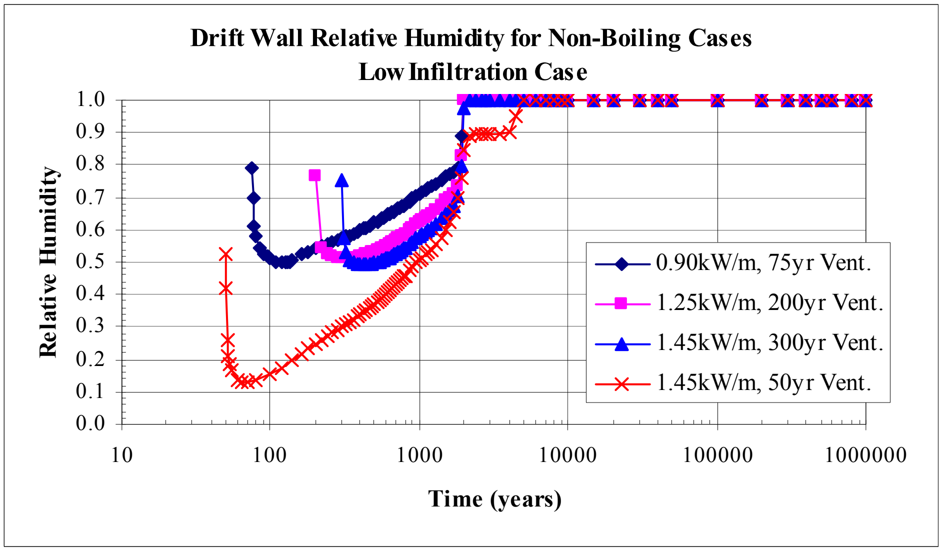

DTN: MO0008SPATHS03.001

Figure III-7. Drift wall relative humidity time-histories of non-boiling cases for low infiltration flux.

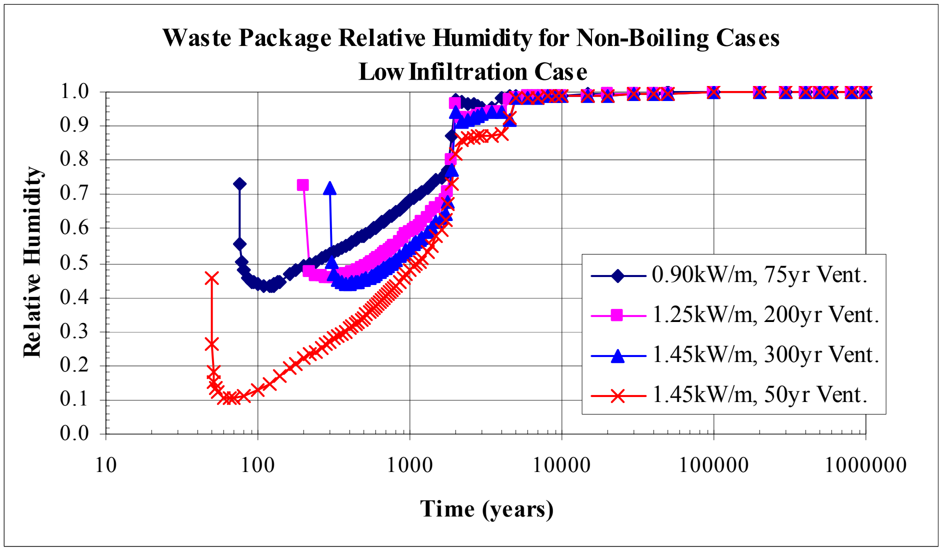

DTN: MO0008SPATHS03.001

Figure III-8. Waste package relative humidity time-histories of non-boiling cases for low infiltration flux.

Table III-2. Summary of TH performance parameters for non-boiling cases in low infiltration flux.

Performance Parameter	Infiltration Flux Case	Linear Heat Load Years of Ventilation			
		0.90kW/m 75 yrs	1.25kW/m 200 yrs	1.45kW/m 300 yrs	1.45kW/m 50 yrs
WP Peak Temperature (Celsius)	Low	97	95	99	172
WP > 115°C Time (Years)	Low	0	0	0	900
WP > 80°C Time (Years)	Low	780	2100	3600	5000
DW Peak Temperature (Celsius)	Low	91	92	96	160
DW > 96°C Time (Years)	Low	0	0	0	2000
¼ Pilr Peak Temperature (Celsius)	Low	68	77	82	97

DTN: MO0008SPATHS03.001

Attachment IV

STRUCTURE OF THE THERMAL-HYDROLOGY SENSITIVITY CALCULATION DATA SUBMITTAL

This attachment presents a list of all the sensitivity calculation runs and the location of the files in the data submittal for the Thermal-Hydrological Sensitivity Calculation (MO0008SPATH03.001 and MO0103MWDTHS03.001). Main directories represent different types of modeling and design parameters such as lower temperature scenarios, DDT/LDTH models, infiltration flux rate, invert materials, ventilation efficiency, and drift to drift spacing. Each sub-directory contains the model runs for varying preclosure duration.

Directories TH_Sensitivity_data1 and TH_Sensitivity_data2 (MO0008SPATH03.001):
input and output files of TH sensitivity NUFT models

1. DDT: 3D, NUFT, drift scale, DDT - thermal (conduction-only) simulations
    1) DDT_0.90: thermal simulations at 0.90kW/m
       50 years of preclosure (ventilation) case
    2) DDT_1.25: thermal simulations at 1.25kW/m
       50 years of preclosure (ventilation) case
    3) DDT_1.45: thermal simulations at 1.45kW/m
       0, 50, 100, 150, and 200 years of preclosure (ventilation) cases
    4) DDT_1.54: thermal simulations at 1.54kW/m
       50 years of preclosure (ventilation) case
    5) DDT_1.57: thermal simulations at 1.57kW/m
       50 years of preclosure (ventilation) case

2. LDTH_low: 2D, NUFT, drift scale, thermal-hydrological simulations with low infiltration
    1) 0.90l.dir: thermal-hydrological simulations at 0.90kW/m
       0, 15, 23, 50, and 100 years of preclosure (ventilation) cases
    2) 1.25l.dir: thermal-hydrological simulations at 1.25kW/m
       0, 15, 50, 100, and 200 years of preclosure (ventilation) cases
    3) 1.45l.dir: thermal-hydrological simulations at 1.45kW/m
       0, 15, 23, 50, 100, 125, 160, 200, 275, and 300 years of preclosure (ventilation) cases
    4) 1.60l.dir: thermal-hydrological simulations at 1.60kW/m
       0, 15, 50, and 100 years of preclosure (ventilation) cases

3. LDTH_mean: 2D, NUFT, drift scale, thermal-hydrological simulations with mean infiltration
    1) 0.90.dir: no-backfill, thermal-hydrological simulations at 0.90kW/m
       0, 15, 50, and 100 years of preclosure (ventilation) cases
    2) 1.25.dir: no-backfill, thermal-hydrological simulations at 1.25kW/m
       0, 15, 50, and 100 years of preclosure (ventilation) cases
    3) 1.45.dir: no-backfill, thermal-hydrological simulations at 1.45kW/m
       0, 15, 23, 50, 100, and 125 years of preclosure (ventilation) cases

4) 1.45wBF.dir: with backfill, thermal-hydrological simulations at 1.45kW/m
50 years of preclosure (ventilation) case for backfill design (~wBF~)
5) 1.60.dir: no-backfill, thermal-hydrological simulations at 1.60kW/m
0, 15, 50, and 100 years of preclosure (ventilation) cases

4. LDTH_high: 2D, NUFT, drift scale, thermal-hydrological simulations with high infiltration
1) 0.90u.dir: thermal-hydrological simulations at 0.90kW/m
0, 15, 23, 50, and 100 years of preclosure (ventilation) cases
2) 1.25u.dir: thermal-hydrological simulations at 1.25kW/m
0, 15, 50, and 100 years of preclosure (ventilation) cases
3) 1.45u.dir: thermal-hydrological simulations at 1.45kW/m
0, 15, 23, 50, 100, and 125 years of preclosure (ventilation) cases
4) 1.60u.dir: thermal-hydrological simulations at 1.60kW/m
0, 15, 50, and 100 years of preclosure (ventilation) cases

5. LDTH_inv_Kth: 2D, NUFT, drift scale, thermal-hydrological simulations with range of invert thermal conductivity values
Two invert thermal conductivity cases of 0.15 (~inv015~) and 0.66 (~inv066~) W/m-K with 50 years preclosure (ventilation)

6. LDTH_vent_eff: 2D, NUFT, drift scale, thermal-hydrological simulations with 50%, 65% and 70% effective heat removal during period of ventilation (70% baseline)
1) 50percent_vent.dir: thermal-hydrological simulations with 50% effective rate of ventilation
26 and 50 years of preclosure (ventilation) cases
2) 65percent_vent.dir: thermal-hydrological simulations with 65% effective rate of ventilation
26 and 50 years of preclosure (ventilation) cases
3) 70percent_vent.dir: thermal-hydrological simulations with 70% effective rate of ventilation (baseline)
26 years of preclosure (ventilation) case

7. LDTH_WPtemp: 2D, NUFT, drift scale, thermal-hydrological simulations with pillar width adjusted thermal loading
Three thermal loading cases of 0.90kW/m (~0.90dx~), 1.25kW/m (~1.25dx~), and 1.60kW/m (~1.60dx~) with 50 years preclosure (ventilation)

Directory TH_Sensitivity_plots (MO0008SPATH03.001):
Excel plots and extracted data from the calculations

1. DDT: 3D, NUFT, DDT - thermal (conduction-only) post-processed data and plots

2. LDTH_low: 2D, NUFT, drift scale, thermal-hydrological post-processed data and plots for low infiltration simulations

3. LDTH_mean: 2D, NUFT, drift scale, thermal-hydrological post-processed data and plots for mean infiltration simulations

4. LDTH_high: 2D, NUFT, drift scale, thermal-hydrological post-processed data and plots for high infiltration simulations

5. LDTH_inv_Kth: 2D, NUFT, drift scale, thermal-hydrological post-processed data and plots for range invert thermal conductivity simulations

6. LDTH_vent_eff: 2D, NUFT, drift scale, thermal-hydrological data and plots with 50%, 65% and 70% effective heat removal during period of ventilation (70% baseline)

7. LDTH_WPtemp: 2D, NUFT, drift scale, thermal-hydrological post-processed data and plots for pillar width adjusted thermal loading simulations

8. CAL-EBS-HS-000003_figures: various figures used in calculation report CAL-EBS-HS-000003

Directory AP314transmittal_00395 (MO0103MWDTHS03.001):
input and output files of TH sensitivity NUFT models for lower temperature operation scenarios

1. 070kWm_FV100yr: Increased waste package spacing scenario, 2D NUFT, 0.70 kW/m, 81m drift spacing, 6 m waste package spacing, 100 years forced ventilation, 28 MTU/acre

2. 100kWm_age30yr_FV75yr: Pre-emplacement fuel aging scenario, 2D NUFT, 1.00 kW/m, 81 m drift spacing, 2 m waste package spacing, 30 years increase of fuel aging, 75 years forced ventilation, 40 MTU/acre

3. 145kWm_dx100kWm_FV300yr: Increased drift spacing scenario, 2D NUFT, 1.45 kW/m, 120 m drift spacing, 0.1 m waste package spacing, 300 years forced ventilation, 40 MTU/acre

4. 030kWm_DS38m_FV0yr: EIS low thermal load scenario, 2D NUFT, 0.30 kW/m, 38 m drift spacing, 18.75 m waste package spacing, 0 years forced ventilation, 25 MTU/acre